

THE INFLUENCE OF LOW MELT POINT, HIGH MODULUS FIBERS IN
BLENDED FIBER BALLISTIC RESISTANT NONWOVENS

Except where reference is made to the work of others, the work described in this thesis is my own or was done in collaboration with my advisory committee. This thesis does not include proprietary or classified information.

Rebecca Ray

Certificate of Approval:

Roy Broughton, Jr.
Professor
Polymer & Fiber Engineering

Howard L. Thomas, Jr., Chair
Associate Professor
Polymer & Fiber Engineering

Sabit Adanur
Professor
Polymer & Fiber Engineering

Peter Schwartz
Professor
Polymer & Fiber Engineering

Karla P. Simmons
Assistant Professor
Consumer Affairs

Joe F. Pittman
Interim Dean
Graduate School

THE INFLUENCE OF LOW MELT POINT, HIGH MODULUS FIBERS IN
BLENDED FIBER BALLISTIC RESISTANT NONWOVENS

Rebecca Ray

A Thesis

Submitted to

the Graduate Faculty of

Auburn University

in Partial Fulfillment of the

Requirements for the

Degree of

Master of Science

Auburn, Alabama
December 15, 2006

THE INFLUENCE OF LOW MELT POINT, HIGH MODULUS FIBERS IN
BLENDED FIBER BALLISTIC RESISTANT NONWOVENS

Rebecca Ray

Permission is granted to Auburn University to make copies of this thesis at its discretion, upon request of individuals or institutions and at their expense. The author reserves all publication rights.

Signature of Author

Date of Graduation

VITA

Rebecca Lori Armstrong, daughter of James and Tanya Armstrong, was born on April 26, 1981, in Nashville, Tennessee. She attended high school at Christ Presbyterian Academy in Nashville, Tennessee, and graduated in May 2000. She entered Auburn University in August 2000, and graduated magna cum laude with a Bachelor of Science in Textile Management and Technology in August 2004. She spent her last semester studying at Reutlingen University in Reutlingen, Germany. On December 18, 2004, she married Adam A. Ray. In August, 2005, she entered graduate school at Auburn University.

THESIS ABSTRACT

THE INFLUENCE OF LOW MELT POINT, HIGH MODULUS FIBERS IN
BLENDED FIBER BALLISTIC RESISTANT NONWOVENS

Rebecca Ray

Master of Science, December 15, 2006
(B.S., Auburn University, 2004)

136 Typed Pages

Directed by Howard L. Thomas

The purpose of this research is to examine the presence of a thermal phase change as a means of energy dissipation in nonwoven needlepunched felts used in soft body armor applications. The investigation was carried out using Differential Scanning Calorimetry, Polarized Light Microscopy and standardized V_{50} ballistic testing. A mathematical formula was developed to approximate the residual kinetic energy of the nonwoven felt. The overall conclusion from the testing is that a thermal phase change does occur as a result of projectile impact; however, the energy dissipation ensuing from this phase change has not proven to be a major contribution to the nonwoven felt's elevated anti-ballistic properties.

ACKNOWLEDGEMENTS

I would like to thank Dr. Howard L. Thomas for providing me with the opportunity to pursue my Masters degree. His consistent wisdom and expertise have been greatly appreciated throughout my undergraduate and graduate experience. I thank my committee members for their guidance throughout the testing and writing phases of this research. I would also like to thank my family, my parents and brothers for their enthusiasm and interest in my education and my husband, Adam, for his unending patience and encouragement in this, and all areas of my life.

Style manual or journal used: The Harvard Journal style

Computer software used: Microsoft Office Word 2003, Microsoft Office Excel 2003,

FlashPath

TABLE OF CONTENTS

NOMENCLATURE	xi
LIST OF FIGURES	xiii
LIST OF TABLES	xviii
CHAPTER ONE: INTRODUCTION.....	1
CHAPTER TWO: LITERATURE REVIEW.....	4
2.1 Standards.....	4
2.1.1 Military Standard	5
2.1.2 NIJ Standard.....	5
2.2 Textile Structures	6
2.2.1 Fiber	6
2.2.1.1 Aramid	7
2.2.1.2 Polyethylene.....	8
2.2.1.3 Liquid Crystal Polymer.....	9
2.2.2 Yarn.....	10
2.2.3 Fabrics.....	11
2.2.3.1 Woven.....	11
2.2.3.2 Nonwoven.....	16
2.3 Textile Failure Mechanisms.....	20
2.3.1 Yarn Pull-Out.....	20

2.3.2 Fiber Cut Energy.....	23
2.3.3 Projectile	25
CHAPTER THREE: METHODS AND MATERIALS	31
3.1 Materials Tested.....	31
3.1.1 Fabric Construction.....	31
3.1.2 Fabric Composition.....	32
3.1.2.1 Fibers.....	32
3.1.2.2 Blending	32
3.2 Tests and Rationale	33
3.2.1 DSC Methodology	33
3.2.1.1 Method	33
3.2.1.2 Output	34
3.2.2 Photographic Methodology.....	35
3.2.2.1 Methodology	35
3.2.2.2 Output	36
3.2.3 Ballistic Limit Testing Methodology.....	36
3.2.3.1 Method	36
3.2.3.2 Output	37
3.2.4 Energy Determination Methodology	37
3.2.4.1 Kinetic Energy	37
CHAPTER FOUR: RESULTS AND DISCUSSION.....	39
4.1.1 DSC.....	39
4.1.1.1 Results.....	39
4.1.1.2 Discussion.....	40
4.1.2 Photographic Images.....	55

4.1.2.1 Results.....	56
4.1.2.2. Discussion.....	62
4.1.3 V ₅₀ Test	63
4.1.3.1 Results.....	63
4.1.3.2 Discussion.....	64
4.1.4 Kinetic Energy Calculation.....	65
4.1.4.1 Results.....	65
4.1.4.2 Discussion.....	66
CHAPTER FIVE: CONCLUSIONS	67
WORKS CITED	70
APPENDICIES.....	73
APPENDIX A: TEST STANDARDS	74
APPENDIX B: FIBER INFORMATION.....	76
APPENDIX C: DEFORMATIONS.....	78
APPENDIX D: IMPACT IMAGES	79
APPENDIX E: NON-IMPACT IMAGES.....	87
APPENDIX F: V ₅₀ TEST RESULTS.....	92
APPENDIX G: DSC PLOTS.....	107

NOMENCLATURE

A	Area
DSC	Differential Scanning Calorimetry
\bar{E}	Energy
$\bar{E}_{Penetration}$	Penetration Energy
$\bar{E}_{Residual}$	Residual Energy
F	Force
FMJ	Full Metal Jacket
FSP	Fragment Simulating Projectile
KE	Kinetic Energy
LCP	Liquid Crystal Polymer
m	Mass
NES	Nonwoven Enhanced Structures
NIJ	National Institute of Justice
OSTR	One Shot Test Response
PE	Polyethylene
r	Radius
RCC	Round Circular Cylinder
SAPI	Small Arms Protective Inserts
SEM	Scanning Electron Microscope

T_g	Glass Transition Temperature
T_m	Melting Temperature
UHMWPE	Ultra High Molecular Weight Polyethylene
v	Strain Wave Velocity
V	Velocity
V_{50}	Velocity at which 50% of Projectiles Penetrate the Armor
μ	Linear density (kg/m)
ρ	Specific gravity (g/cc)

LIST OF FIGURES

Figure 1. Woven Fiber-to-Fabric Process.....	12
Figure 2. Nonwoven Fiber-to-Fabric Process.....	17
Figure 3. Sample 37 Non-Impact.....	41
Figure 4. Sample 37 Impact.....	42
Figure 5. Sample 40 Non-Impact.....	43
Figure 6. Sample 40 Impact.....	43
Figure 7. Spectra® 6.3 Non-Impact DSC.....	45
Figure 8. Spectra®6.3 Impact DSC.....	45
Figure 9. Spectra® 2.2 Non-Impact DSC.....	46
Figure 10. Spectra® 2.2 Impact DSC.....	47
Figure 11. Spectra®2.2 Impact DSC (sample 32).....	48
Figure 12. Spectra® 2.2 Non-Impact DSC (sample 32).....	48
Figure 13. Spectra® 3.6 Non-Impact DSC.....	49
Figure 14. Spectra® 3.6 Impact DSC (Sample 33).....	50
Figure 15. Spectra® 3.6 Impact DSC (Sample 34).....	50
Figure 16. Spectra® 3.6 Impact DSC (Sample 13).....	51
Figure 17. Spectra® 3.6 Impact DSC (Sample 37).....	52
Figure 18. Dyneema® Non-Impact DSC.....	53
Figure 19. Dyneema® Impact DSC (Sample 27).....	54
Figure 20. Dyneema® Impact DSC (Sample 29).....	54

Figure 21. Dyneema® Impact DSC (Sample 30)	55
Figure 22. Needlepunched Twaron® (L) (154x) and Impact Twaron® (R) (154x).....	56
Figure 23. Needlepunched KM2® (L) (139x) and Impact KM2® (R) (167x).....	57
Figure 24. Needlepunched K129® (L) (167x) and Impact K129® (R) (139x).....	57
Figure 25. Needlepunched (L) (294x) and Impact (R) (294x) Spectra® 2.2.....	58
Figure 26. Needlepunched (L) (227x) and Impact (R) Spectra® 3.6	58
Figure 27. Needlepunched (L) (172x) and Impact (R) (172x) Spectra® 6.3.....	59
Figure 28. Needlepunched (L) (286x) and Impact (R) (214x) Dyneema®	59
Figure 29. Needle Punched (L) (173x) and Impact (R) (173x) Vectran®.....	60
Figure 30. Polarized Dyneema® (250x).....	60
Figure 31. Polarized Spectra® 3.6(273x)	61
Figure 32. Polarized Vectran® (173x/328x).....	62
Figure 33. Ballistic Testing Set-Up (Bhatnagar, pg 139, 2006)	74
Figure 34. Ballistic Testing Shot Pattern (Bhatnagar, pg 243, 2006).....	74
Figure 35. V ₅₀ Limit for RCC FSP	75
Figure 36. Para-Aramid Structure (Bhatnagar, pg 249, 2006).....	76
Figure 37. Liquid Crystal Polymer (Bhatnagar, pg 192, 2006)	77
Figure 38. Comparison of Tensile Properties (Bhatnagar, pg 338, 2006)	77
Figure 39. Deformations (Bhatnagar, 2006).....	78
Figure 40. Spectra ® 3.6(205x)	79
Figure 41. Spectra ®3.6.....	80
Figure 42. Spectra® 3.6 (205x)	80
Figure 43. Spectra® 2.2 (294x)	81
Figure 44. Spectra® 2.2 (294x)	81
Figure 45. Spectra® 6.3 (172x)	82

Figure 46. Twaron® (154x).....	82
Figure 47. Dyneema® (214x).....	83
Figure 48. KM2® (111x).....	83
Figure 49. KM2® (111x).....	84
Figure 50. KM2® (167x).....	84
Figure 51. K129® (139x)	85
Figure 52. K129® (139x)	85
Figure 53. Vectran® (173x).....	86
Figure 54. Vectran® (173x).....	86
Figure 55. Spectra® 3.6 (227x)	87
Figure 56. Spectra® 2.2 (294x)	88
Figure 57. Spectra® 2.2 (294x)	88
Figure 58. Spectra® 6.3 (172x)	89
Figure 59. Spectra®3.6 (363x)	89
Figure 60. Dyneema® (286x).....	90
Figure 61. Twaron® (154x).....	90
Figure 62. KM2® (139x).....	91
Figure 63. K129® (167x)	91
Figure 64. Sample 13 (Spectra®3.6/KM2®).....	92
Figure 65. Sample 25 (Dyneema®/KM2®)	93
Figure 66. Sample 26 (Dyneema®/KM2®/Vectran®).....	94
Figure 67. Sample 27(Twaron®/Dyneema®)	95
Figure 68. Sample 28 (Twaron®/Dyneema®)	96
Figure 69. Sample 29(Vectran®/Dyneema®/Twaron®).....	97
Figure 70. Sample 30 (Vectran®/Dyneema®/Twaron®).....	98

Figure 71. Sample 31(Twaron®/Spectra® 2.2).....	99
Figure 72. Sample 32 (Twaron®/Spectra® 2.2/Vectran®).....	100
Figure 73. Sample 33 (Spectra ®3.6/Twaron®).....	101
Figure 74. Sample 34 (Spectra ®3.6/KM2®).....	102
Figure 75. Sample 38 (8 oz. K129®/Dyneema®)	103
Figure 76. Sample 37 (8.5 oz. K129®/Spectra® 3.6).....	104
Figure 77. Sample 39 (5.8 oz K129®/Dyneema®)	105
Figure 78. Sample 40 (8 oz. K129®/Dyneema®)	106
Figure 79. Sample 13: Spectra® 3.6 Impact.....	107
Figure 80. Sample 25: Dyneema® Impact	108
Figure 81. Sample 26: Dyneema® Impact	108
Figure 82. Sample 27: Dyneema® Impact	109
Figure 83. Sample 28: Dyneema® Impact	109
Figure 84. Sample 29: Dyneema® Impact	110
Figure 85. Sample 30: Dyneema® Impact	110
Figure 86. Sample 31: Spectra® 2.2 Impact.....	111
Figure 87. Sample 31: Spectra® 2.2 Non-Impact.....	111
Figure 88. Sample 32: Spectra® 2.2 Impact.....	112
Figure 89. Sample 32: Spectra ®2.2 Non-Impact.....	112
Figure 90. Sample 33: Spectra® 3.6 Impact.....	113
Figure 91. Sample 34: Spectra ®3.6 Impact.....	113
Figure 92. Sample 34: Spectra® 3.6 Non-Impact.....	114
Figure 93. Sample 35: PET Impact.....	114
Figure 94. Sample 35: PET Non-Impact.....	115
Figure 95. Sample 37: Spectra® 3.6 Impact.....	115

Figure 96. Sample 38: Spectra® 6.3 Impact.....	116
Figure 97. Sample 38: Spectra® 6.3 Non-Impact.....	116
Figure 98. Sample 39: Dyneema® Impact	117
Figure 99. Sample 40: Dyneema® Impact	117
Figure 100. Sample 40: Dyneema® Non-Impact	118

LIST OF TABLES

Table 1. Fiber Descriptions.....	32
Table 2. NES Sample Composition	33
Table 3. DSC Data	40
Table 4. V_{50} Test Results	63
Table 5. KE Calculation Data	66
Table 6. Fiber Combinations used in Research	76

CHAPTER ONE: INTRODUCTION

The purpose of this study is to provide an empirical analysis of energy dissipation as a physical phenomenon in fiber structures. This physical phenomenon is used to explain the circumstances under which a multi-fiber nonwoven material in combination with woven layers is able to more efficiently stop a projectile than the current woven ballistic standard or a single fiber nonwoven material. The suspected reason for this superiority is the presence of a phase change during impact which contributes to the energy dissipation of the material.

A literature review of this area yields multiple studies focusing on the reactions of fibers, yarns, and projectiles to the ballistic environment. The fiber reactions have been studied as both cut energy and breakage, while most yarn reactions are studied as pull-out phenomena. Projectile reaction studies focus on loss of mass and deformation as they are affected by impact with soft body armor.

The methods used to investigate the presence of a thermal phase change in the multi-fiber nonwoven sample are *Differential Scanning Calorimetry* (DSC), observation and recording of photographic evidence with Optical Microscopy, standardized ballistic resistance testing, and a mathematical formula of the structure's residual kinetic energy. The DSC data was gathered using a heat flux TA Instruments 2920 Modulated DSC, and the photographic images were gathered using an Olympus BH-12® with an Olympus DP10® camera and FlashPath® software. Both pieces of equipment were provided by

and used in the Auburn University Polymer and Fiber Engineering laboratories. The ballistic resistance data were gathered based on military specifications from H. P. White Laboratories, an independent source approved by the Department of Defense and the National Institute of Justice.

The DSC testing was performed on impact and non-impact samples from each fiber variety used in the *Nonwoven Enhanced Structures* (NES) structures. The DSC plots did not provide conclusive evidence of a phase change but discrepancies between the impact and non-impact samples were consistently found. Further testing and investigation would be required in order for these discrepancies to be adequately interpreted.

The microscope images showed that the needlepunching process did not significantly damage the NES and that the fibers experienced the same impact reactions in the blended NES that they do in their woven counterparts. The use of polarized light microscopy showed that melting did occur in the *Ultra High Molecular Weight Polyethylene* (UHMWPE) and Vectran® samples. This melting is evidence of a phase change; however, the testing was not performed to determine the significance that this phase change has on the NES energy dissipative abilities.

Ballistic V_{50} testing results show that most of the NES samples pass NIJ and military standards and that the best performance combination is a 50/50 blend of K129® and any UHMWPE. It was also observed that Vectran® decreased the V_{50} limits when combined with aramids and UHMWPE and was not a beneficial addition to the blend for the purposes of this research.

The determination of residual kinetic energy provided approximations on the various NES samples' ballistic performance. Based on these approximations the highest

residual energy, and therefore poorest performance, occurred in a 50/50 Twaron®/Dyneema® blend. The lowest residual energy, and therefore best performance, occurred in a 50/50 Spectra® 2.2/Twaron® blend.

The main conclusions drawn from this research are that NES are superior to traditional woven armor on a mass basis and that there is evidence of a phase change in the NES. What cannot be concluded from this research is the magnitude and significance of the energy dissipated by the phase change and if this dissipation is an explanation for the superior performance.

CHAPTER TWO: LITERATURE REVIEW

Over the entire span of recorded history, textiles have played a major role in protecting humans from many different hazards, such as animals, insects, and climate. During the evolution of these "protective" textiles, there have also been many attempts to use them for protecting humans from other humans. Since the work of Carothers at DuPont in the early 1930s, protective textiles have seen a rebirth in the area of soft armor in both military and civilian applications (Laible, 1980). This field has changed dynamically with the invention of new high strength fibers. It is toward the optimization of these fibers, through fabric forming and blending, that the present research is directed.

The purpose of this chapter is to highlight key innovations in the area of soft body armor pertaining to this thesis. The chapter describes the fibers, yarns, and fabrics used in this research, and explores their past uses in other armor applications. Mechanisms of fiber, yarn, and fabric failure are discussed along with the effect of impact upon them and the projectile.

2.1 Standards

An agreed upon standard of ballistic armor performance is essential to the acceptance of body armor as a trusted means of protection. Standards have been established by various organizations and countries but the benchmark standards are those established by the United States. The most common, and most relevant to this research

are the military standard MIL-STD-662F and standard 0101.04 from the *National Institute of Justice* (NIJ).

2.1.1 Military Standard

The military standard MIL-STD-662F establishes the V_{50} of a ballistic material as a determinate of its ballistic limit. The V_{50} is calculated by taking the average velocity of an equal number of partial and complete penetrations within a predetermined velocity range. This standard also specifies the equipment, conditions, and procedure for conducting V_{50} tests on a material (Bhatnagar, pp128-9, 2006). The standard developed for the testing of NES is found in Appendix A, Figure 35.

2.1.2 NIJ Standard

The National Institute of Justice is the governmental body responsible for the approval of soft body armor. The NIJ stated purpose is to “Advance scientific research, development, and evaluation to enhance the administration of justice and public safety (NIJ, 2006).” In order to evaluate the public safety of soft body armor, the NIJ has established parameters to approve armor at levels in accordance with their impact resistance to various projectiles. The most widely used NIJ standard is number 0101.04, was first issued in the year 2000. In this standard, the test methods and requirements are established for body armor protection against rifles and handguns. This standard categorizes munitions threats into levels I, IIA, II, IIIA, III, IV, and specifies the minimum V_{50} values required to protect against each layer (Bhatnagar, pp128-136,2006). The testing set up, and the shot patterns are found in Appendix A, Figure 33 and Figure 34.

2.2 Textile Structures

An understanding of fiber, yarn, and fabric structures is necessary in order to evaluate the properties of various soft body armor materials. The NES tested for this research shared similar constructions but are composed of varying fiber combinations. The basic construction from face to back consists of two needlepunched nonwoven layers, followed by a minimum of thirty woven layers, and ending with two additional needlepunched nonwoven layers. The nonwoven layers are even blends in varying combinations of aramid, UHMWPE and *Liquid Crystal Polymer* (LCP) fibers. Although most ballistic materials are not blended, a fiber hybrid effect has been shown to benefit impact response in fabrics. The different fiber strengths can be utilized together to defeat a projectile in multiple ways. One method is to utilize the high frictional properties of aramid fibers in order to strip the metal jacket from a projectile, and then the non-linear visco-elastic polyethylene properties in order to defeat the deformed soft metal fragments (Bhatnagar, pp. 69, 2006).

2.2.1 Fiber

A polymer can be simply defined as a high molecular weight group of smaller molecular weight monomers joined together through polymerization (Brown, 2000). The materials used in soft body armor are synthetic polymers with properties, such as high tensile strength and low fiber elongation, which make them able to withstand certain ballistic impact conditions. The fiber properties originate from the polymer morphology, chain linearity, and from the orientation achieved in spinning. The controlled property of fiber denier (g/9,000m) has also proven to determine fiber ballistic performance. Although higher denier fibers lead to faster and simpler production, they tend to

experience a "bundle effect" in which fibers do not spread evenly. This ultimately causes uneven engagement of the ballistic impact. Lower denier fibers are known to excel over high denier fibers in ballistic resistance and have lower weights (Bhatnagar, pp. 2-3, 68, 2006). The synthetic polymers relevant to this study are aramid, UHMWPE and LCP fibers. A chart of the tensile properties of various anti-ballistic yarns can be seen in Appendix B, Figure 38.

2.2.1.1 Aramid

Aramid fibers are defined by the *Federal Trade Commission* (FTC) as “a manufactured fiber in which the fiber forming material is a long chain synthetic polyamide having at least 85% of its amide linkages attached directly to two aromatic rings (Man Made Fiber and Textile Dictionary, 1978).” Aramid fibers used in ballistic protection are known chemically as poly (p-phenylene terephthalamide) and more commonly by the trade names, Kevlar® (DuPont) and Twaron® (Akzo). The molecular structure of para-aramid can be found in Appendix B, Figure 36.

The non-thermoplastic aramid polymer has an approximate density of 1.48 gm/cm³ and a tensile modulus ranging from 6,000-160,000 MPa (poly (p-phenylene terephthalamide), 2006). The polymers high strength to weight ratio stems from the aromatic ring structure which encourages crystallization. This is the reason for para-aramids impressive ability to deter projectile penetration (Billmeyer, pp. 410-11, 1984). Para-aramid fibers are also well suited for ballistic applications because of their thermal properties. Kevlar® and Twaron® fibers reach their glass transition temperature between 307-347°C, and begin melting at approximately 497°C. The polymers upper use temperature is approximately 250°C, with decomposition beginning at 460°C, although

temporary use at 300°C has been recorded. These high thermal values allow the polymer to endure substantial impact temperatures without melting or decay, reinforcing their ability to be used for anti-ballistic purposes. Para-aramids also possess other fiber properties less directly related to their ballistic abilities; these properties include good biological stability, high electrical resistance, low flammability, and chemical stability to formaldehyde, gasoline, fluorocarbons, and phosphoric acids (poly (p-phenylene terephthalamide), 2006).

It has been established that para-aramid fibers respond to projectile impact through axial splitting or fibrillation (Hearle, pp. 390, 1989). This fibrillation has been shown to result from both transmitted stress wave failure, and in shear failure modes (Carr, 1999). Axial splitting occurs in aramid fibers due to a lack of fiber uniformity and pure tension. Stresses on the fiber, like those associated with impact, travel parallel to the fiber axis and therefore produce fibrillation. These stresses are able to increase shear stress at fiber defects to a point where an axial split is formed. While a small shear force will break only the intermolecular forces between bonds, a high tensile stress will break the covalent bonds within the polymer chain (Hearle, pp. 54-56, 1989).

2.2.1.2 Polyethylene

Polyethylene (PE) is an olefin fiber which is defined as an ethylene-based semi-crystalline polymer which is capable of being branched or linear. PE's versatile structure allows for many varieties of the polymer with divergent characteristics. A PE fiber variety useful in anti-ballistic applications is *Ultra High Molecular Weight Polyethylene* (UHMWPE), also known by the trade names Spectra® (Honeywell) or Dyneema® (DSM). This fiber is gel spun to optimize crystallinity and orientation and to produce a

fiber strong enough to withstand ballistic impact. The density of UHMWPE is approximately 0.93 g/cm^3 , with a tensile modulus ranging from 650-150,000 MPa depending on the degree of orientation and spinning methods (“UHMWPE”, 2006). These properties allow Spectra® and Dyneema® to have high strength-to-weight ratios which, as with para-aramids, allows a high level of ballistic protection for a relatively low weight of material. While the strength-to-weight ratio resembles that of aramid fibers, the thermal properties of UHMWPE are very different. Spectra® and Dyneema® fibers melt at approximately 125-145°C, depending on the degree of crystallinity and the heat history of the particular sample (“UHMWPE”, 2006). UHMWPE exhibits excellent impact toughness, even under extremely cold temperatures, and has the highest abrasion resistance of all thermoplastics. This polymer also exhibits better chemical stability than other polyethylene fibers (“UHMWPE”, 2006).

It is clear that the high tensile strengths and low densities make UHMWPE fibers well suited for use in soft body armor. Prevorsek et al. (1988) attribute Spectra®’s ability to dissipate energy to the fibers tensile strain wave velocities. The velocities are approximated to be 12,300 m/s, making them the highest known for any fiber (Prevorsek, 1988). In a previously mentioned study, Carr (1999) explored the effects of UHMWPE’s relatively low melting temperatures as they affect the fiber's impact response. The results of the study showed that UHMWPE fibers absorb energy under impact by both fiber melting and fiber shearing (Carr, 1999).

2.2.1.3 Liquid Crystal Polymer

In the early 1970s, research into liquid crystals led to the development of thermotropic polymers. These polymers are able to produce high strength and high

modulus fibers when subjected to a lengthy heat treatment just below their melting temperatures (Plate, pp 399-401. 1993). Vectran® is the only melt spun Liquid Crystal Polymer (LCP) on the market and is most often spun into high strength multi-filament yarns. The density of Vectran® is approximately 1.4 g/cm³ with an elongation at break around 3.5%. The high strength characteristics are shown in the fiber's optimum tensile strength ranging from 2840-3210 MPa. The fibers tensile modulus ranges from 64.8-72.4 GPa. Vectran® exhibits relatively high thermal properties with a melting point of 330°C. These LCP are able to maintain their properties under both hot and cold temperatures, and have a low thermal expansion coefficient. In addition to the density, strength, and thermal properties, Vectran® fibers are also resistant to creep, abrasion, moisture absorption, and chemical degradation. The moderate density, high strength, and high thermal properties combine to make a fiber which has excellent impact resistance and is well suited for anti-ballistic applications (“Vectran® LCP Fiber”, 2006). An image of LCP molecular structure can be viewed in Appendix B, Figure 37.

2.2.2 Yarn

Staple yarns are most common in natural fiber sources and are defined as fibers that are short in length (1-10cm) and require twist in order to bind the fibers together and form a yarn structure of useful strength. The twist adds strength to the yarn by increasing the amount of fiber to fiber friction within the structure (Laible, 1980).

Filament yarns are made with a slight twisting (1 turn/cm) of filament fibers. These yarns have tensile strengths that are equivalent to the tensile strengths of each individual fiber (Laible, 1980). The only naturally occurring filament yarn is silk and

therefore the majority of filament yarns are made from synthetic fibers (Bhatnagar, pp. 252, 2006).

The majority of yarns used to weave bullet resistant fabrics are made from filament fibers. Filament yarns are preferable to staple yarns because they outperform them in ballistic resistance testing (Laible, 1980). Yarns made from filament fibers are more suitable for body armor than those made from staple fibers because the filament fibers have higher strength values than the staple fibers (Hearle, 1989). Filament yarns are able to absorb impact along the entire length of the yarn whereas a staple yarn is held together with friction and has unavoidable weak places which interrupt absorption (Bhatnagar, pp. 254, 2006).

2.2.3 Fabrics

2.2.3.1 Woven

Woven fabrics can be either two or three dimensional, with two dimensional being plain, basket, twill, or satin weaves, and three dimensional being similar in structure to a braided fabric (Bhatnagar, pp. 212-15, 2006). Two dimensional fabrics are made by interlacing yarns at 90° angles to each other in order to form a thin structure with a large surface area (Adanur, 2001). Three dimensional fabrics are created by interlacing with the introduction of a third fabric plane. Composites of 3-D fabrics show good impact resistance but are not able to absorb kinetic energy as well as the lightweight 2-D woven structures (Bhatnagar, pp. 214-15, 2006). A simplified flow chart of the fiber to woven fabric process is shown in Figure 1.

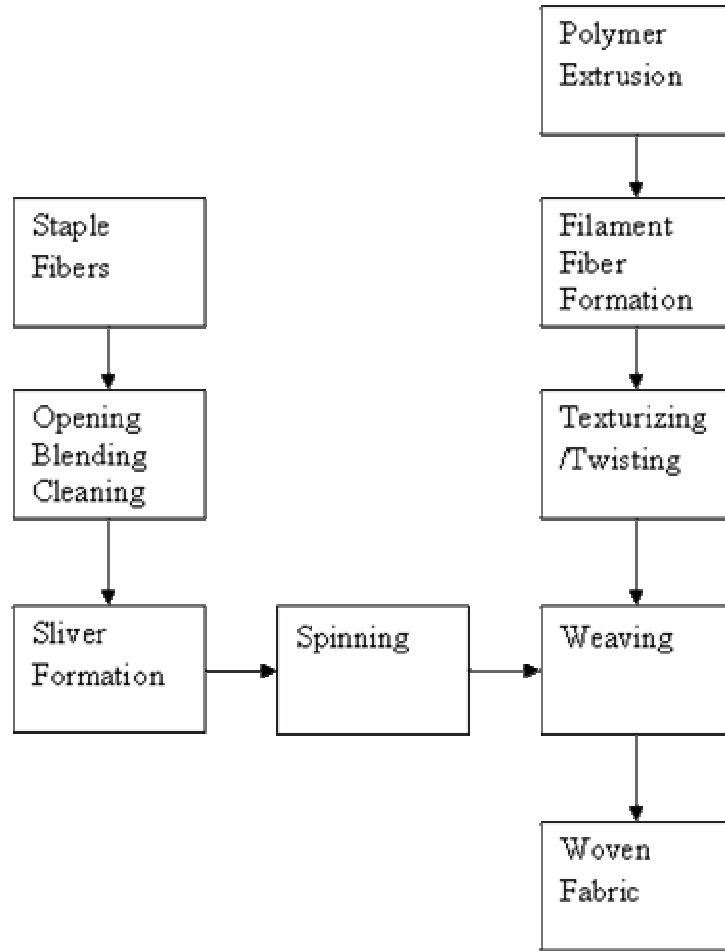


Figure 1. Woven Fiber-to-Fabric Process

Although the use of fabrics and textiles in protective armor has been documented throughout history, the relevant use of synthetic fibers to replace metals began with military flak jackets in the 1940's. Early flak jackets were 32 layers of five ply, 207 denier (23 tex), 34 filament nylon yarns in a 2x2 basket weave. The use of this vest spawned new research and testing of fibers for anti-ballistic applications, and lead to the development of soft body armor as a substantial field of military research (Laible, 1980). The flak jacket replacement vest is known as the Interceptor®, and weighs 7.5 kg (16.4 lbs), considerably less than the PASGT flak jackets weight of 11.4 kg (25.1 lbs). The

Interceptor® is composed of two sections: an *outer tactical vest* (OTV) and *small arms protective inserts* (SAPI). The OTV is composed of densely woven KM2® and weights 3.8 kg (8.4 lbs). The SAPI are protective panels that can be inserted into the jacket in the front and back in an attempt to further protect vital organs (Interceptor Body Armor, 2006). The Interceptor® armor is designed to provide protection from fragments, multi-hit handguns, and full metal jacket projectiles (Bhatnagar, pp366, 2006).

All soft body armor defeats projectiles through the method of strain wave propagation and by the penetration strength of the material (Hearle, 1974). Strain wave velocity is described as:

$$v = \sqrt{F / \mu} \quad (1)$$

where:

v = strain wave velocity

F= force applied to fiber

μ = linear density (kg/m)

This equation can also be described as:

$$v = \sqrt{E / \rho} \quad (2)$$

where:

E= Young's modulus of material

ρ=material specific gravity

These two equations can be combined to determine the impact energy dissipation optimum of the material (Bhatnagar, pp. 263, 2006).

$$F = \sqrt{\frac{E\mu}{\rho}} \quad (3)$$

Fabric strength is primarily determined by the intrinsic strength of its fibers and yarns, but is also affected by its weave design (Adanur, 2001). Tensile strength is the amount of force a linear structure can resist before breaking and multiple tests have been established to determine this property in textile materials. Some commonly used ASTM tests for tensile strength are: D5035, D4595, and D4848. Under normal uni-axial load, a woven fabric experiences a series of events beginning with the crimp exchange. When the yarns have been stretched out, they begin to engage the load. Next, the warp and filling yarns begin to deform from exchanged forces (Adanur, 2001). When the yarns reach their tensile limits, they begin to break apart causing fabric failure. While the above tests give insight into potential ballistic performance, specific tests have been designed to imitate forces perpendicular to the fabric face. The ASTM standardized tests for the burst resistance of fabrics are the Mullen Burst Test ASTM D3786 and the Ball Burst Test ASTM D3787 (Adanur, 2001).

An analysis of a woven fabric's response to impact was performed by Phillip Cunniff (1992) at the U.S. Army Natick research center. In this study, the steps of ballistic impact are traced based on photographic evidence, and show how single and multi ply woven structures are able to defeat high speed projectiles. Upon impact, the fabric forms a conical shaped, transverse deformation with the bullet forming the apex of the cone. Simultaneous with the transverse wave formation is the development of longitudinal (strain) waves at the point of impact. The strain waves spread from the impact point out into the yarns at the speed of sound. When the longitudinal waves are propagating along the yarns, they are also forcing the material to flow back toward the impact point where they feed the energy of the forming tent. Crossovers, or orthogonal

yarns, are involved in the system when the strain wave transfers energy to them. This energy is then sent along their yarn axis, furthering energy dissipation away from the impact site (Cunniff, 1992).

The most prevalent soft body armor is made of filament yarns in a plain weave construction. The reason for this structure's dominance lies in the woven fabrics ability to dissipate energy along each yarn axis and through each yarn crossover point. Since balanced weave fabrics contain the highest number of crossover points, they have made up the majority of soft body armor (Adanur, 1995). A balanced weave is ideal because it provides the maximum engagement of both warp and weft yarns in the energy absorption. This density allows the fabric to most efficiently spread the impact energy over a greater area of the armor structure (Adanur, 2001).

In a recent study, Kirkwood, et al. (October 2004) stated that a fabric's ability to defeat a projectile depends on: yarn uncrimping, stretching, breaking, and pull-out. Although many of these properties depend on the strength of the materials used, Kirkwood suggests that increased yarn contact points provide increased yarn to yarn friction and therefore more uncrimping and higher ballistic performance (Kirkwood, October 2004). This study reinforces the concept that in order to achieve optimum fabric impact resistance the number of yarn crossover points must be maximized. In the study by Cunniff, the role of transverse and longitudinal wave propagation was considered in reference to an unbalanced weave design. Based on his own investigation and that of Prosser (Part 1, 1985), Cunniff concludes that lower values of yarn to yarn friction in an unbalanced weave results in more yarn slippage upon impact. When slippage occurs the

projectile has contact with fewer yarns allowing less material to propagate the longitudinal and transverse forces away from the point of impact (Cunniff, 1992).

Freeston, et al. (1973) investigates the role of a fixed end (representative of a crossover point) in a strain wave's propagation from the point of impact. It is understood that a strain wave traveling along a yarn will be interrupted by the crossover and some of the wave's energy will be reflected while some will continue to spread. Freeston attempts to develop a model for determining the amount of energy reflected by the crossover points. From this model, he determines that yarn interlacing disrupts the strain wave minimally (Freeston, 1973). This study shows that a majority of the energy from the ballistic impact is absorbed via strain wave propagation along the yarn axis. Very little energy is absorbed by the crossover points. This indicates that the density of warp and weft yarns do more to spread out the energy over a higher number of yarns and that this, not the increased number of crossover points, is responsible for the higher impact performance of balanced weave fabrics. In either case, it is well established that balanced weaves have better anti-ballistic properties than other weave designs.

2.2.3.2 Nonwoven

Nonwoven fabrics are fibrous assemblies fixed together by entanglement, bonding, or heat fusion (Man Made Fiber and Textile Dictionary, 1978). Nonwoven fabrics are unlike conventional woven fabrics because the fibers are not oriented into a yarn before being made into a fabric. One main branch of nonwovens, needlepunched nonwovens, are made from staple fibers which are oriented and formed into a mat structure which is then bound together by needlepunching (Bhatnagar, pp. 256-262, 2006). A flow chart of the process is given in Figure 2.

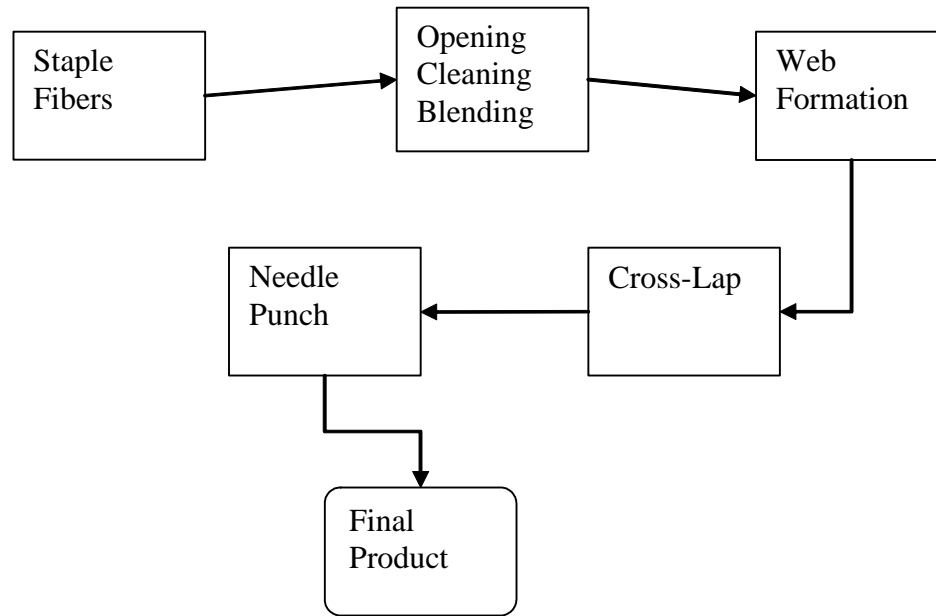


Figure 2. Nonwoven Fiber-to-Fabric Process

Military studies were first to introduce needlepunched nonwovens to soft body armor applications. These felts tend to have high strength-to-weight ratios along with good drape making them ideal for soft body armor applications. While most of the early studies were limited to nylon and polypropylene fibers they did help to establish the potential of felt body armor.

In his book, “Ballistic Materials and Penetration Mechanics,” R.C. Laible (1980) describes some early army tests and explores the mechanisms that make felt armor an anti-ballistic option. Laible states that the primary means of projectile deflection in felts is the presence of intra-fiber friction. Laible (1980) divides the properties of ballistic resistance of felts into two categories: fiber and fabrication.

In the fiber category, Laible describes the importance of molecular type and weight, along with tenacity, elongation, and the fiber surface. At the time of Laible’s study polyamides had superior ballistic resistance to polypropylenes, and nonwoven

aramids had not yet been studied in detail. Molecular weight affects a materials ballistic performance because higher weight yields better mechanical properties and better ballistic resistance. Tenacity is the value of a fiber's strength to a fiber's linear density. A material with higher tenacity typically exhibits increased ballistic resistance.

In the fabrication category, Laible addresses the role of needling type, needling angle, felt thickness and ply angle but emphasizes fiber length and felt density. Fiber length is a determinant of armor quality because longer fibers have typically proven to produce a more ballistic resistant felt structure. Based on his own research, Laible determines that multi-layered lightly needled nylon felts have superior V_{50} values to a heavily needled nylon felt (Laible, 1980).

A felt fabric's impact response is very different than that of a woven fabric. Woven fabrics absorb impact by uncrimping, elongation, and eventual breakage. Felt response to impact was studied by Wittrock and Ipson (1966) using photographic data. This study concluded that felt fabrics are able to counteract only small forces from a projectile but can do this over such a large area that they are useful in armor applications. The study concluded that felts were useful only at or below the materials ballistic limit.

In another military report, Hearle and Purdy (1971) investigate the ballistic penetration of felt materials by taking high speed photographic images of layered felts. In order to determine how the layers interacted with each other, each layer was dyed a different color. The resulting impact revealed the various colored fibers around the impact point. The purpose of this study was to identify which layers were involved in the impact and how the projectile carried the layers through the material while being stopped.

Hearle and Purdy observed that, rather than pushing through the multiple layers of felt individually, the projectile compressed all the layers together as it pushes into the material. Based on these results, the authors concluded that multiple layers of needlepunched felt are more effective than one ultra thick layer.

The study also introduced the concept of an optimum needling density. Their tests show that high needling density leads to restricted fiber movement, which, in turn, increase the force of resistance. This remains a positive relationship until the needling density becomes so high that the fabric does not deform therefore robbing the material of a primary energy dissipation mechanism. Conversely, if needling density is too low the fiber friction is not adequate to prevent slippage thus decreasing the ballistic resistance of the felt (Hearle, 1971).

In Laible's experiments on nylon needlepunched felts, it was found that felts are able to stop a projectile by spreading the energy out over a large impact area rather than by a high degree of fabric displacement. These felts were able to dissipate more energy over a long period of time while the woven samples were able to dissipate energy quickly over a short period of time. For this reason, Laible concludes, that nylon felts are more effective in stopping low-velocity projectiles, while wovens are more effective in high-velocity applications (Laible, 1980).

There are three major disadvantages when using nylon felts in soft body armor. As discussed in the preceding paragraph, at high velocities, the short impact time hinders nylon felt's ability to dissipate a projectile's kinetic energy. Another disadvantage of any felt is that the fabric can absorb up to seven times its weight in water, even if composed of hydrophobic fibers. Felts must therefore be protected with water resistant coverings if

they are to be trusted for ballistic resistance. A third disadvantage is that, in the past, ballistic felts have required high bulk in order to meet body armor specifications. This causes limited mobility and increased discomfort to the wearer of nylon needlepunched felt armor (Laible, 1980).

2.3 Textile Failure Mechanisms

In past research, three primary methods have been used to determine energy dissipation in soft body armor: yarn pull-out, fiber shearing, and projectile deformation. Each of these methods defeats the projectile through the absorption, and dissipation of *kinetic energy* (KE). In yarn pull-out and fiber shearing, tensile straining and breakage of fibers are major sources of KE absorption by a soft body armor structure. Projectile deformation allows the structure to more easily dissipate the KE throughout the armor by increasing the surface area of the projectile and causing more fiber-projectile interaction (Bhatnagar, pp. 221, 53-70, 2006).

2.3.1 Yarn Pull-Out

Yarn pull-out is a method of energy absorption in woven ballistic structures. A pull-out test is performed by applying a force to a single fiber in a woven structure and measuring the load force versus the displacement as the fiber is pulled out from the fabric. Kirkwood et al. (2004) define yarn pull-out as a two part process based on a force-displacement curve. The first part involves the initial stretching of the yarn up to its peak load point and is referred to as “yarn uncrimping.” The second part involves the effects of the yarn after the peak load has been reached and is referred to as “yarn translation.” The total area under the force-displacement curve created by these two

processes represents the total amount of energy necessary for yarn pull-out (Kirkwood, 2004).

Martinez, et al. (1993) performed friction and yarn pull-out tests on Kevlar Ht®, Kevlar 29®, and Kevlar 49® woven fabrics. The friction testing involved an estimation of the static mutual friction based on ASTM D4917 (15.09) and dynamic wear tests utilizing a TE-77 hi-frequency Cameron-Plint® friction tester. The yarn pull-out test was performed using a weighted string attached to single yarns in each of the three fabrics. The overall results from the yarn pull-out test showed the Kevlar 29® to be the most ballistic resistant fabric. This high performance was due to the increased number of yarns per unit length in this fabric. The conclusion from this study is that more energy is required for yarn pull-out when there are a large number of yarns per unit length (Martinez, 1993).

In 1997, Bazhenov (1997) published the results for the testing he completed on five, 10mm x 10mm woven aramid structures, of either 900 or 530 denier, with varying yarn densities. The pull-out method involved fixing the fabric at one end with a C-shaped clamp and applying force to one yarn from within the unbound center of the clamp until complete pull-out occurred. The results lead Bazhenov to conclude that there is a proportional relationship between sample length and the amount of energy transfer in the fibers. He also observed that increases in fabric density resulted in higher forces of friction. This coincides with the results of Martinez et al. (1993) in the previous paragraph.

In a another study, Shockey, et al. (2001) used impact testing to compare the response of high performance fibers to *fragment simulating particles* (FSP) in order to

develop a method for minimizing the damage caused by civilian airplane engine bursts. They tested samples of woven Zylon® (PBO), Kevlar® (aramid), and Spectra® (PE) with stitch densities ranging from 12 x 12 yarns/cm to 18 x 18 yarns/cm (30 x 30 yarns/in to 45 x 45 yarns/in). The fabric's areal densities ranged from 0.013g/cm³ to 0.166g/cm³. Three different fragment simulating particles were used: a large blunt edge FSP, a small blunt edge FSP, and a sharp edge FSP. Each had masses less than 1.94grams. The quasi-static penetration testing was performed at both private and military test sites, with both producing similar results. Apart from the initial superiority of PBO, the most notable result from this study was that, in yarn pull out testing, fabrics with two clamped edges absorbed 25-60% more energy than fabrics with all four edges clamped.

Kirkwood et al. (2004) performed pull-out testing on 600 denier Kevlar® KM2 yarns in plain weave structures containing 13.386 yarns per centimeter. The test method used an Instron 4206® universal testing machine. The fabric was clamped from the top and bottom edges. Pull-out testing was done on various lengths of the KM2® fabric targeting single warp yarns, multiple warp yarns, and adjacent warp yarns. The single yarn tests showed that the peak load is proportional to sample length while sample width had no effect on the pull-out energy. The test also showed that fabric tension and yarn pull-out energy were proportional. The multiple yarn pull-out tests revealed that “initial pull-out energy increased as a power law of the number of yarns” (Kirkwood, 2004). Multiple pull-out testing also showed that pull-out energy is higher when pulling multiple adjacent yarns rather than multiple isolated yarns. Kirkwood et al. (2004) determined that, in the case of these particular yarns, the pull out energy is affected by the fabric length, transverse tension, quantity of yarns being pulled simultaneously, the pattern of

the pull and the distance pulled. Kirkwood et al. (2004) also developed a semi-empirical model to find the correlation between the energy required to pull out a yarn and the pull-out distance (Kirkwood, 2004).

2.3.2 Fiber Cut Energy

When a projectile impacts a bullet resistance material, fibers are often cut or sheared. The energy that dissipates into the fabric structure is referred to as fiber cut energy. This is a heavily studied area of soft body armor.

In one study, Hearle et al. (1974) try to gain a basic understanding of fiber impact by examining the energy absorption of various fabrics in a controlled environment. The study involved *scanning electron microscopy* (SEM) of the fractured fibers in an attempt to better understand the way individual fibers dissipate energy. The study used a Webley Mark 3® air rifle which fired 0.88 gram, 0.22 caliber waisted lead pellet projectiles, at 346 meters per second. Velocity was measured using two methods; photographic and photo-cell. A variety of materials were tested: Polyethylene film, woven steel fabric, spun bonded nonwoven polyester filaments, bonded nonwoven polyester fibers, spun bonded nonwoven polypropylene filaments, bonded nonwoven nylon, woven cotton, needlepunched nylon, warp knitted nylon, and woven Kevlar®. The actual impact testing varied by changing target weight while maintaining constant velocity and by changing impact velocity. The materials were also subjected to a slow speed penetration test, tensile testing, and dynamic modulus testing. Test results showed that fiber fracture is a means of energy dissipation in the cotton, warp knit nylon, steel, and woven nylon fabrics. Plastic deformation absorbs energy in polypropylene fabrics and fibrillation absorbs energy in Kevlar® fabrics (Hearle, 1974).

In another study, Carr (1999) compares para-aramid and UHMWPE fibers and their responses to ballistic impact. The testing utilized a 0.69 gram steel sphere inside a 7.62mm NATO capped cartridge. The cartridge was fired from a pressure housing towards a 0.57 meter single yarn of each material and was observed by a Hadland Imacon 468® high speed imaging system. The testing velocity ranged from 346-720 meters per second and fifty test were run on five varieties of Kevlar® and Dyneema®. Carr states that yarn failure in all fibers was attributed to either the transmitted stress wave or the yarn shear failure. He defined the critical impact energy for each material based on the failure by either of the aforementioned means. The para-aramid material critical impact energy was 130 Joules and the UHMWPE critical impact energy was 160 Joules. Carr also noted that para-aramid yarns failed as a result of fibrillation in both transmitted stress wave failure and shear failure, but with the greater fibrillation occurring in the transmitted stress wave scenario. For Dyneema® yarn, failure by transmitted stress waves was evidenced by fractured surfaces and shear bands in areas near the impact. The same evidence was seen in failure by shearing; however, this failure mechanism also included melt damage, which was suggested to explain the increased energy absorption shown in shearing versus transmitted stress waves (Carr, 1999).

Erlich et al. (2003) performed a study on slow penetration of Zylon® fabrics in an effort to record the influence of projectile shape on yarn breakage. The authors used a quasi-static push test and video camera to study penetration with both a blunt edged projectile and a sharp edged projectile. As anticipated, sharp edges lead to increased fiber breakage and decreased energy absorption by the yarns. This study also identified three distinct means of fabric failure: local yarn rupture, pull-out, and remote yarn failure. Yarn

pull-out was discussed in the previous section. Elrich et al. (2003) describes local yarn rupture as the breaking of fibers within the area of impact. This was shown to be the primary reason for fabric failure in bi-axially fixed yarns when sharp projectiles were used. Remote yarn failure occurs when individual fibers in a yarn show breakage at locations distant from the area of impact. This method of fiber failure was the primary means of fabric failure in uni-axially fixed yarns. This study addresses the issue of yarn breakage, divides breakage into local yarn failure and remote yarn failure, and matches primary energy absorption means to the various sample types depending on the projectile and the yarn axis.

In a study by Robert Prosser of Natick Research and Development Center (1988), the significance of shear forces and tensile forces in ballistic penetration is examined. The materials tested in the study were ballistic nylon panels which were fired upon using a 0.22 caliber steel FSP. The impact point was then examined and observations were used to determine if tensile or shear failure had occurred. Prosser argues that the primary means of fiber breakage is shear failure since the projectile will follow the path of least resistance (and nylon has lower shear strength than tensile strength). It was concluded that shearing is the primary penetration mechanism in nylon ballistic panels and consequently that tensile failure is only a secondary penetration mechanism (Prosser, 1988).

2.3.3 Projectile

In any anti-ballistic armor design it is important to consider the material properties of not only the fibers and fabrics, but also the projectile itself. The study of projectile deformation is critical to the development of armor because it examines the

projectiles ability to enter and damage armor or tissue. This gives insight in to how the fibrous structure can be optimally designed to prevent penetration.

Backman and Goldsmith (1978) use the properties of length, diameter, nose shape, mass, and density as properties that can be used to determine a projectile's ballistic value. They do however, note one tradeoff associated with length: long projectiles aid in penetration but make the projectile more susceptible to instability in firing and bending under impact (Backman, 1978).

In his book, Laible (1980) describes several projectile characteristics which can lead to infiltration of an armor body: high velocity, high strength, high density, length in penetration direction, and a small impact surface. These characteristics enable a projectile to apply large amounts of energy onto a small point and to maintain that energy during penetration (Laible, 1980).

Most *Full metal jacket* (FMJ) projectiles are sharp and hard allowing them to pierce more effectively than blunt projectiles while damaging a smaller, though not necessarily less lethal, area of soft tissue (Bhatnagar, pp 29-71, 2006). A sharp projectile has a nose half angle of 14° , or has a nose length-to-diameter ratio greater than or equal to one. Sharp projectiles penetrate by piercing the target and therefore target failure is found around the projectile axis (Backman, 1978). FMJ bullets are lead filled and coated with a jacket of copper, brass, or steel. The hard jackets allow the bullet to penetrate and shed, exposing the soft deformable core (Bhatnagar, pp53-4, 2006).

Handgun bullets are typically made of deformable materials that help to increase tip surface area upon impact (Bhatnagar, pp 29-71, 2006). A blunt projectile has a nose half angle of 90° , or has a nose length-to-diameter ratio of less than one. The primary

means of target penetration is through plugging and therefore target failure occurs as a cylindrical or conical surface (Backman, 1978).

In one experiment, a blunt-end projectile and a sharp-end projectile were compared according their velocity and penetration into a ceramic target. The projectiles were both 0.30 caliber steel cylinders, the sharp-end projectile having a cone angle of 55°. The results of the experiment show that the sharp-end bullet was able to penetrate the thick ceramic at a lower velocity than the blunt-end bullet. However, when the ceramic was thinner, the blunt-end bullet appeared to penetrate at a lower velocity. This is due to the effect of work hardening and frictional effects on a projectile as it slows and nears the end of the target. A plug is more easily pushed by a blunt-end projectile than a sharp-end projectile when a large deformation has occurred and frictional forces increase (Laible, 1980).

The penetration mechanisms of various projectiles greatly affect the level and means of deformation. Some factors which determine the bullet deformation are: kinetic energy (KE), drag effects, firearm design, and target composition (Bhatnagar, pp 53, 2006). The KE of a bullet is closely related to the mass and velocity of the projectile. The equation for KE can be applied to projectiles in the following manner:

$$KE = \frac{1}{2}(mV)^2 \quad (4)$$

where:

KE= kinetic energy

m= mass (of projectile)

V= Velocity (of projectile)

The KE is dissipated by the target through three mechanisms: penetration, deformation, and conversion into heat energy. Penetration and deformation are affected by the projectile's physical properties and dimensions. A bullet's mass is determined by the composition, diameter, and length. This determines the projectile energy since the *kinetic energy* (KE) is proportional to the mass and therefore high mass results in high KE. The bullet velocity is also important because of the effects on the KE of the projectile. Based on the KE equation, if the velocity is doubled while mass remains constant the resulting KE will be quadrupled (Bhatnagar, pp 52-7, 2006).

Drag is defined as the resistance of air on an airborne projectile. This is related to the bullet velocity, shape, and size, and is affected by the air density, temperature and pressure. Fragments react to drag force differently than bullets because they are not aerodynamically designed but formed from explosions and are random in shape and direction. This random shape allows air drag to slow fragments in the air much more than a bullet. Upon impact fragments typically do not undergo much deformation except, depending on velocity, the dulling of sharp edges.

Other factors affecting bullet deformation and penetration deal more with the firing apparatus and the conditions during firing. The barrel twist acts to stabilize the bullet and maintain a straight path toward the target. Barrel length is proportional to the bullet acceleration and therefore a longer barrel fires a projectile with more force. The distance from the muzzle affects the bullet/target relationship because the longer the bullet is in the air the more drag it experiences.

The target itself affects the projectile's tendency to deform and penetrate depending on the armor's fiber, and impact response characteristics. Fiber strength

determines the target's ability to deform and defeat penetration while fiber response to strain waves determines its ability to dissipate the projectile energy efficiently. Fiber to fiber friction aids in stripping the FMJ from the bullet, allowing the soft metal to deform and increase the area of armor/bullet contact. Friction also binds the armor together and promotes higher impact resistance within the fabric. Fibers used in ballistic armor can enhance their frictional properties through coatings, orientation, and quilting (Bhatnagar, pp29-71, 2006).

In a report for the U.S. Naval Weapons Center, Backman and Goldsmith (1978) discuss the relationship between the target and projectile and the deformation of each during impact. In the beginning of the report the authors outline seven common mechanisms of projectile penetration into a target: stress wave fracture, spall failure, plugging, radial fracture, petaling (front and rear), fragmentation, and ductile hole enlargement (Backman, 1978). In low density, low strength targets, target fracture can take place as a result of the initial strain wave when that wave supersedes the compressive strength of the material. Spall failure or scabbing occurs when the target material has inadequate tensile properties to reflect impact compression. In blunt projectile use, plugging occurs when the target forms a cylindrical plug modeled after the bullet itself. The plug acts to shear the target around the area of the projectile, decreasing target strength and aiding penetration. Radial fracture occurs in brittle targets where the material's tensile strength is lower than its compressive strength resulting in radial cracking. The stress from the initial impact wave causes a bending moment in the target material in front of the projectile, deforming the target around the impact point (Backman, 1978). Schematics of the various deformation methods are shown in

Appendix C. The three means of investigation, according to this article, are: the measurement of crater dimensions, the final projectile properties, and metallurgical inspection of projectile cross sections. The crater can be measured for depth and diameter while the projectile can be analyzed based on length, nose shape, mass, and diameter. The metallurgical analysis of the projectile cross sections can reveal information on the micro structural differences, the internal fracturing, and adiabatic shearing (either localized or plug related).

A common projectile deformation, called mushrooming, occurs when impact with the armor causes the bullet tip to spread apart (and increase in bulk) at the tip while maintaining a cylindrical shape in the rear. A projectile that deforms this way is easier for armor to defeat because the kinetic energy goes from being concentrated in a small area with limited armor contact to being concentrated in a larger area with greater armor contact (Laible, 1980). It is interesting to note that, in the absence of armor, a bullet with this behavior could damage a larger surface area than a bullet that maintained its shape throughout penetration.

In addition to deformation, projectiles can also experience mass losses during impact. One method by which mass loss takes place occurs is when the shock propagation from impact causes debris from both the target and bullet to spray from the impact point (Backman, 1978).

CHAPTER THREE: METHODS AND MATERIALS

This chapter describes the materials tested and the methods of testing to gather data for further analysis. The materials tested are described based on their construction and composition. Method and rationale for use are described for the DSC, light microscopy, V_{50} , and KE methods used in this research.

3.1 Materials Tested

Fifteen different varieties of armor material NES were tested to gather energy dissipation data.

3.1.1 Fabric Construction

The NES structure begins with two needlepunched nonwoven layers, followed by thirty-seven to thirty-nine layers of woven Twaron®, and ends with two additional layers of needlepunched nonwoven fabric. The differences in the samples tested lay in their nonwoven layer fiber populations, which were composed of equal parts of various combinations of aramid, UHMWPE, and LCP fibers. The needlepunched nonwoven layers have a punch density between 118 and 236 needles per square centimeter (300 and 600 needles per square inch) and a weight of 2.3 kg/m^2 (7.6 oz/ft^2). The woven middle layers are 100% plain weave 840 denier Twaron® in an approximately square sett. The complete NES structure weighs 7.7 kg/m^2 (25.3 oz/ft^2).

3.1.2 Fabric Composition

The fifteen NES were each composed of ballistic fiber combinations which varied by fiber types, fiber blend ratios, fiber deniers and punch densities.

3.1.2.1 Fibers

The fibers used in the samples are aramid, polyethylene, and liquid crystal polymers, and were described in more detail in Chapter 2, Section 2.2.1. The fiber trade names and deniers are shown in Table 1.

Fiber Type	Trade Name®	Approx. Denier (g/9,000 m)
Aramid	KM2	1.5
	Twaron	0.7
	K129	1.5
Polyethylene	Spectra	2.2
	Spectra 3.6	3.6
	Spectra 6.3	6.3
	Dyneema	1.5
Liquid Crystal Polymer	Vectran	5

Table 1. Fiber Descriptions

3.1.2.2 Blending

The nonwoven layers are composed of blends of the above fibers, manufactured into fifteen different combinations. The woven fabric was 100% Twaron® in each sample. The nonwoven combinations are numbered based on their V_{50} testing order and are presented in Table 2.

Sample No.	Nonwoven Composition®	No. of Woven Layers
13	Spectra 3.6/KM2	37
25	Dyneema/KM2	37
26	Dyneema/KM2/Vectran	37
27	Twaron/Dyneema	37
28	Twaron/Dyneema	37
29	Twaron/Dyneema/Vectran	37
30	Twaron/Dyneema/Vectran	37
31	Twaron/Spectra 2.2	37
32	Twaron/Spectra 2.2/Vectran	37
33	Twaron/Spectra 3.6	37
34	Spectra 3.6/KM2	37
37	Spectra 3.6/K129 (8.5oz.)	37
38	Spectra 6.3/K129 (8oz.)	38
39	K129 (5.8oz.)/Dyneema	39
40	K129 (8oz.)/Dyneema	38

Table 2. NES Sample Composition

3.2 Tests and Rationale

The four test methods used on the NES samples (DSC, microscopy, V_{50} , and KE calculation) and the rationale behind their use are explained in this section.

3.2.1 DSC Methodology

A general account of the DSC technique, and resulting plots, is provided in order to better understand this test's use in this research.

3.2.1.1 Method

DSC is a method of thermal analysis that uses pyrometry, thermal conductivity, and glass viscosity to measure the temperature differences between a reactive material and a non-reactive standard. There are two types of DSC instruments: the power compensated DSC and the heat flux DSC.

The power compensated DSC is designed with two temperature controlled chambers-one for the material and one for the standard. As the DSC chambers are heated any transformations are detected and the temperatures are adjusted to maintain a “null balance” between the material and the standard. The instrument measures the electrical energy needed to sustain this “null balance”. This energy is proportional to the sample’s release of heat as a function of time.

The heat flux DSC instrument uses one chamber for both the material and the standard. As the material experiences temperature changes, it will respond with either exothermic (release) or endothermic (absorption) heat. Computer software and a calibration constant are used to translate the amplified differential thermocouple voltage to energy per unit time (Speyer, 1994).

For the research presented in this thesis, a heat flux TA Instruments 2920 Modulated DSC was used for temperature analysis. The materials tested were taken from the back side of the soft armor’s first nonwoven layer. Two material samples were taken from each of the fifteen fabrics-one sample from the damaged impact area and one sample from a non-impact area. The DSC was set to run the samples at a rate of 10°C per minute in both the ramp up and the ramp down. The aim of this testing was to determine if there are differences in the thermal properties of the impacted and non-impacted samples.

3.2.1.2 Output

The result of a typical DSC test is a plot of the melt and glass transition temperature differences as a function of time. This plot can be analyzed to reveal information about the transition temperatures, thermodynamics and kinetics of the

reactive material. Since the DSC measures the material's heat transfer over time, the output is plotted in watts per degree Celsius (Speyer, 1994).

3.2.2 Photographic Methodology

The common methods used to obtain images from microscopes, and the method used in this research, are explained in the following section.

3.2.2.1 Methodology

Photographic examination of ballistic impact effects on fibers has been established by past studies since the re-birth of soft body armor (Hearle, 1971, 1989 and Wilde, 1973). The diminutive nature of fibers and yarns necessitates the use of a microscope to identify impact effects. Two microscopic instruments commonly used are the light microscope and the *scanning electron microscope* (SEM).

A SEM forms an image using electrons and therefore is able to achieve great magnification and resolution. SEMs also have a long working distance, detailed surface images, and a large depth of focus. Some disadvantages of SEMs are their inability to perceive color, high cost, and destruction of the sample (due to the fact that it must be coated in gold).

Light microscopes have several advantages over SEM's including perception of color, internal and surface detail, and the option for polarized light microscopy. The disadvantages are low magnification and resolution, small depth of focus, and short working distance (Hearle, 1989).

Light microscopy was chosen for NES testing due to the need for low cost and color images. The microscope used was an Olympus BH-12® with an Olympus DP10® camera and FlashPath® software.

3.2.2.2 Output

Images were taken from the back side of the first nonwoven layer for each of the fifteen samples. Three areas of the armor were captured in the images: the nonwoven layer at an impact site, each fiber type at a non-impact site, and each fiber type at an impact site. The purpose of these images is to show the fabric impact area and the individual fiber reactions to needling and impact.

3.2.3 Ballistic Limit Testing Methodology

Common ballistic testing procedures and their results are described in the following sections.

3.2.3.1 Method

It was established in Chapter 2, Section 2.1 that soft body armor must meet certain governmental standards before being approved for use in police and military applications. Currently, two test methods are used for comparing prototype armors against governmental standards: ballistic resistance testing and ballistic limit (V_{50}) testing. Ballistic resistance testing uses fixed performance requirements to evaluate a material and provides only pass/fail data while V_{50} testing is used to establish the performance limitations of a material. These tests are performed on numerous identical samples and the results are plotted as go/no-go points on a curve of penetration to projectile velocity.

There are four different ways to perform a V_{50} test: Probit Method, Langlie Method, *One Shot Test Response* (OSTR) Method, and the Bruceton Method. The most commonly used V_{50} test is the MIL-SD-662F, which is an adapted form of the Bruceton

Method. In this method, the initial firing occurs at the velocity likely to produce fifty percent penetration. Velocity variations are then used around this fifty percent point and firings continue until an even amount of trials have been acquired. The V_{50} values (the velocity at which 50% of projectiles penetrate) are evaluated against the NIJ standard for the various threat levels.

3.2.3.2 Output

In this research ballistic limit testing was performed according to MIL-SD-622, by the NIJ certified H. P. White testing facility. The testing report contains information regarding the sample such as, size, conditioning, and owner in addition to the V_{50} values. For further clarification the test report also includes information about test conditions and projectile caliber, shape, construction, weight, stability and impact obliquity.

3.2.4 Energy Determination Methodology

The mathematical formula for estimating residual KE, used in this research, is described in the following sections.

3.2.4.1 Kinetic Energy

In order to determine the transfer of energy throughout the NES, the equation for KE (equation 4) is used. Projectile penetration of an armor structure has three main occurrences of KE: the KE of the projectile (\bar{E}), the KE of penetration ($\bar{E}_{Penetration}$), and the residual KE from the exiting projectile ($\bar{E}_{Residual}$). For \bar{E} , the V_{50} is obtained from the V_{50} testing data. For $\bar{E}_{Penetration}$ the V_{50} is obtained from the velocity of the complete penetrations detailed in the V_{50} testing. For $\bar{E}_{Residual}$ the V_{50} is not specifically known but

is known to be greater than the V_{50} data since it exceeded the ballistic limit of the fabric and exited the armor.

These equations can be combined to estimate the residual energy after armor contact:

$$\bar{E}_{Residual} = \bar{E}_{Penetration} - \bar{E}, \quad (5)$$

or, rewritten as:

$$\bar{E}_{Residual} = \frac{1}{2} [m(V_{50Penetration})^2 - m(V_{50})^2] \quad (6)$$

For this equation to be true several parameters must remain constant including projectile shape, size and ballistic stability, impact velocity, fixation/backing of the target and composition/dimensions of target materials.

CHAPTER FOUR: RESULTS AND DISCUSSION

This chapter presents the results gathered from the DSC, Microscope, V_{50} and KE testing described in Chapter 3. These results are analyzed in reference to their effect on the overall research objectives of this thesis.

4.1.1 DSC

DSC tests were performed on each of the NES combinations with samples taken from both the impact and non-impact sites. Testing was performed on fibers from each NES impact site and from a non-impact site for each fiber type. The following section only describes the Spectra® and Dyneema® samples, since aramid fibers have thermal temperatures above ballistic impact temperatures.

4.1.1.1 Results

The DSC plots show characteristic spikes indicating the *glass transition temperature* (T_g) and the *melting temperature* (T_m) for each of the tested samples. These temperatures are compared between the impact and non-impact sites to determine if any noticeable changes occurred in the fibers' thermal properties due to impact. The non-impact T_m is subtracted from the impact T_m and the difference is converted into a percentage. The results from this calculation are shown in Table 3.

The lowest temperature difference occurs in sample number forty (50/50 K129®/Dyneema®) which has a post-impact T_m of -0.45%. The highest temperature

difference occurs in sample number thirty-seven (50/50 K129®/Spectra® 435) which has a post-impact melting point of 1.09% above the non-impact melting point. The DSC graphs for sample numbers thirty-seven and forty are shown in Figure 3 - Figure 6. These results are not typical of all the samples. The average % difference between the non-impact and impact melting temperatures is 0.12 with a standard deviation of 0.47. From the NES samples, half the samples show negative percent differences indicating that the impact T_m is higher than the non-impact T_m . The other half of the samples show positive percent differences indicating that the impact T_m is higher than the non-impact T_m . The DSC plots from each of the tested samples are found in Appendix G.

Sample #	Fiber Type®	T_m Non-Impact (°C)	T_m Impact (°C)	% Difference
13	Spectra 3.6	154.19	154.71	-0.33
25	Dyneema	154.73	154.38	0.22
26	Dyneema	154.80	154.80	-0.05
27	Dyneema	154.73	154.86	-0.08
28	Dyneema	154.73	154.82	-0.05
29	Dyneema	154.73	154.43	0.19
30	Dyneema	154.73	155.01	-0.18
31	Spectra 2.2	154.19	153.60	0.38
32	Spectra 2.2	153.36	152.91	0.29
33	Spectra 3.6	156.26	154.64	1.04
34	Spectra 3.6	156.26	156.67	-0.26
37	Spectra 3.6	156.26	154.56	1.09
38	Spectra 6.3	155.29	154.47	0.53
39	Dyneema	154.73	155.41	-0.44
40	Dyneema	154.73	155.42	-0.45

Table 3. DSC Data

4.1.1.2 Discussion

The highest positive difference between the non-impact T_m and the impact T_m is found in sample thirty-seven, which contains Spectra® 435. The DSC graph of this fiber

before impact is shown in Figure 3. The lowest point on this graph indicates the melting temperature (156.26°C for this sample) since, at that temperature, the heat flow is the lowest and the temperature is the highest. The DSC graph of sample number thirty-seven after impact is shown in Figure 4 and has a T_m of 154.56°C. The range for all four Spectra® 435 samples is from 1.09 to -0.33%, with an average of 0.39% above the non-impact T_m . The Spectra® 2.2 ranges from 0.29 to 0.38%, with an average of 0.34% above the non-impact T_m . The Spectra® 650 is only present in one of the samples and is 0.53% above the non-impact T_m . The seven Spectra® samples tested show an average of 0.32%, and all but two of the samples (numbers 13 and 34) show negative percentages.

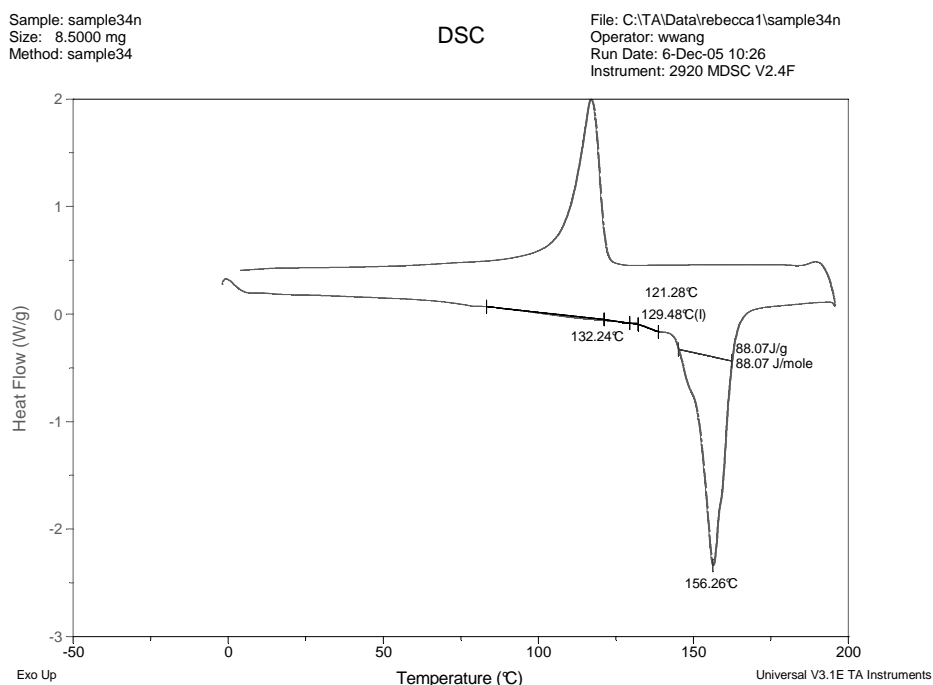


Figure 3. Sample 37 Non-Impact

Sample: sample372
Size: 7.1000 mg
Method: sample31

DSC

File: C:\TA\Data\rebecca1\sample372
Operator: skh
Run Date: 28-Feb-06 13:45
Instrument: 2920 MDSC V2.4F

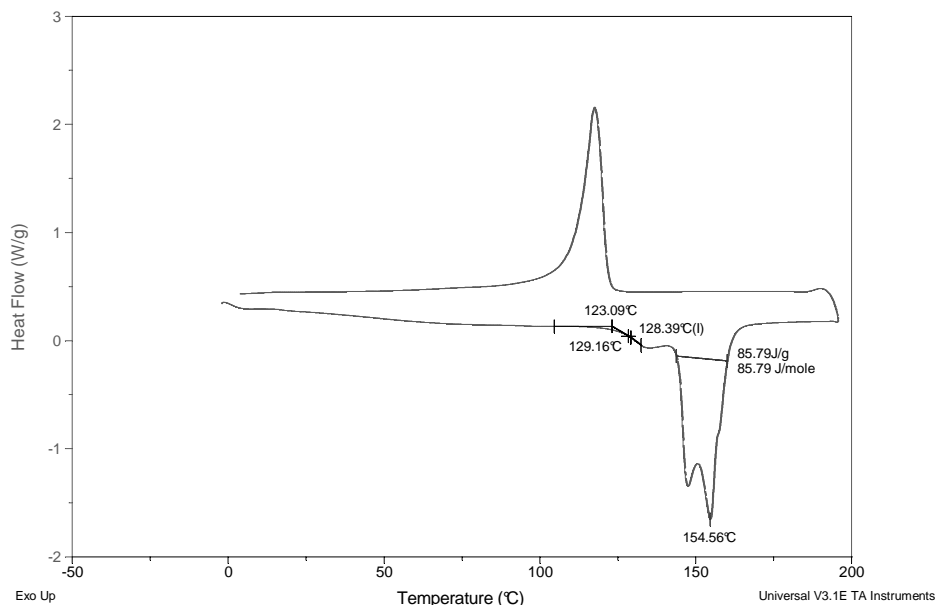


Figure 4. Sample 37 Impact

The Dyneema® used in this research was all the same type (1.5 denier per filament) and therefore there is no denier distinction as with the Spectra®. The lowest percent below the non-impact T_m is sample forty with -0.45% difference between the non-impact T_m and the impact T_m . The DSC plot for sample forty non-impact Dyneema® is shown in Figure 5 and reveals a T_m of 154.73°C. Figure 6 shows sample forty after impact and reveals a T_m of 155.42°C. The average for the Dyneema® samples is -0.11% and six of the eight samples tested have negative percent values.

Sample: sample40n
Size: 9.0000 mg

DSC

File: C:\TA\Data\rebecca1\sample40n
Operator: wwang
Run Date: 2-Dec-05 09:57
Instrument: 2920 MDSC V2.4F

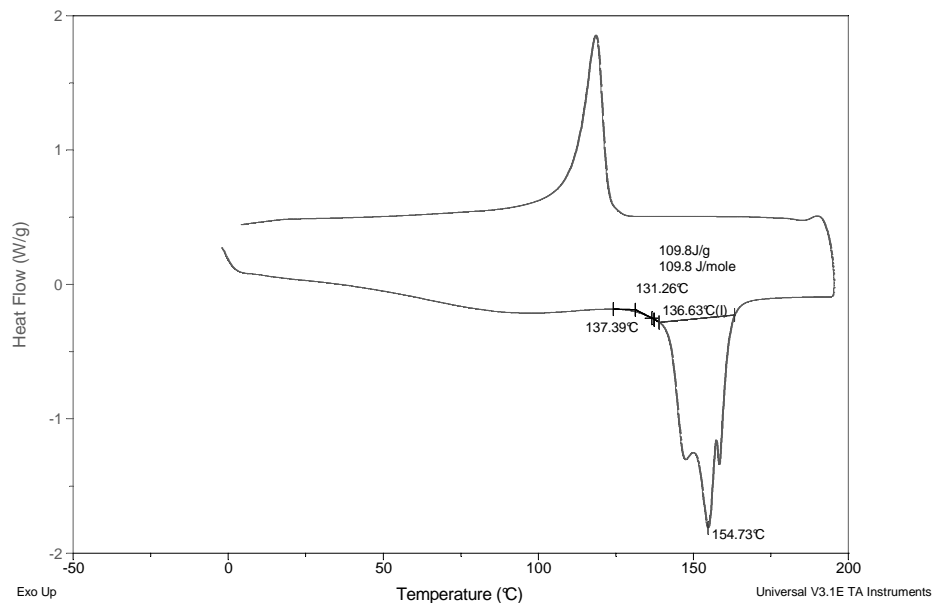


Figure 5. Sample 40 Non-Impact

Sample: sample 40
Size: 9.2000 mg

DSC

File: C:\TA\Data\rebecca1\sample40
Operator: wwang
Run Date: 30-Nov-05 15:56
Instrument: 2920 MDSC V2.4F

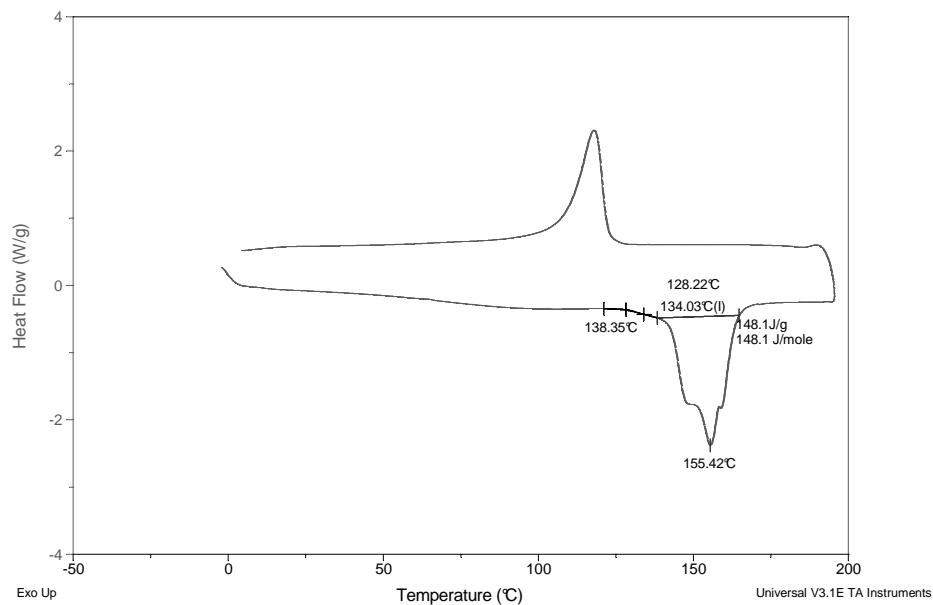


Figure 6. Sample 40 Impact

The differences seem weightier when the actual fiber-projectile interaction is considered. A two grain projectile has a diameter of 0.28 cm (0.11in) and, since it is a *right circular cylinder* (RCC), a circular surface area of:

$$A = \pi r^2 = \pi(0.28\text{cm})^2 = 0.246 \text{ cm}^2 \quad (7)$$

All the blends are either one half or one third Spectra® or Dyneema® fibers. In two layers of NES, which contain 2.3 kg/m² (7.6 oz/yd²) of fibers per layer, the PE fibers would only come in contact with the projectile in a 0.246 cm² (0.003 in²) area and only thirty or fifty percent of that area, depending on the blend, would be Polyethylene fibers. This means that there is very little PE fiber-projectile interaction and therefore a phase change would only occur in a small number of fibers (and those would constitute an even smaller number of the fibers selected for DSC testing). The low percentages shown in the DSC test could be a reflection of this low fiber-projectile interaction.

The DSC plots exhibit some unusual patterns when examined according to fiber type. The Spectra®6.3 was only used in sample 38 and therefore only one DSC was performed on an impact and non-impact sample. These plots, shown in Figure 7 and Figure 8, show similar patterns in both the impact and non-impact samples. The basic pattern consists of a pronounced peak halfway down into the T_m trough and a very subtle peak on the way up from the trough.

Sample: sample38n
Size: 9.4000 mg
Method: sample38

DSC

File: C:\TA\Data\rebecca1\sample38n
Operator: wwang
Run Date: 2-Dec-05 13:24
Instrument: 2920 MDSC V2.4F

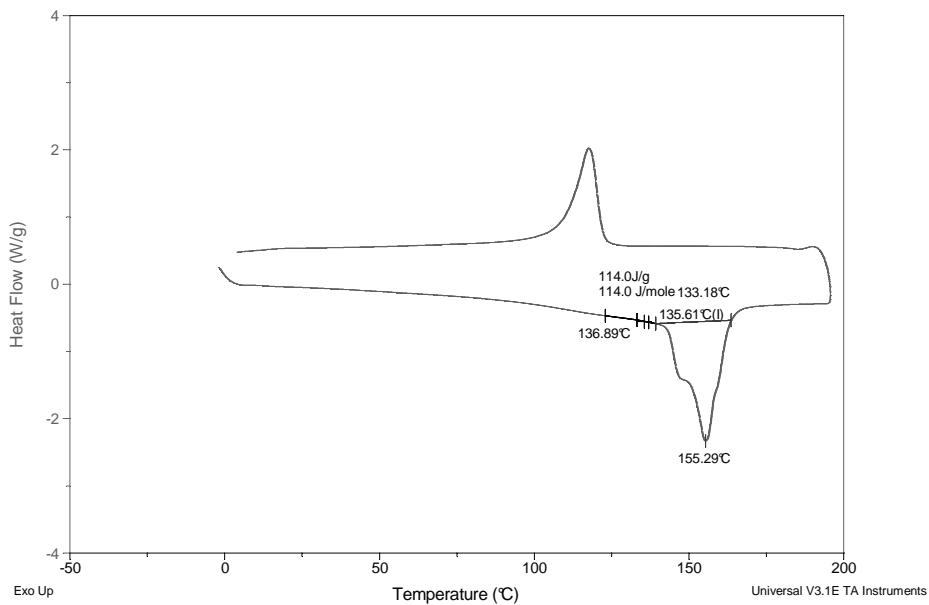


Figure 7. Spectra® 6.3 Non-Impact DSC

Sample: sample38
Size: 9.0000 mg
Method: sample38

DSC

File: C:\TA\Data\rebecca1\sample38
Operator: wwang
Run Date: 2-Dec-05 12:36
Instrument: 2920 MDSC V2.4F

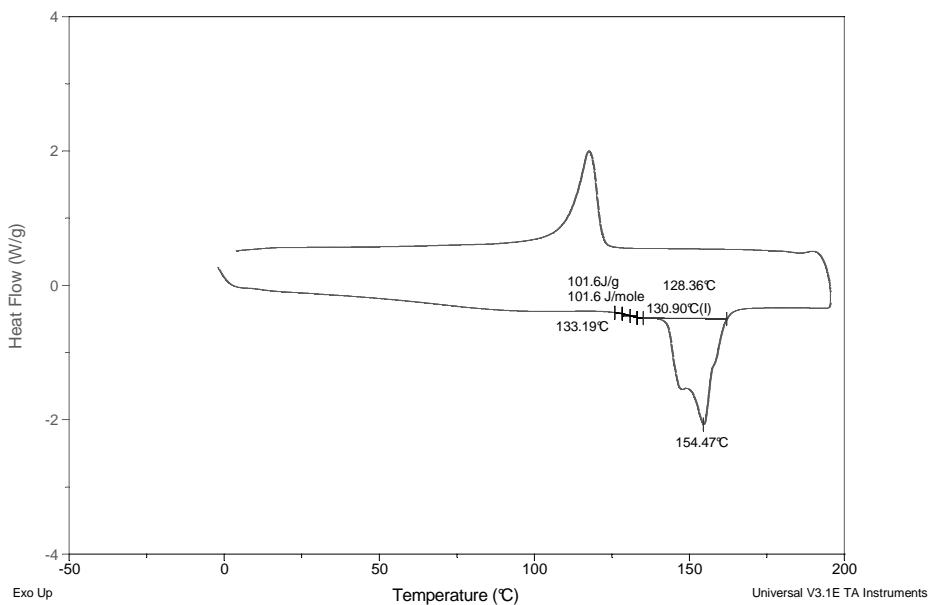


Figure 8. Spectra®6.3 Impact DSC

The Spectra® 2.2 samples 31 and 32 were plotted by the DSC and produced varied results. Sample 31 non-impact shows a slight peak halfway down into the T_m trough and a slight return peak a third of the way up the trough. The impact sample follows the same pattern but has a much more pronounced halfway peak. These plots can be seen in Figure 9 and Figure 10.

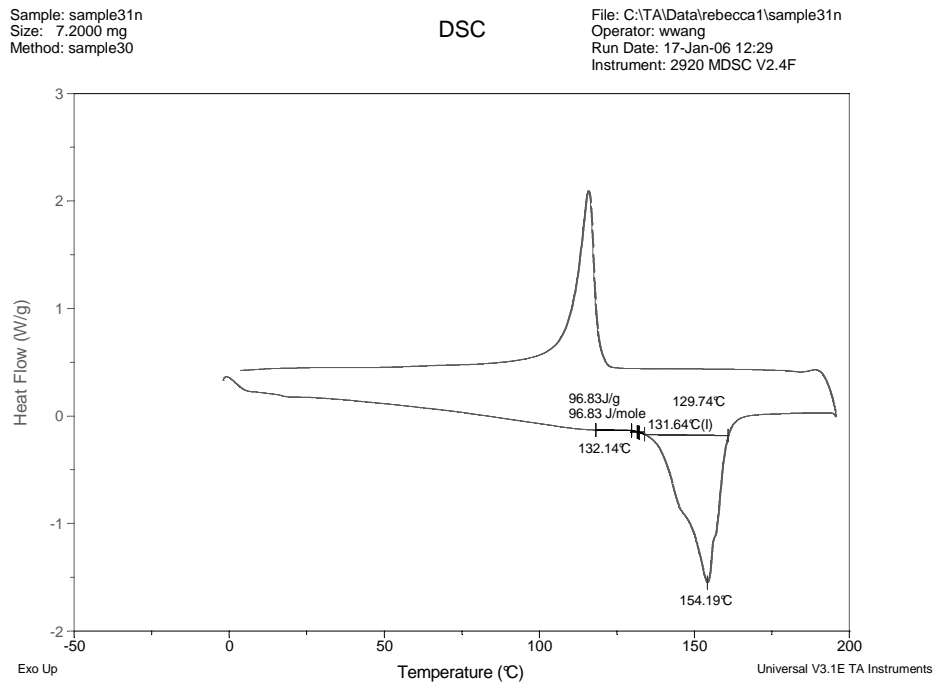


Figure 9. Spectra® 2.2 Non-Impact DSC

Sample: sample31
Size: 5.3000 mg
Method: sample31

DSC

File: C:\TA\Data\rebecca1\sample31
Operator: skh
Run Date: 28-Feb-06 12:36
Instrument: 2920 MDSC V2.4F

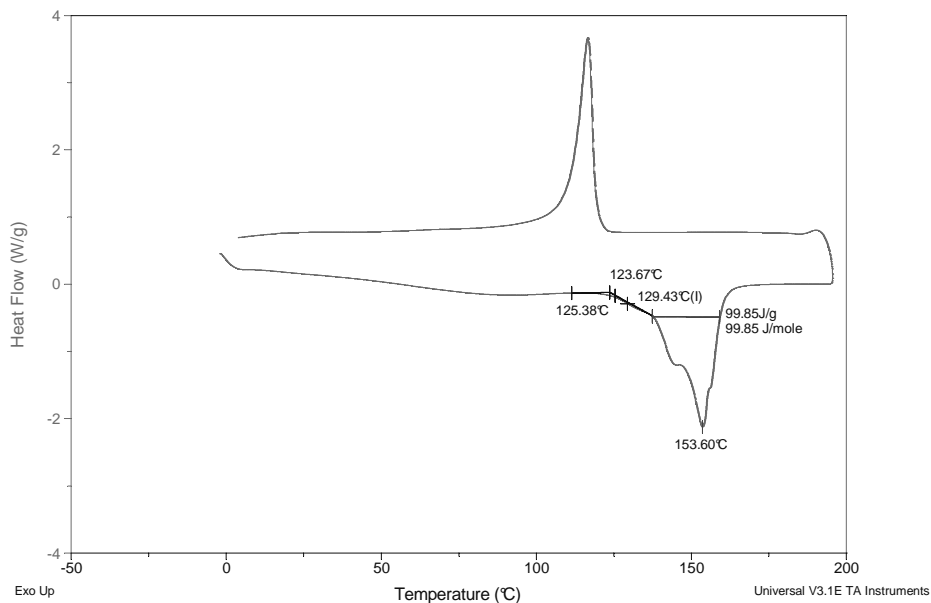


Figure 10. Spectra® 2.2 Impact DSC

The plots of Sample 32 are shown in Figure 11 and Figure 12, and do not follow similar patterns. The non-impact sample has a halfway peak and a subtle return peak. The impact sample shows a pronounced peak during the initial curve down into the T_m trough and a less pronounced halfway peak and similar return peak.

Sample: sample32
Size: 9.0000 mg
Method: sample37

DSC

File: C:\TA\Data\rebecca1\sample32
Operator: wwang
Run Date: 9-Dec-05 11:03
Instrument: 2920 MDSC V2.4F

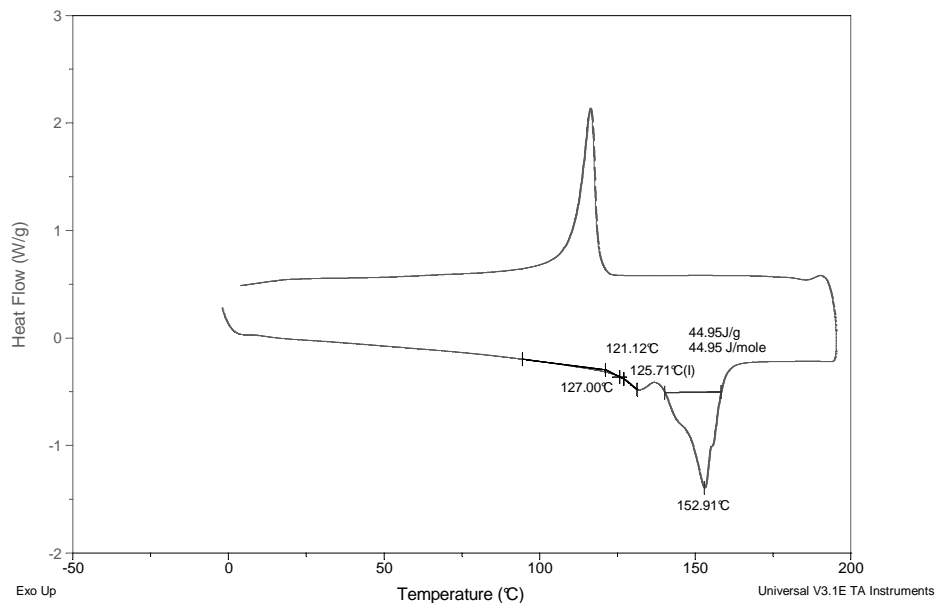


Figure 11. Spectra®2.2 Impact DSC (sample 32)

Sample: sample32n
Size: 8.3000 mg
Method: sample37

DSC

File: C:\TA\Data\rebecca1\sample32n
Operator: wwang
Run Date: 9-Dec-05 11:52
Instrument: 2920 MDSC V2.4F

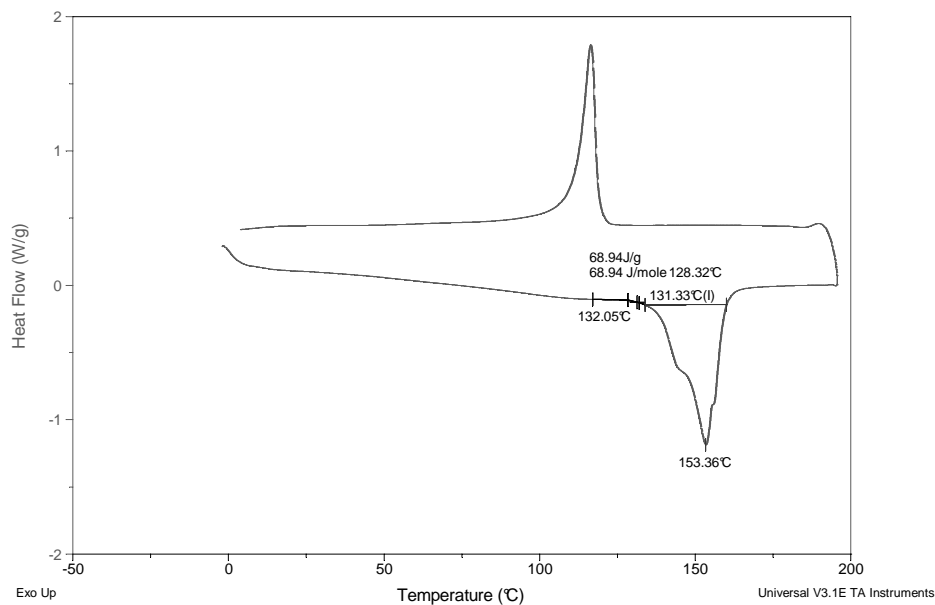


Figure 12. Spectra® 2.2 Non-Impact DSC (sample 32)

For the Spectra®3.6, four impact samples were tested and one non-impact sample was tested. The non-impact sample shows subtle initial, halfway and return peaks which can be seen in Figure 13.

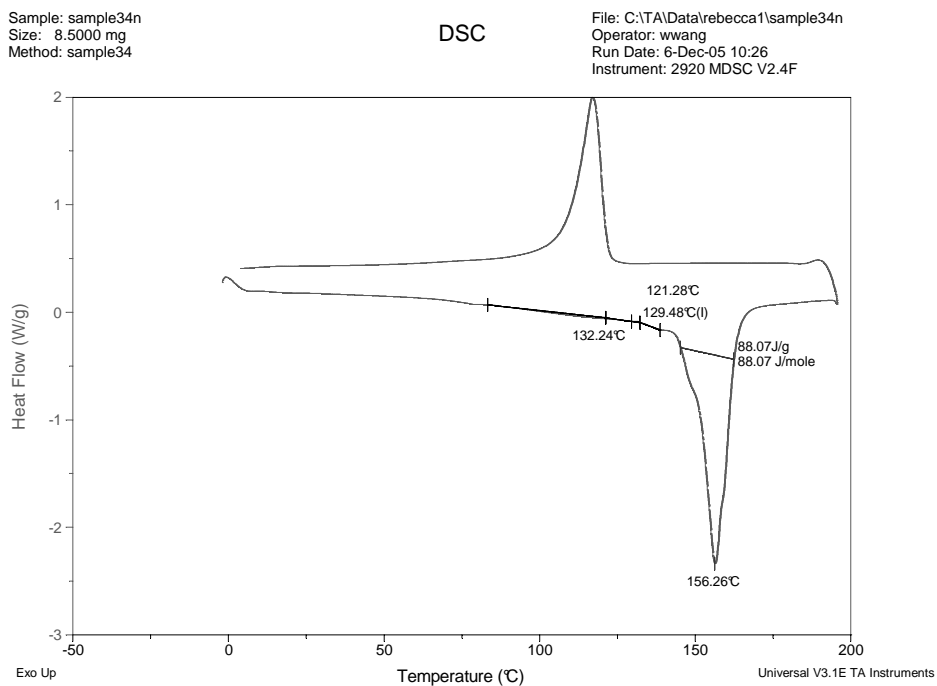


Figure 13. Spectra® 3.6 Non-Impact DSC

The Spectra® 3.6 plots from samples 33 and 34 follow the same basic pattern as the non-impact plot except in both cases the initial peak is more pronounced. These plots can be seen in Figure 14 and Figure 15.

Sample: sample33
Size: 9.1000 mg
Method: sample33

DSC

File: C:\TA\Data\rebecca1\sample33
Operator: wwang
Run Date: 6-Dec-05 11:26
Instrument: 2920 MDSC V2.4F

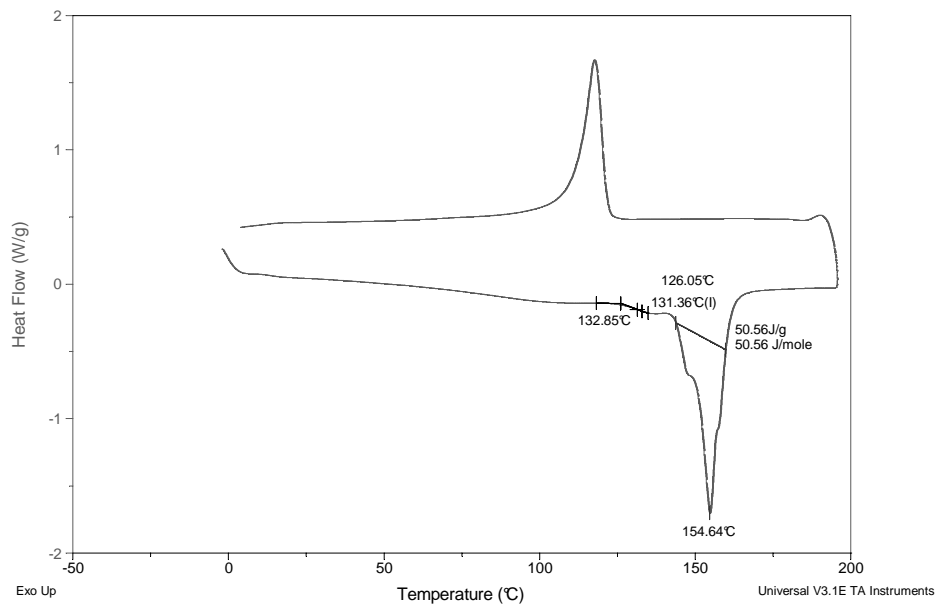


Figure 14. Spectra® 3.6 Impact DSC (Sample 33)

Sample: sample34
Size: 8.9000 mg
Method: sample34

DSC

File: C:\TA\Data\rebecca1\sample30
Operator: wwang
Run Date: 6-Dec-05 09:35
Instrument: 2920 MDSC V2.4F

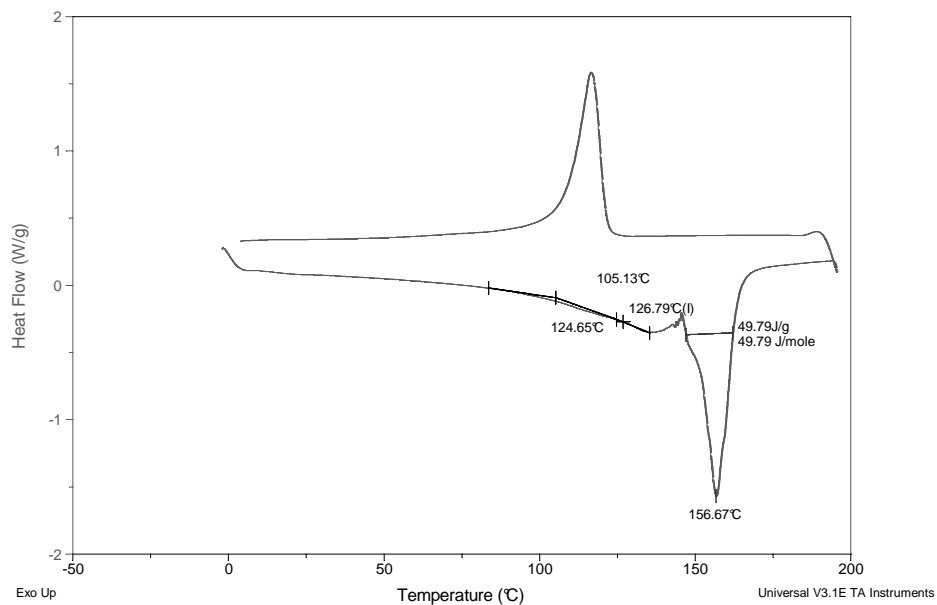


Figure 15. Spectra® 3.6 Impact DSC (Sample 34)

The DSC plots of Spectra® 3.6 in sample 13 and 37 show patterns very different from the non-impact sample but similar to each other. In each plot the halfway peak, shown in Figure 16 and Figure 17, is dramatically more pronounced than in the non-impact sample.

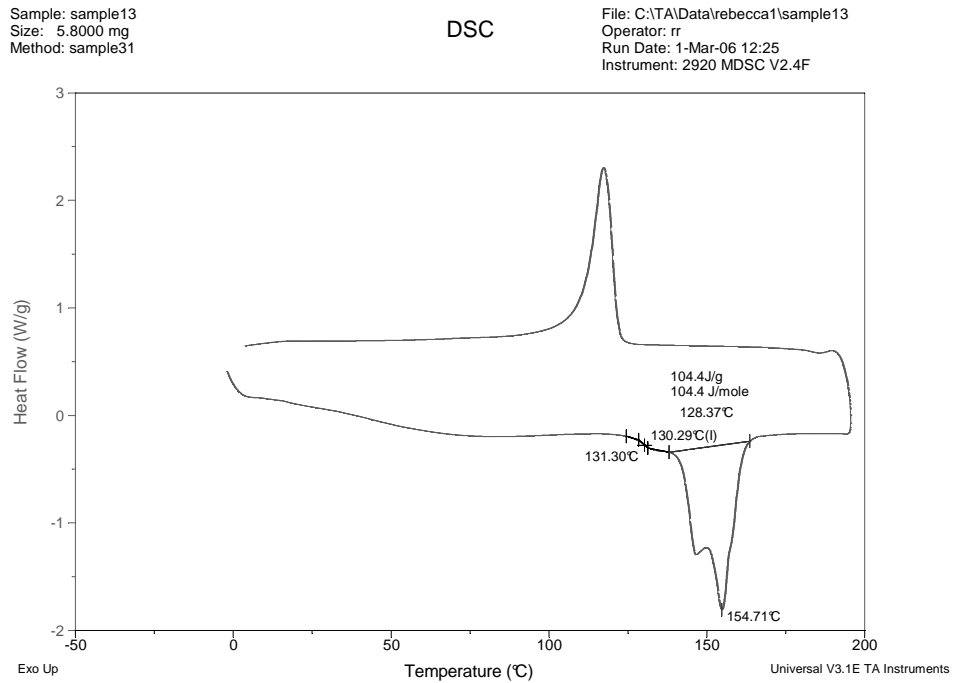


Figure 16. Spectra® 3.6 Impact DSC (Sample 13)

Sample: sample372
Size: 7.1000 mg
Method: sample31

DSC

File: C:\TA\Data\rebecca1\sample372
Operator: skh
Run Date: 28-Feb-06 13:45
Instrument: 2920 MDSC V2.4F

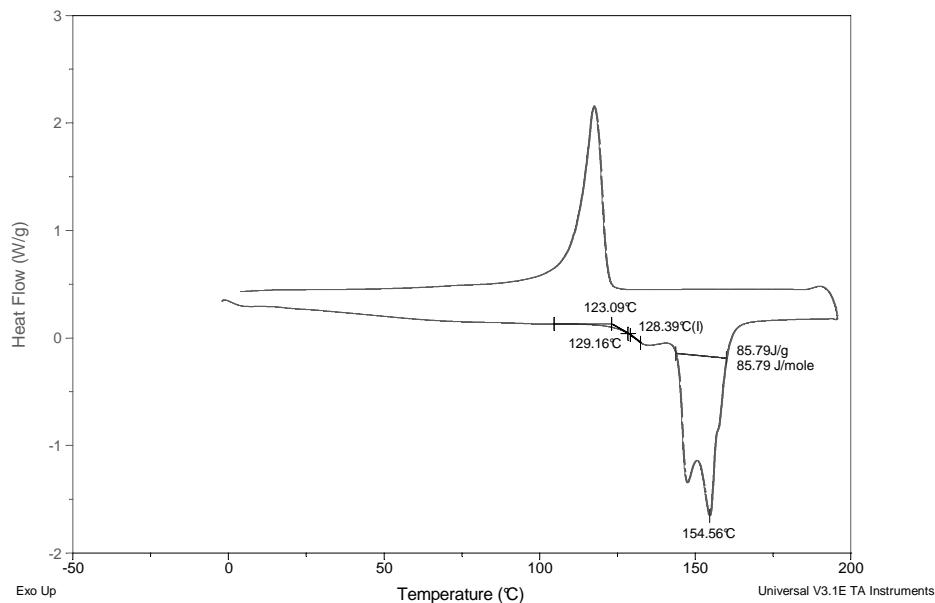


Figure 17. Spectra® 3.6 Impact DSC (Sample 37)

The Dyneema® was used in the greatest number of samples and therefore was the most thoroughly tested by DSC. In total, seven Dyneema® impact samples were plotted but only one non-impact sample was plotted. The non-impact plot, shown in Figure 18, is of sample 40 and shows a pattern with a slight initial peak, a pronounced halfway peak and a sharp return peak.

Sample: sample40n
Size: 9.0000 mg

DSC

File: C:\TA\Data\rebecca1\sample40n
Operator: wwang
Run Date: 2-Dec-05 09:57
Instrument: 2920 MDSC V2.4F

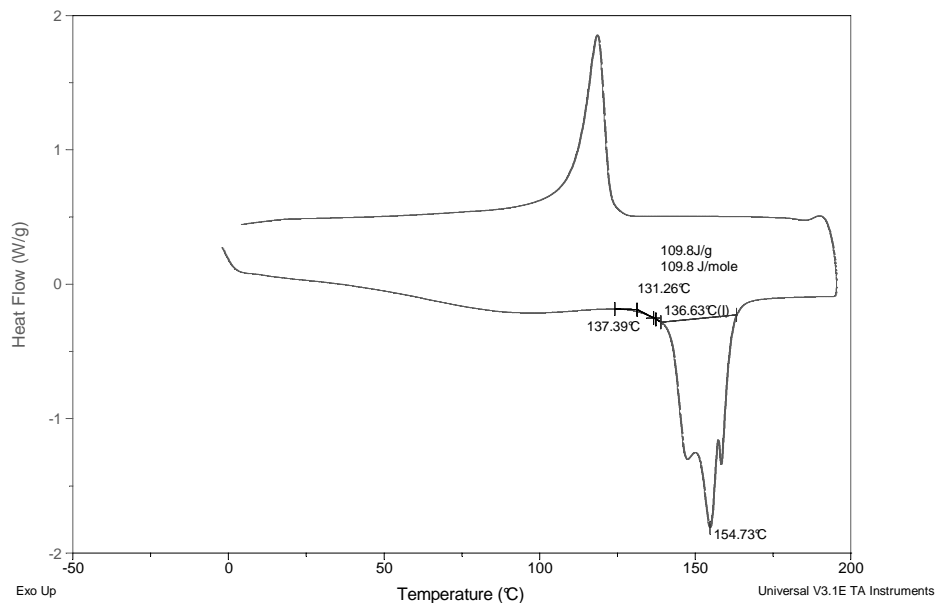


Figure 18. Dyneema® Non-Impact DSC

From the seven impact plots, four samples (25, 26, 39 and 40) exhibit patterns very similar to those in the non-impact sample. Samples 27, 29 and 30 all produced DSC plots with initial peaks significantly more pronounced than that of the non-impact plot. These plots are shown in Figure 19, Figure 20, and Figure 21.

Sample: sample27
Size: 6.7000 mg
Method: sample31

DSC

File: C:\TA\Data\rebecca1\sample27
Operator: rr
Run Date: 1-Mar-06 09:29
Instrument: 2920 MDSC V2.4F

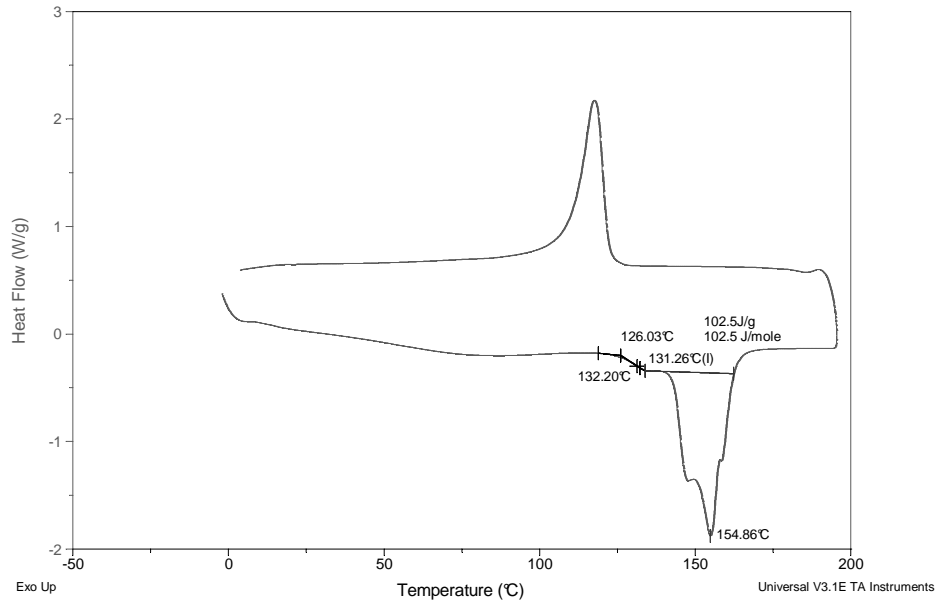


Figure 19. Dyneema® Impact DSC (Sample 27)

Sample: sample29
Size: 6.2000 mg
Method: sample31

DSC

File: C:\TA\Data\rebecca1\sample29
Operator: rr
Run Date: 28-Feb-06 14:31
Instrument: 2920 MDSC V2.4F

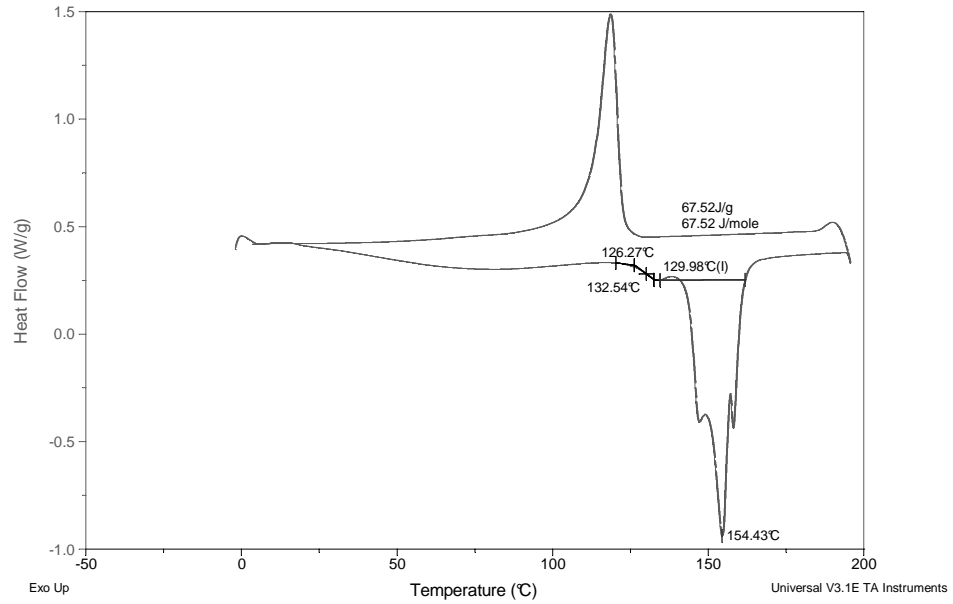


Figure 20. Dyneema® Impact DSC (Sample 29)

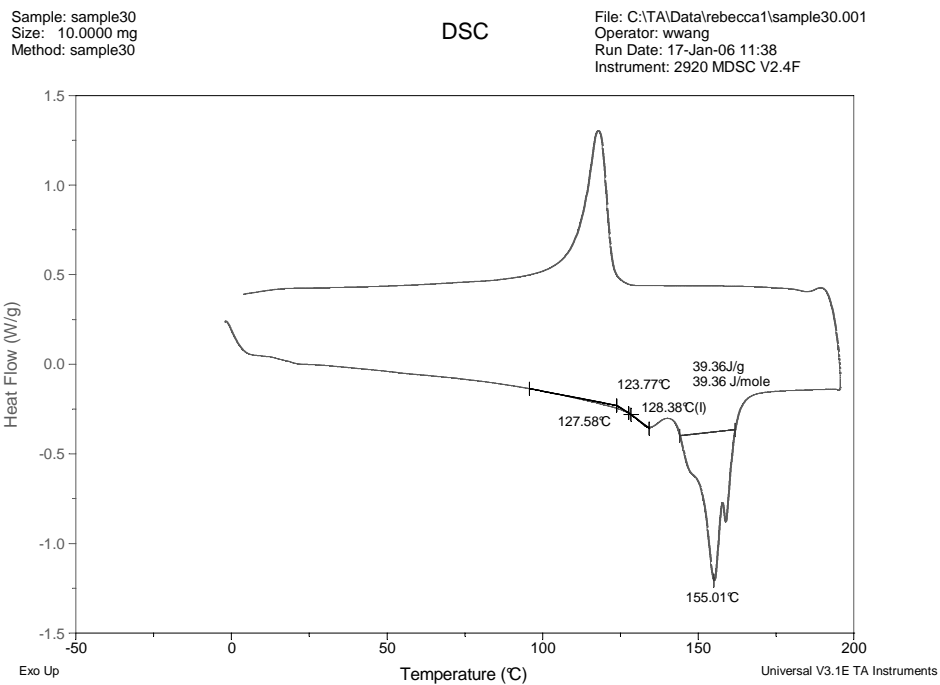


Figure 21. Dyneema® Impact DSC (Sample 30)

The DSC testing provided no conclusive evidence of a phase change; however, some of the anomalies found in the various samples are indications that there was some thermal activity which left the impacted samples permanently changed. In order to determine the reliability or magnitude of these anomalies further, testing would be required.

4.1.2 Photographic Images

The analysis of the fiber images provides information on fiber damage resulting from both needling and impact. In order to distinguish between the two, images were taken from impact and non-impact sites. Images were taken for each of the fibers used in the samples. For a complete set of images see Appendices D and E.

4.1.2.1 Results

The aramid fiber images in Figure 22 - Figure 24 show characteristic axial splitting, fibrillation under impact, and a lack of sizable needling damage. The axial splitting occurs in the impact fibers because the force during impact was great enough to break the intermolecular and covalent bonds of the aramid polymer. This allowed cracks to form which split the fiber along its axis (Fibrillation in aramid fibers is discussed in Section 2.2.1.1 of Chapter 2).

Figure 22 shows the needlepunched Twaron® fiber on the left side which exhibits no noticeable damage and no signs of axial splitting. The impact image in Figure 22 shows the axial splitting on the right side of the fiber which is identifiable by the small fiber strands extending out from the main strand and in the decreased diameter of the main fiber as splitting takes place.

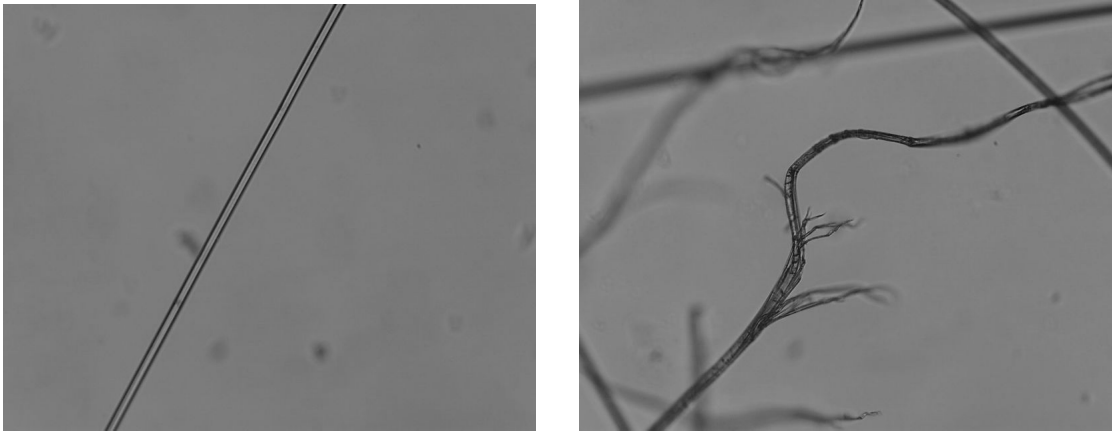


Figure 22. Needlepunched Twaron® (L) (154x) and Impact Twaron® (R) (154x)

The axial splitting of the impact KM2® in Figure 23 is very pronounced and can be seen surrounding the main fiber.

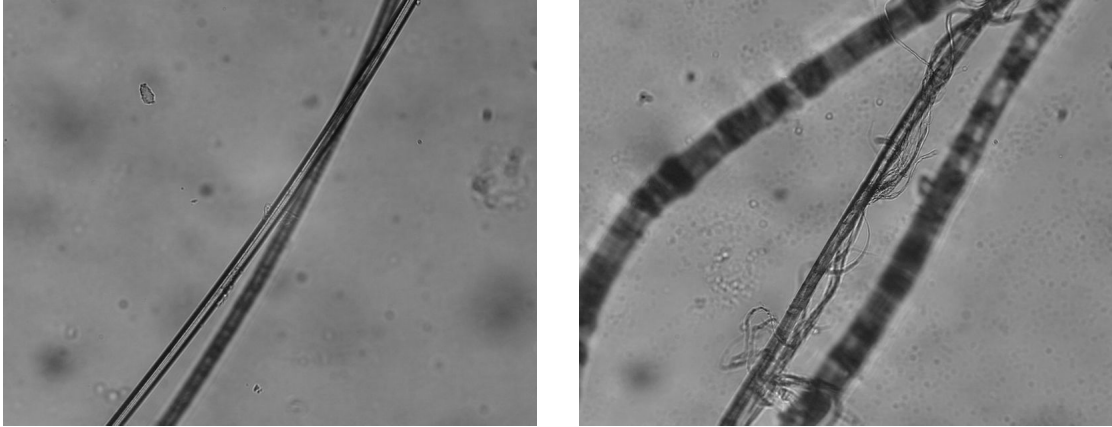


Figure 23. Needlepunched KM2® (L) (139x) and Impact KM2® (R) (167x)

The impact of K129® in Figure 24 shows axial splitting along the underside of the main fiber and is a clear example of how axial splitting depletes the main fiber structure and can result in thin, fragmented fiber ends.

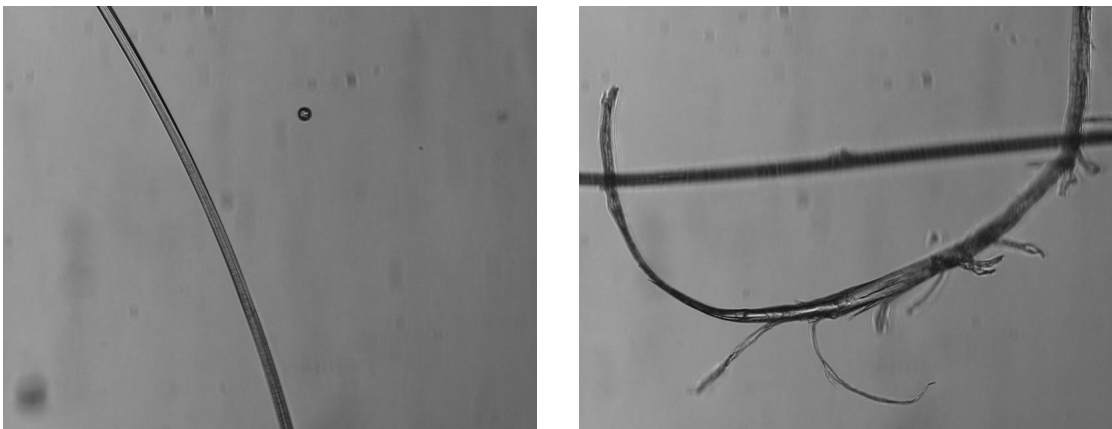


Figure 24. Needlepunched K129® (L) (167x) and Impact K129® (R) (139x)

The Spectra® and Dyneema® fiber images, in Figure 25 - Figure 28, show the melting, scarring and shearing that was discussed in Section 2.2.1.2, Chapter 2. It is also evident from the needlepunched images in Figure 25 - Figure 28 that impact is the primary cause of damage and that needlepunching damages are not significant.

The left image in Figure 25 shows the needlepunched, non-impact image of Spectra® 2.2 which exhibits some fiber damage in the form of shallow nicks and bands

on the fiber surface. The right image shows the surface scarring characteristic of post impact polyethylene fibers.

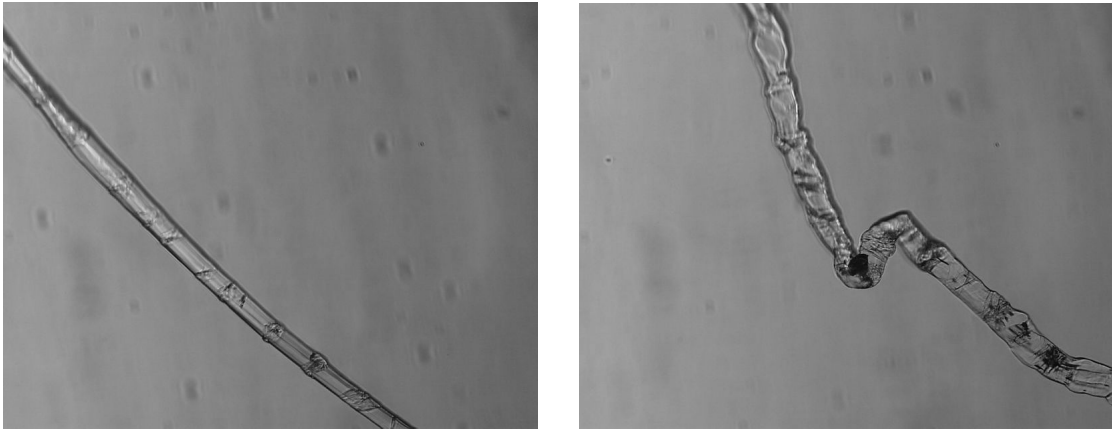


Figure 25. Needlepunched (L) (294x) and Impact (R) (294x) Spectra® 2.2

Figure 26 shows a needlepunched image of Spectra® 3.6 with shallow nicks and bands similar to those seen in Figure 25. The impact image in Figure 26 shows surface scarring and melting on the end of a Spectra® 3.6 fiber.

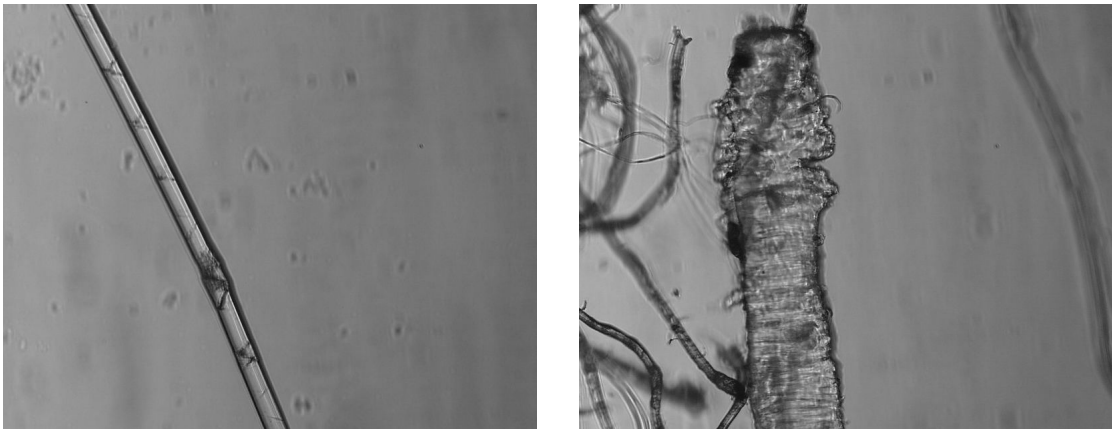


Figure 26. Needlepunched (L) (227x) and Impact (R) Spectra® 3.6

In Figure 27, the needlepunched Spectra® 6.3 shows little damage and the characteristic kink bands perpendicular to the fiber axis. The impacted Spectra® 6.3 image in Figure 27 shows clear signs of melting and ball formation along with some minor axial splits near the base of the melted ball.

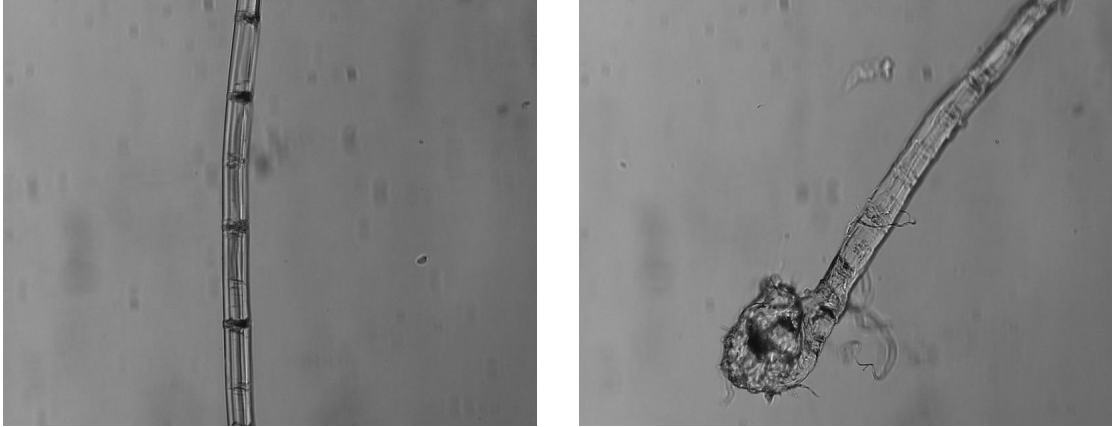


Figure 27. Needlepunched (L) (172x) and Impact (R) (172x) Spectra® 6.3

In Figure 28, the needlepunched and impact images of Dyneema® are shown. The needlepunched image shows some shallow cuts, bands and scales perpendicular to the fiber axis but overall the fiber is not damaged. The impact image on the right shows melting, visible at the balled ends, and some fiber scarring visible by the high number of closely spaced kink bands.

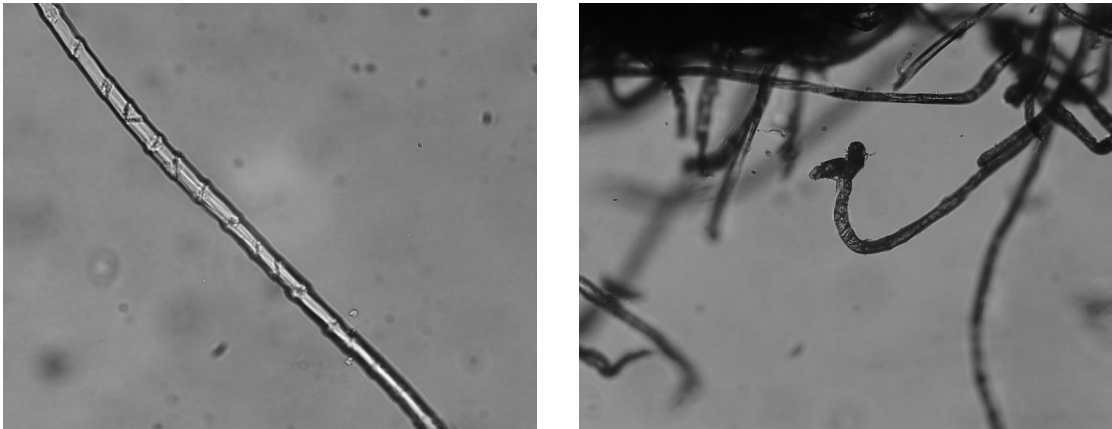


Figure 28. Needlepunched (L) (286x) and Impact (R) (214x) Dyneema®

The Liquid Crystal Polymer fiber, Vectran®, was used in four of the NES samples and the impacted image is shown in Figure 29. The image shows fibrillation and melting in the impacted area of the fiber. The needlepunched Vectran® fiber image shows no significant signs of damage.

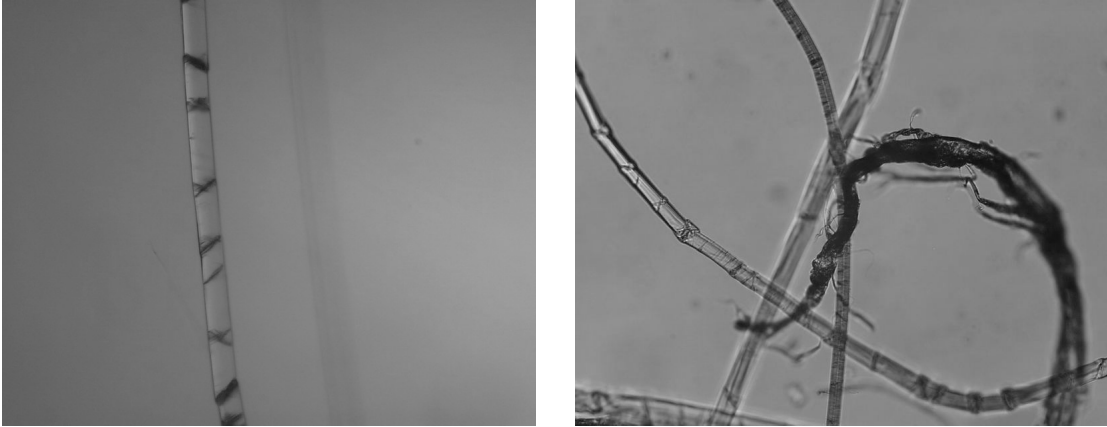


Figure 29. Needle Punched (L) (173x) and Impact (R) (173x) Vectran®

The fiber melting is evidence of a phase change resulting from projectile impact. In order to determine that actual melting occurred, images were taken under polarized light to observe a color band change in the fiber sections. Polarized images were taken for Spectra® 3.6, Dyneema® and Vectran® since these are the fibers that could experience melting during impact.

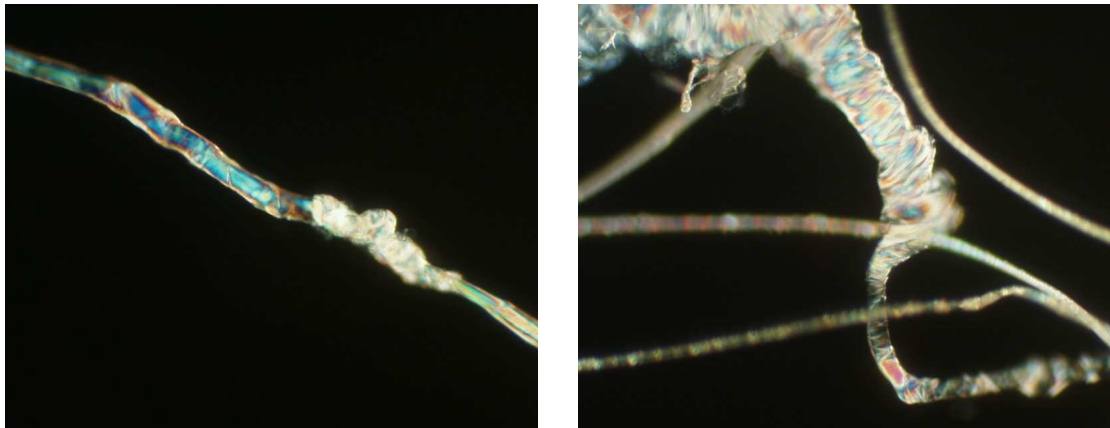


Figure 30. Polarized Dyneema® (250x)

The two Dyneema® images in Figure 30 both show colored bands in the pre-melt fiber which are distorted in the melted section. The image on the left shows a pre-melt fiber with a blue center and orange edges which deforms into a white clump in the melted fiber

section. In the lower right quadrant of the right image, a pre-melt fiber section with a red center and white edges deforms upward into a melted fiber clump with white, orange, blue, and green areas of color.

The Spectra® 3.6 polarized images, shown in Figure 31, exhibit clear signs of melting. The topmost fiber is a non-impact Spectra® 3.6 which shows distinct stripes of color with yellow in the center, blue on the bottom, and orange on the top. The melted fiber shows the same colors but in distorted bands clearly interrupted by the melting phase change.

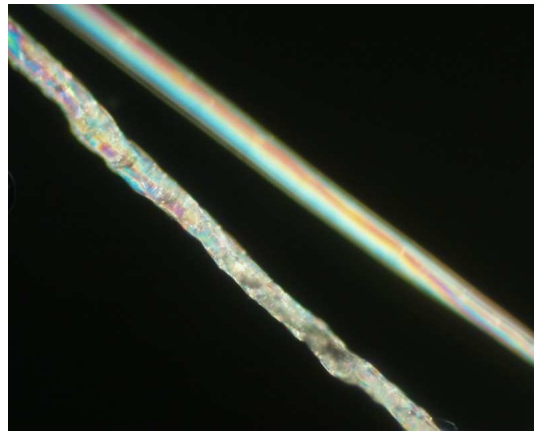


Figure 31. Polarized Spectra® 3.6(273x)

The Vectran® polarized images, in Figure 32, show changes in translucence rather than color.

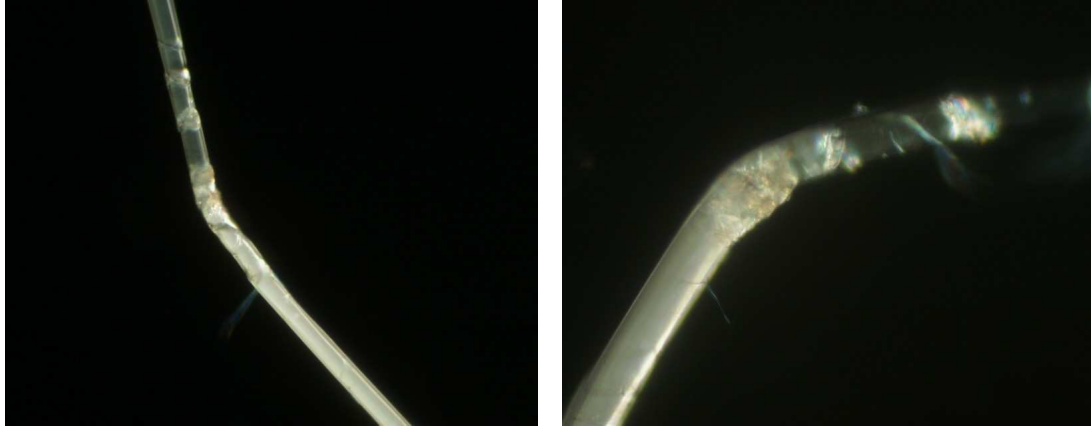


Figure 32. Polarized Vectran® (173x/328x)

These images show a transition from the clear pre-melted fiber to the opaque melted fiber. In the left image, the transition can be seen in the top left quadrant where some deformation and fibrillation begins. The right image shows a more magnified view of this transition as the fiber becomes opaque at the fiber bend where deformation and fibrillation begin.

4.1.2.2. Discussion

The impact damage seen in the photographic images is characteristic of the fibers tested based on the research found in Section 2.2.1, Chapter 2. The aramid fibers showed axial splitting, the UHMWPE fibers showed melting and surface scarring, and the Vectran® fibers exhibited both melting and axial splitting.

The polarized light images do show band color changes in the Dyneema® and Spectra®3.6 samples, and translucency changes in the Vectran® fibers. This is confirmation that the fibers experienced a phase change. It does not, however, give information regarding how much energy dissipation can be attributed to this phase change and if that dissipated energy is a legitimate contributor to the blend's superiority over the standard woven armor.

Another observation based on the photographic images is that the needlepunch fabric formation process did not significantly damage the fibers.

4.1.3 V₅₀ Test

Ballistic V₅₀ testing was performed according to military standard MIL-STD-622F at H. P. White Laboratories, an independent NIJ certified testing facility in Street, Maryland. This testing provides the velocity at which 50% of the projectiles pass through the fabric. More information on the V₅₀ test procedure can be found in Section 3.2.3 of Chapter 3.

4.1.3.1 Results

The V₅₀ test results in Table 4 show that the sample with the highest V₅₀ is the Dyneema®/KM2® combination with a value of 1038.5 m/s (3404 ft/sec).

Sample	Sample Composition®	Punch Density punches/cm ² (punches/in ²)	Woven Layers	V ₅₀ (m/s)	V ₅₀ (ft/s)	Pass/Fail
13	SPECTRA 3.6/KM2	118(300)	37	986.3	3236	F
25	DYNEEMA/KM2	118(300)	37	1038	3404	F
26	DYNEEMA/KM2/VECTRAN	118(300)	37	994.3	3262	P
27	DYNEEMA/TWARON	118(300)	37	1001	3284	P
28	DYNEEMA/TWARON	236(600)	37	979	3212	F
29	DYNEEMA/TWARON/VECTRAN	118(300)	37	974.4	3197	F
30	DYNEEMA/TWARON/VECTRAN	118(300)	39	995.2	3265	P
31	SPECTRA 2.2/TWARON	118(300)	37	1004	3294	P
32	SPECTRA 2.2/TWARON/VECTRAN	118(300)	37	978	3210	F
33	SPECTRA 3.6/TWARON	118(300)	37	990	3248	P
34	SPECTRA 3.6/KM2	118(300)	38	1023	3356	P
37	8.5OZ. SPECTRA 3.6/K129	118(300)	37	1006	3299	P
38	8 OZ. SPECTRA 6.3/K129	118(300)	37	994.6	3263	P
39	5.8 OZ. DYNEEMA /K129	118(300)	37	1004	3294	P
40	8 OZ. DYNEEMA /K129	118(300)	37	1002	3286	P

Table 4. V₅₀ Test Results

The sample with the lowest V_{50} value is the Vectran®/Dyneema®/Twaron® combination with a value of only 974.4 m/s (3197 ft/sec). The NES V_{50} values are evaluated on a pass/fail basis according to the parameters of the military standard MIL-STD-662F. This standard specifies that soft body armor must have V_{50} values of 1005.8 m/s (3300 ft/s) with an allowable deviation of 19 m/s (62.5 ft/s) which passes V_{50} values in the range of 986.8 m/s (3237.5 ft/s) to 1024.8 m/s (3392.5 ft/s).

4.1.3.2 Discussion

The majority of the NES samples performed well under V_{50} testing, with ten of fifteen passing the military standard and one sample (13) failing by only 0.5 m/s. Observation of the data provided in Table 4 shows four main trends: success of K129®, V_{50} lowering of Vectran®, the effect of higher punch density, and the raising of V_{50} by the addition of woven layers.

The most consistent results come from the 50/50 K129®/UHMWPE blends. Each of the four NES samples containing this combination have V_{50} test results not only within the passing range but within a 10 m/s spread of the desired V_{50} .

In samples 26, 29, 30 and 32 Vectran® is added to the UHMWPE/aramid combination. The NES samples with Vectran® had lower V_{50} values than the UHMWPE/aramid combination in three out of the four samples.

Samples 27 and 28 share the same fiber composition but have different punch densities. This difference in punch density resulted in Sample 27, with a punch density of 118 punches/cm² (300 punches/in²), passing and Sample 28, with a punch density of 236 punches/cm² (600 punches/in²), failing. The V_{50} for sample 28 was 22 m/s lower than

sample 27. While the ideal punch density for this material cannot be calculated from this data, it is clear that 118 punches/cm² is better than 236 punches/cm².

A well known trend shown by the V_{50} data is that increasing fabric layers results in higher V_{50} values. This is shown in two sample pairs: 13 and 34, 29 and 30. In samples 13 and 34 the addition of one woven layer in sample 34 raised the V_{50} by 37 m/s and allowed sample 34 to pass while sample 13 failed. A similar situation occurred in samples 29 and 30, where the addition of two layers in sample 30 allowed the V_{50} to rise by 20.8m/s and the sample to pass. These test results show that the NES can provide protection against two grain, RCC FSP and has potential to protect against higher threat levels. The preliminary V_{50} test results from H.P. White are provided in Appendix F.

4.1.4 Kinetic Energy Calculation

In order to determine the residual KE of the NES system, an equation was developed in Chapter 3, Section 3.2.4. This calculation is performed for each NES sample and is discussed in the following section.

4.1.4.1 Results

The data to calculate the formula was gathered from the V_{50} test which provided the V_{50} and the complete penetration velocity for each of the NES samples. The basic calculation is shown in equation 6. Each NES sample was calculated according to this data and the results are shown in Table 5.

Sample	Composition®	V₅₀ m/s (ft/s)	Penetration (Complete) V m/s(ft/s)	Residual KE (joules)
13	SPECTRA 3.6/KM2	986(3236)	1045(3429)	7.79
25	DYNEEMA/KM2	1036(3404)	1080(3542)	6.05
26	DYNEEMA/KM2/VECTRAN	994(3262)	1055(3462)	8.12
27	TWARON/DYNEEMA	1001(3284)	1062(3485)	8.18
28	TWARON/DYNEEMA	979(3212)	1039(3409)	7.87
29	VECTRAN/DYNEEMA/TWARON	974(3197)	1027(3369)	6.89
30	VECTRAN/DYNEEMA/TWARON	995(3265)	1046(3433)	6.77
31	TWARON/SPECTRA 2.2	1004(3294)	1056(3466)	6.96
32	TWARON/SPECTRA 2.2/VECTRAN	978(3210)	1037(3402)	7.73
33	SPECTRA 3.6/TWARON	990(3248)	1025(3362)	4.58
34	SPECTRA 3.6/KM2	1023(3356)	1062(3483)	5.29
37	8.5OZ. K129/SPECTRA 3.6	1006(3299)	1054(3459)	6.43
38	8 OZ. K129/SPECTRA 6.3	995(3263)	1045(3427)	6.63
39	5.8 OZ. 50/50 K129/DYNEEMA	1004(3294)	1057(3467)	7.10
40	8 OZ. K129/DYNEEMA	1002(3286)	1053(3454)	6.81

Table 5. KE Calculation Data

4.1.4.2 Discussion

The results from this calculation show which samples dissipated the greatest energy and therefore permitted the least amount of energy to exit the armor. The results show an average residual energy of 6.88 joules with a standard deviation of 1.02 joules. The highest residual energy (the poorest anti-ballistic performance) was 8.18 joules and occurred in sample 27, a 50/50 Twaron®/Dyneema® blend. The lowest residual energy (best anti-ballistic performance) was found in sample thirty-three, a 50/50 Spectra® 3.6/Twaron® blend, with a residual energy of 4.58 joules.

CHAPTER FIVE: CONCLUSIONS

The purpose of this research was to determine if a phase change occurred within the NES samples and if that phase change dissipated enough energy to be a contributing factor in the superiority of the NES over the traditional woven structure. The testing implemented was DSC, Microscopy, V_{50} , and KE calculations.

The DSC plots of the UHMWPE and Vectran® fibers from impact sites and from non-impact sites did not follow the same thermal patterns. Despite the apparent phase change support, these results were not conclusive because further testing and a larger sample group are required to eliminate mere anomalies.

The microscopic images were used to show that the needlepunching process did not significantly damage the NES and that the fibers responded to impact in this structure with the same energy dissipation mechanisms observed in woven structures. The aramid fibers underwent axial splitting, the UHMWPE fibers experienced deformation and melt, and the Vectran® fibers experienced both phenomena. The melting seen in the UHMWPE and Vectran® fibers was further solidified through the use of polarized light. These polarized images show how the non-melt fiber reflects the light in axial color bands while the melted fiber areas exhibit interrupted and distorted areas of color. This evidence of melting shows that a phase change occurred within the NES structure as a result of impact.

The overall ability of the NES to function as soft body armor was proven by the V_{50} ballistic testing. The results of this test show a majority of the NES samples pass governmental standards with the most suitable sample being a 50/50 blend of K129® and any UHMWPE. It was also observed that Vectran® consistently decreased the V_{50} limits when combined with aramids and UHMWPE and that a NES with a punch density of 118 punches/cm² (300 punches/in²) produced better V_{50} results than a NES with a punch density of 236 punches/cm² (600 punches/in²).

The calculation of residual kinetic energy provided approximations on the ballistic performance of the various NES. Based on these approximations a 50/50 Spectra® 3.6/Twaron® blend had the lowest residual energy, and therefore provided the best anti-ballistic protection. The highest residual energy, and therefore poorest anti-ballistic performance, occurred in a 50/50 Twaron®/Dyneema® blend. While these are the two outliers, each of the samples had residual kinetic energies within a 4 joule spread of each other.

Further research is needed to determine the magnitude of energy dissipation resulting from the phase change and this dissipation's relationship to the NES performance. DSC testing could be conducted with a larger sample population and a higher number of tests in order to determine if permanent thermal disruptions are evident in impacted samples. Another suggestion for future work would involve further testing on LCP fibers in a 50/50 Vectran®/aramid blend which would then be subjected to V_{50} testing and residual KE calculations.

The overall conclusion that can be drawn from this research is that there is evidence of a phase change in the NES and that the NES structures outperform woven

armor on a mass basis. What can no be concluded is whether this phase change dissipates enough energy to be a contributing factor to the NES superiority. The phase change is most strongly evidenced by the microscopic signs of melting and is potentially supported by the irregular DSC thermal patterns in impacted fibers. The V_{50} passing values and residual KE approximations further evidence the NES ability to compete with woven armor.

WORKS CITED

- Adanur, Sabit 2001, *Handbook of Weaving*. Technomic Publishing Company, Inc. Lancaster, PA.
- Adanur, Sabit 1995, *Wellington Sears Handbook of Industrial Textiles*. Technomic Publishing Company, Inc. Lancaster, PA.
- Backman, Marvin, E., and Werner Goldsmith 1978, 'The Mechanics of Penetration of Projectiles into Targets.' *International Journal of Engineering Science*. Volume 16, pp.1-99.
- Bazhenov, S., 1997. 'Dissipation of Energy by Bulletproof Aramid Fabric.' *Journal of Materials Science*. Volume 32, pp 4167-4173.
- Bhatnagar, Ashok (ed.) 2006, *Lightweight Ballistic Composites: Military and Law-enforcement Applications*, Woodhead Publishing Limited, Cambridge, England.
- Billmeyer, Fred W. Jr., 1984. *Textbook of Polymer Science*. John Wiley and Sons, Ltd. New York, NY.
- Carr, D.J., 1999. 'Failure Mechanisms of Yarns Subjected to Ballistic Impact.' *Journal of Materials Science Letters*. Volume 18, pp 585-588.
- Cunniff, Philip M., 1992. 'An Analysis of the System Effects in Woven Fabrics Under Ballistic Impact.' *Textile Research Journal*. Volume 62, Issue 9, pp 495-509.
- Cunniff, Philip M., 1996. 'A Semi-Empirical Model for the Ballistic Impact Performance of Textile Based Personnel Armor.' *Textile Research Journal*. Volume 66, Issue 1, pp 45-59.
- Erlich, D.C., D.A. Shockey, and J.W. Simons. "Slow Penetration of Ballistic Fabrics." *Textile Research Journal*. Volume 73, Issue 2, pp 179-184, 2003.
- Hearle, J.W.S. 1989. 'Mechanics of Yarns and Nonwoven Fabrics' in *Textile Structural Composites*. Ed. Tsu-Wei Chou, and Frank K. Ko, Elsevier Publishing Company, NY, NY.
- Hearle, J.W.S., and A.T. Purdy, 1971. 'Research on Energy Absorption by Nonwoven Fabrics.' Contract Number DAJA37-71-C-0554, European Research Office, London, England.
- Hearle, J.W.S., B. Lomas, W.D. Cooke, and I.J. Duerden, 1989. *Fibre Failure and Wear of Materials*. John Wiley and Sons, Ltd. New York, NY.
- Hegde, Raghavendra R., Atul Dahiya, M. G. Kamath, Ramaiah Kotra and Xiao Gao, 2004. 'Polyester Fibers.' *University of Tennessee*. Available at: <http://www.engr.utk.edu/mse/pages/Textiles/Polyester%20fiber.htm>. Accessed July, 17, 2006.
- 'Interceptor Body Armor,' [Online] Accessed 8/1/06. *Global Security*, <http://www.globalsecurity.org/military/systems/ground/interceptor.htm>.

- Jacobs, M.J.N., and J.L.J. Van Dingenen, 2001. 'Ballistic Protection Mechanisms in Personal Armor'. *Journal of Materials Science*. Volume 36, pp 3137-3142.
- Kirkwood, Keith M., John E. Kirkwood, Young Sil Lee, Ronald G. Egres Jr., Eric Wetzel, and Norman J. Wagner, October 2004. 'Yarn Pull-Out as a Mechanism for Dissipating Ballistic Impact Energy in Kevlar® KM-2, Part 1: Quasi-Static Characterization of Yarn Pull-Out.' *Textile Research Journal*. Volume 74, pp. 920-928.
- Kirkwood, Keith M., John E. Kirkwood, Young Sil Lee, Ronald G. Egres Jr., Eric Wetzel, and Norman J. Wagner, November 2004. 'Yarn Pull-Out as a Mechanism for Dissipating Ballistic Impact Energy in Kevlar® KM-2, Part 2: Predicting Ballistic Performance.' *Textile Research Journal*. Volume 74, pp. 939-948.
- Laible, Roy C., 1980. *Ballistic Materials and Penetration Mechanics*. Elsevier Scientific Publishing Company, New York, NY.
- Lim, C.T., V.P.W. Shim, and Y.H. Ng, 2003. 'Finite Modeling of Ballistic Impact of Fabric Armor.' *International Journal of Impact Engineering*. Volume 28, pp 13-31.
- Man Made Fibers*, 1978. Celanese Corporation. New York, NY.
- Martinez, M.A., C. Navarro, R. Cortes, J. Rodriguez, and V. Sanchez-Galvez, 1993. 'Friction and Wear Behavior of Kevlar Fabrics.' *Journal of Materials Science*. Volume 28, pp 1305-1311.
- National Institute of Justice, 'Mission Statement', [Online], Accessed 7/26/06. <http://www.ojp.usdoj.gov/nij/about.htm>.
- NIJ Standard-0101.04 P-BFS performance test summary, Accessed 7/26/06. <http://www.nlectc.org/pdf/files/0101.04RevA.pdf>.
- Plate, N.A., 1993. *Liquid-Crystal Polymers*. Plenum Press. New York, NY.
- 'Poly (p-phenylene terephthalamide).' *Polymers: A Property Database*. [Online] Accessed 7/12/06. <http://www.polymersdatabase.com.spot.lib.auburn.edu/polymer/polymer-frame.asp?entry-id=1770&search-term=twaron>.
- Porwal, P.J., and S.L. Phoenix, 2005. 'Modeling System Effects in Ballistic Impact into Multi-Layered Fibrous Materials for Soft Body Armor.' *International Journal of Fracture*. Volume 125, pp 217-249.
- Prevorsek, D.C., G.A. Harpell, W.D. Kwon, K.L. Li, and S. Young. March 7-10, 1988. 'Ballistic Armor from Extended Chain Polyethylene Fibers.' *33rd SAMPE Symposium*. Anaheim, CA. pp1685-1689.
- Prosser, R.A. 'Penetration of Nylon Ballistic Panels by Fragment Simulating Projectiles, Part I: Linear Approximation of the Relationship Between the Square of the V50 or VC Striking Velocity and the Number of Layers of Cloth in the Ballistic Panel.' U.S. Army Natick Research, Development and Engineering Center, Natick, MA. Technical Report NATICK/TR-85/027L, August, 1985.
- Prosser, Robert, 1988. 'Penetration of Nylon Ballistic Panels by Fragment Simulating Projectiles, Part II: Mechanism of Penetration.' *Journal of the Textile Research Institute*. Volume 58, Issue 3, pp 161-165.
- Shockey, D.A., D.C. Erlich, and J.W. Simons. "Improved Barriers to Turbine Engine Fragments: Interim Report II." DOT/FAA/AR-99/8, II, 2001.
- Speyer, Robert F., 1994. *Thermal Analysis of Materials*. Marcel Dekker, Inc., NY, NY,

- Termonia, Yves, 2004. 'Impact Resistance of Woven Fabrics.' *Textile Research Journal*. Volume 74, Issue 8, pp 723-729.
- "Vectran® LCP Fiber", *MatWeb*, [Online] Accessed July13, 2006 <http://www.matweb.com/search/SpecificMaterial.asp?bassnum=PCELAN00>.
- Vinson, J.R., and J.A. Zukas, 1975. 'On the Ballistic Impact of Textile Body Armor.' *Journal of Applied Mechanics*. Volume 42, pp 263-268, June 1975.
- Wilde, A.F., D.K. Roylance, and J.M. Rogers, 1973. 'Photographic Investigation of High-Speed Missile Impact upon Nylon Fabric, Part I: Energy Absorption and Cone Radial Velocity in Fabric.' *Textile Research Journal*. Volume 43, pp 753-761.
- Wittrock, E.P., and T.W. Ipson. "Response on Nonwoven Synthetic Fiber Textiles to Ballistic Impact." Report Number USA-NLABS-TR-67-8-CM. pp 124. Headquarters Quartermaster Research and Development Command, Natick, MA, 1966.

APPENDICIES

APPENDIX A: TEST STANDARDS

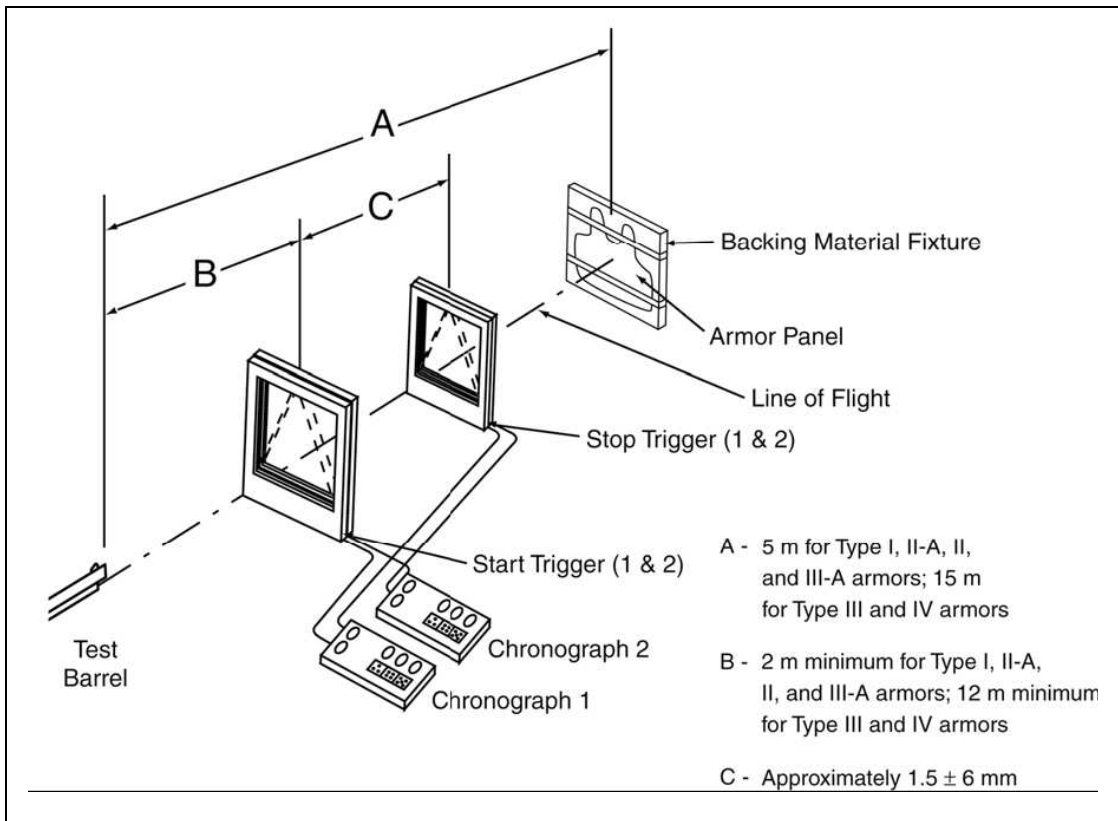


Figure 33. Ballistic Testing Set-Up (Bhatnagar, pg 139, 2006)

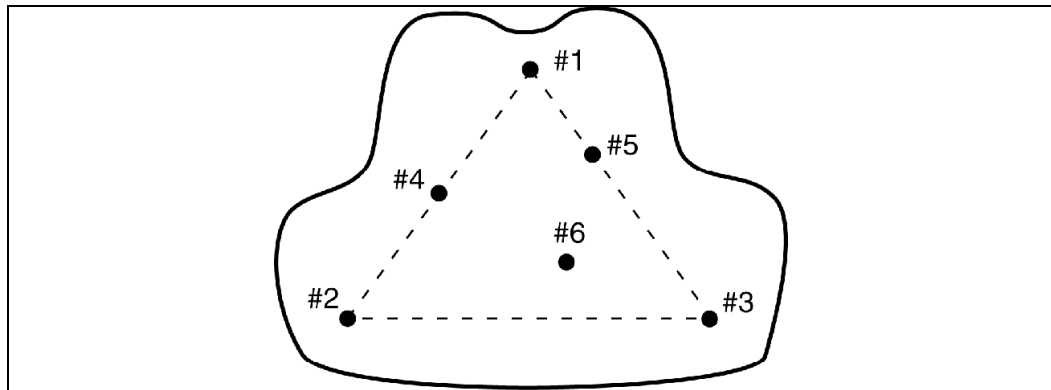


Figure 34. Ballistic Testing Shot Pattern (Bhatnagar, pg 243, 2006)

4.4.4.1 Ballistic Resistance Testing. The flexible body armor components shall be tested IAW MIL-STD-662F except for mounting of the sample which shall be in accordance with MIL-C-44050A, Section 4.3.6.f for testing against 2-, 4-, 16-, and 64-grain right circular cylinders with a L/D=1 at 0 degrees obliquity. V50 ballistic protection limits (no clay) shall be not less than 2-grain – 3300 ft/sec, 4-grain – 2700 ft/sec, 16-grain – 2225 ft/sec, and 64-grain – 1825 ft/sec when using a 10-shot V50 (5 partial penetrations and 5 complete penetrations) with a maximum spread of 125 feet per second. The flexible body armor components shall also be tested IAW NIJ 0101.04 against the 9 mm x 19 mm bullet. The flexible body armor shall have no complete penetrations when tested IAW the NIJ 0101.04 methodology for this specific projectile with the exception that the velocity will be 1500 ft/sec. A V50 ballistic protection limit shall be established based on first article for quality assurance testing of future lots for fragmentation protection performance (IAW MIL-STD-662 and MIL-C-44050A) and for the 9 mm (IAW NIJ 0101.04). For the 9mm V50, no complete penetration shall occur at a velocity less than the 1500 ft/sec requirement and be acceptable.

V50 ballistic evaluation of the flexible vest for quality conformance/lot acceptance testing shall be conducted with the 4-grain RCC, 16 grain RCC, 64-grain RCC or the 9mm bullet. The government shall select one projectile for each lot testing. It is anticipated that the projectiles will be selected randomly. Based on the results of First article tests, the government may chose to accept a certificate of compliance for the ballistic properties of the ballistic cloth in lieu of additional testing. The Certificates of Compliance shall contain verifiable ballistic test and inspection data. The Government reserves the right to inspect and test the material to verify the validity of the certification. The Government also reserves the right to inspect purchase documentation to verify that specified materials were purchased.

Figure 35. V₅₀ Limit for RCC FSP

APPENDIX B: FIBER INFORMATION

Sample No.	Nonwoven Composition	No. of Woven Layers
13	Spectra 3.6/KM2	37
25	Dyneema/KM2	37
26	Dyneema/KM2/Vectran®	37
27	Twaron/Dyneema	37
28	Twaron/Dyneema	37
29	Twaron/Dyneema/Vectran®	37
30	Twaron/Dyneema/Vectran®	37
31	Twaron/Spectra 2.2	37
32	Twaron/Spectra/Vectran®	37
33	Twaron/Spectra 3.6	37
34	Spectra 3.6/KM2	37
35	Polyester	37
37	Spectra 3.6/K129(8.5oz.)	37
38	Spectra 6.3/K129 (8oz.)	38
39	K129 (5.8oz.)/Dyneema	39
40	K129 (8oz.)/Dyneema	38

Table 6. Fiber Combinations used in Research

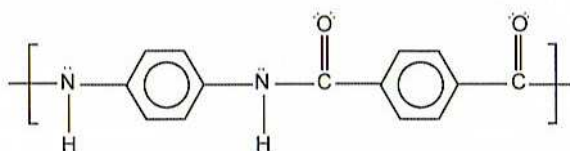


Figure 36. Para-Aramid Structure (Bhatnagar, pg 249, 2006)

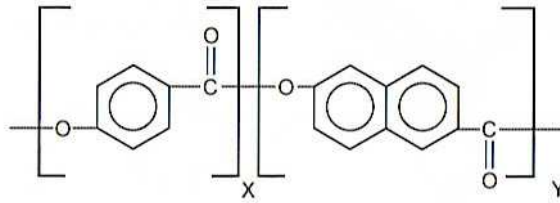


Figure 37. Liquid Crystal Polymer (Bhatnagar, pg 192, 2006)

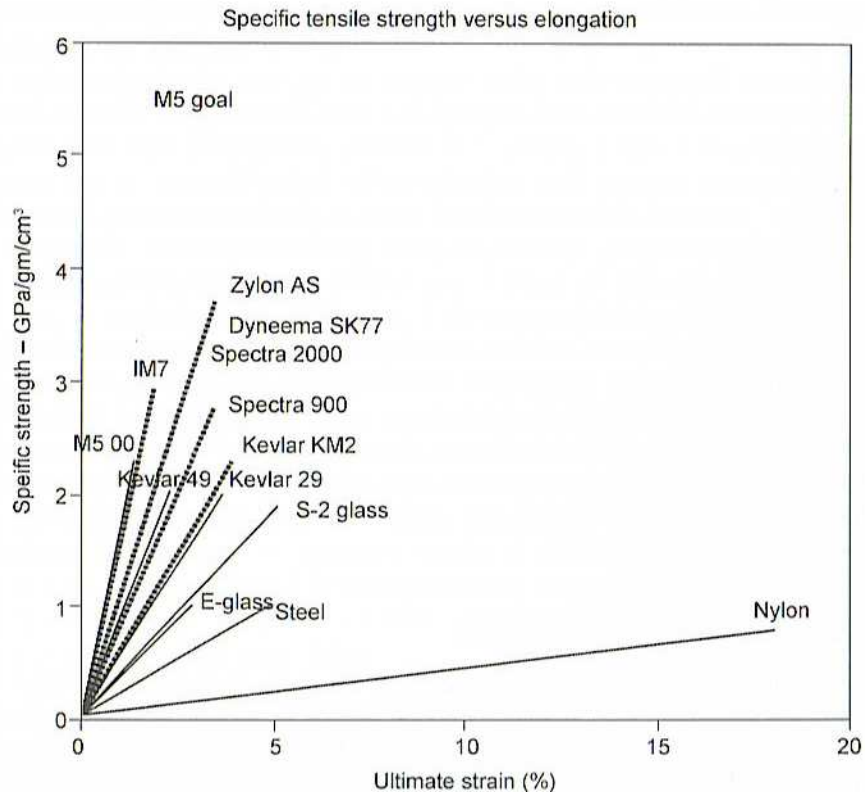
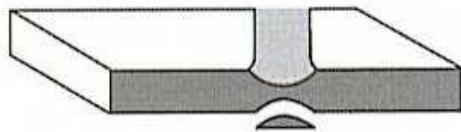


Figure 38. Comparison of Tensile Properties (Bhatnagar, pg 338, 2006)

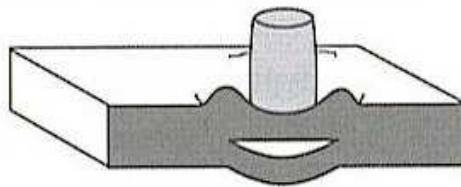
APPENDIX C: DEFORMATIONS



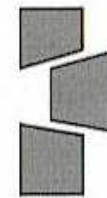
(a) Fracture due to initial stress wave



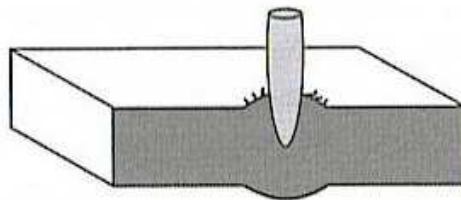
(b) Radial fracture behind initial wave in brittle target



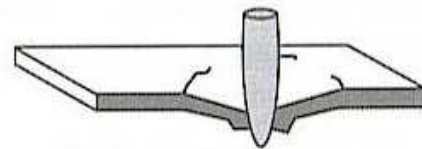
(c) Spall failure (scabbing)



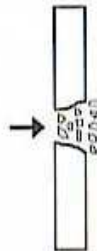
(d) Plugging



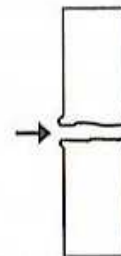
(e) Petalling (frontal)



(f) Petalling (rearwards)



(g) Fragmentation



(h) Ductile hole enlargement

Figure 39. Deformations (Bhatnagar, 2006)

APPENDIX D: IMPACT IMAGES



Figure 40. Spectra ® 3.6(205x)

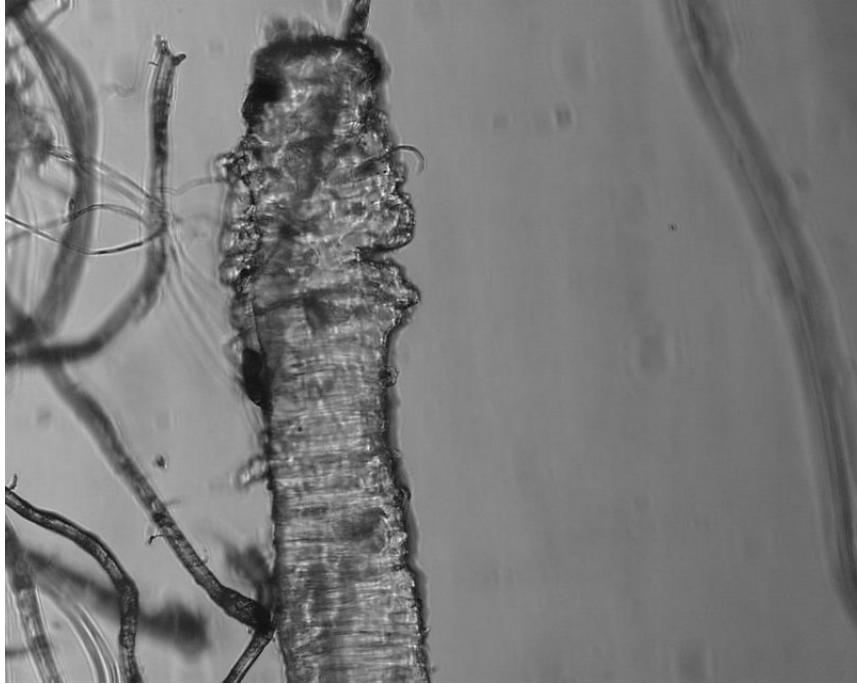


Figure 41. Spectra ®3.6



Figure 42. Spectra® 3.6 (205x)



Figure 43. Spectra® 2.2 (294x)

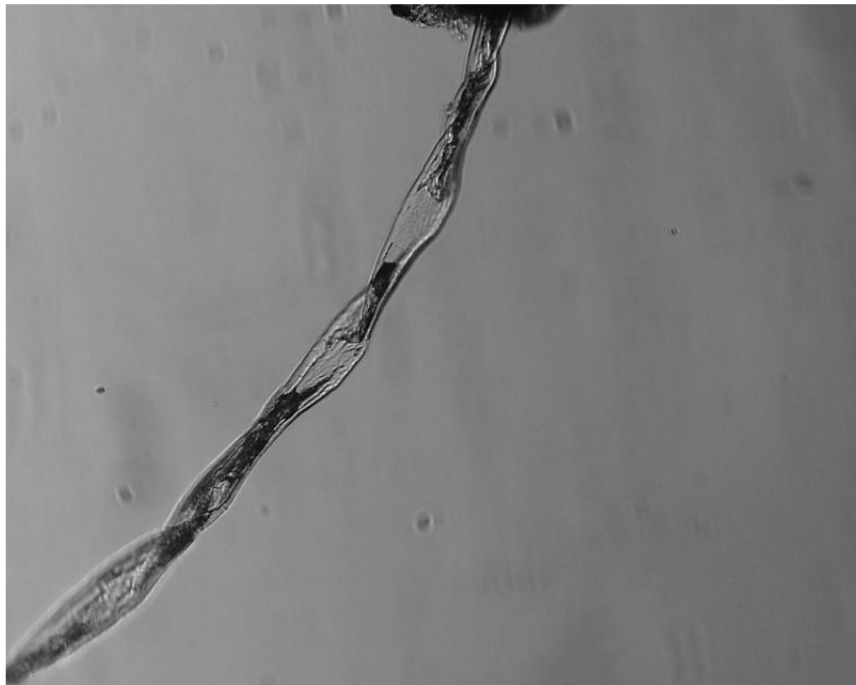


Figure 44. Spectra® 2.2 (294x)



Figure 45. Spectra® 6.3 (172x)

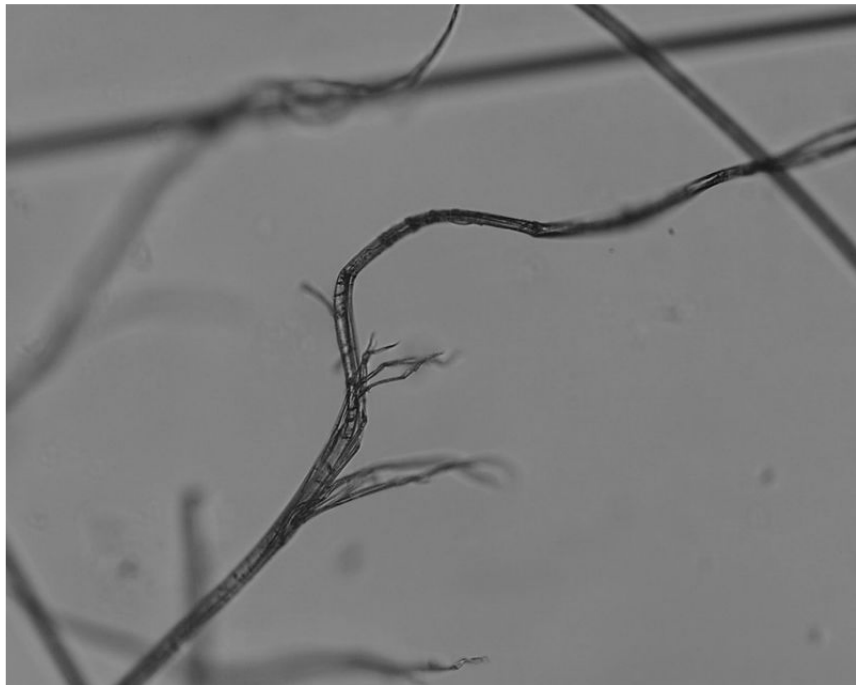


Figure 46. Twaron® (154x)



Figure 47. Dyneema® (214x)



Figure 48. KM2® (111x)



Figure 49. KM2® (111x)

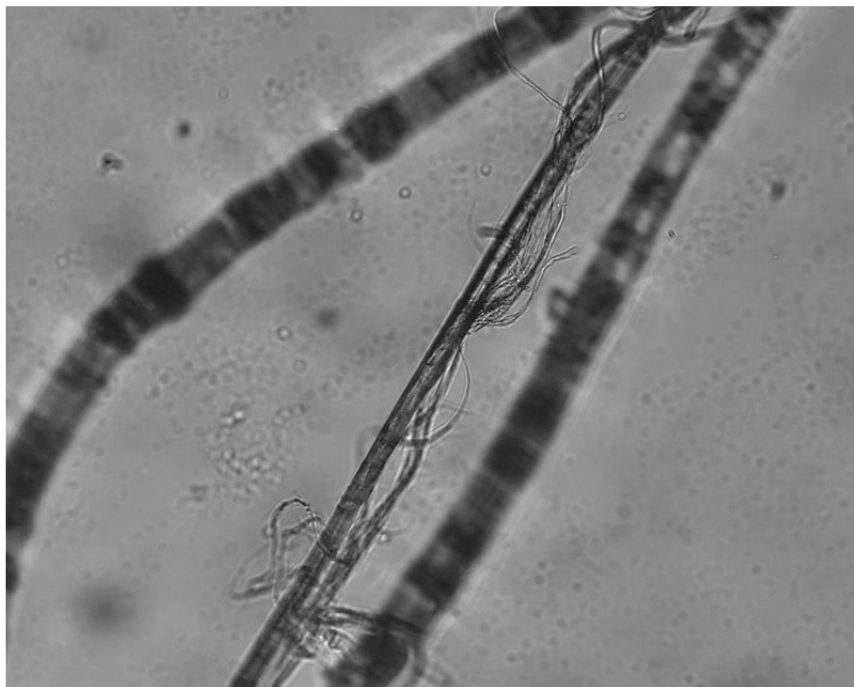


Figure 50. KM2® (167x)



Figure 51. K129® (139x)



Figure 52. K129® (139x)



Figure 53. Vectran® (173x)

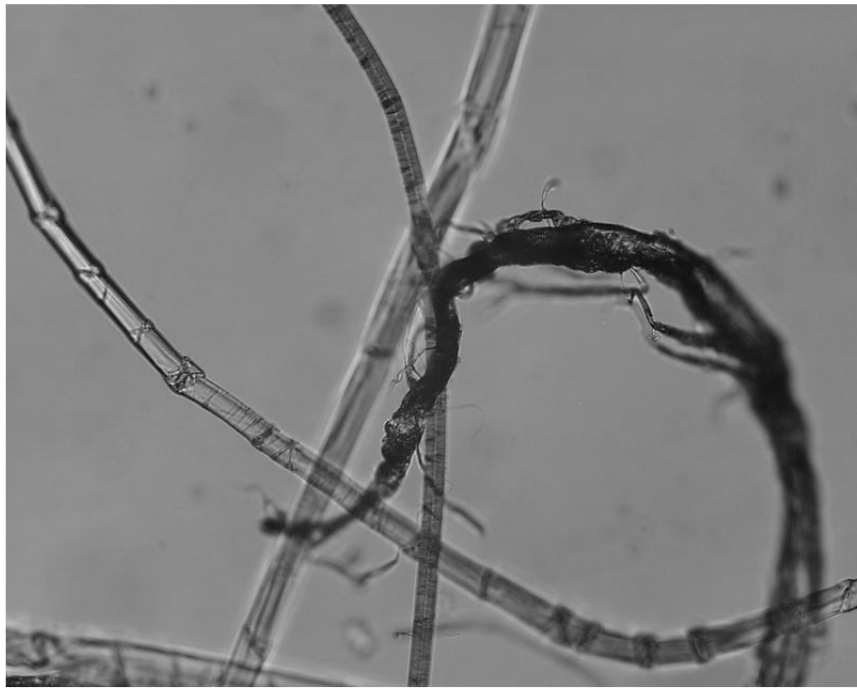


Figure 54. Vectran® (173x)

APPENDIX E: NON-IMPACT IMAGES

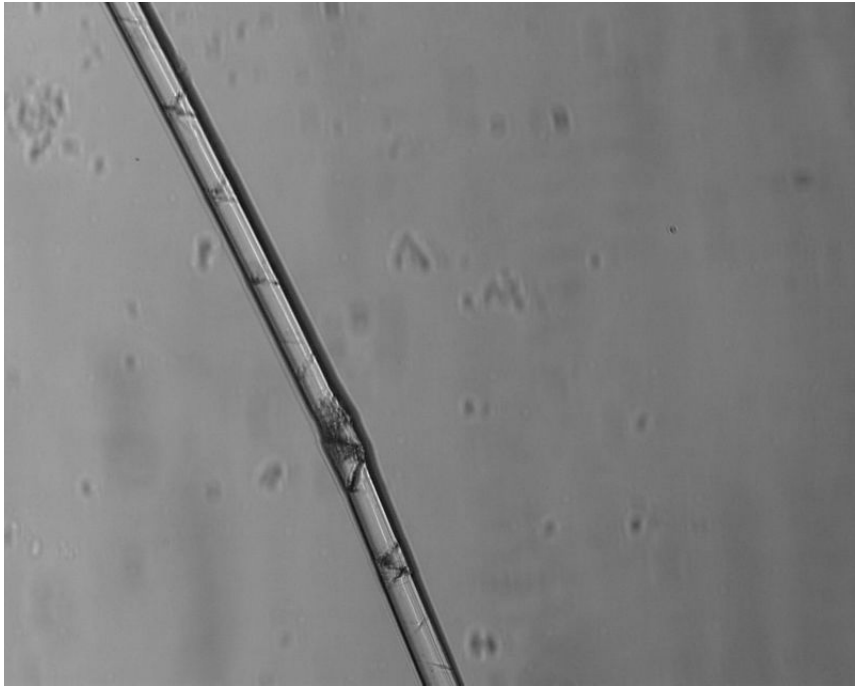


Figure 55. Spectra® 3.6 (227x)

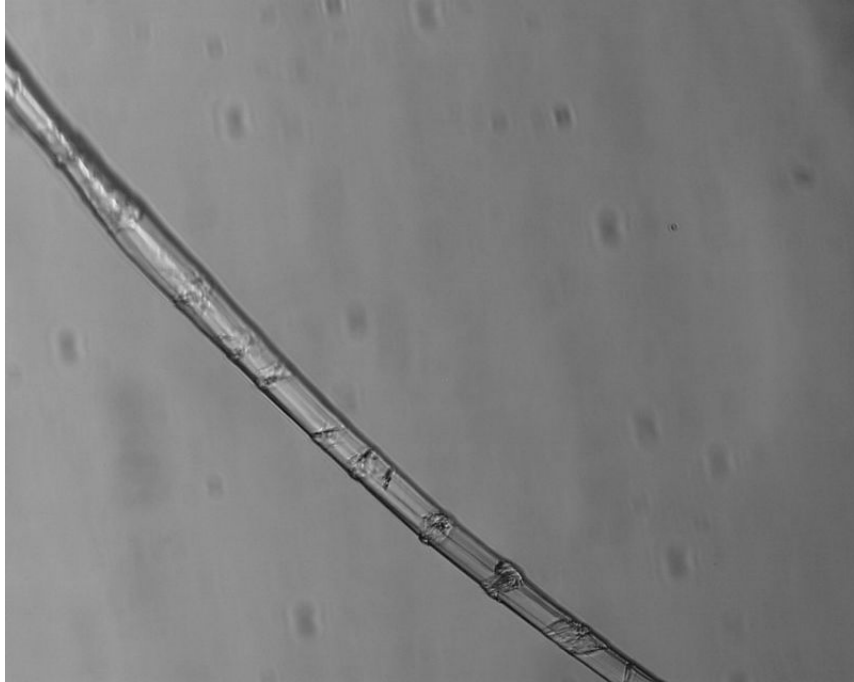


Figure 56. Spectra® 2.2 (294x)

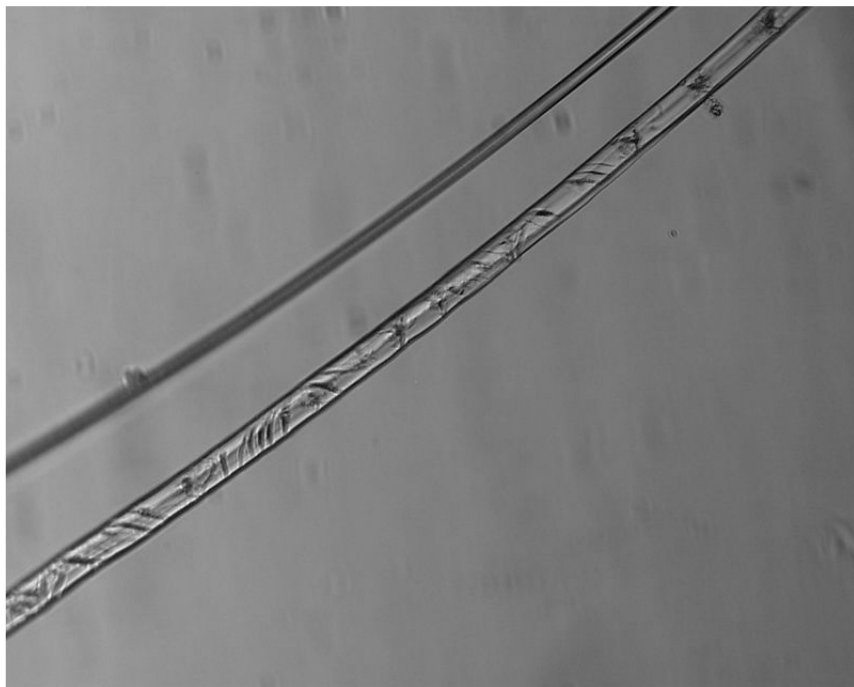


Figure 57. Spectra® 2.2 (294x)



Figure 58. Spectra® 6.3 (172x)

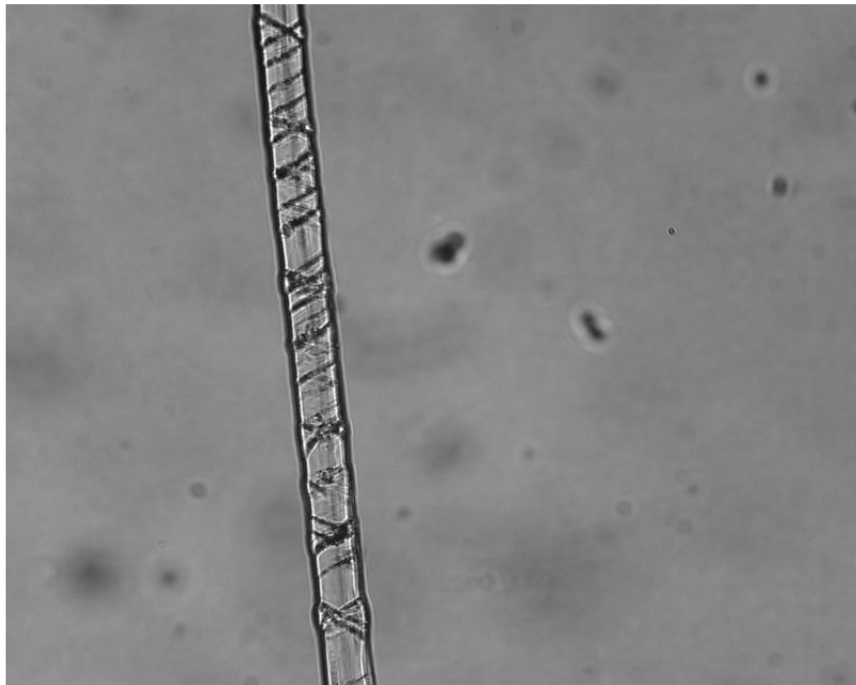


Figure 59. Spectra® 3.6 (363x)



Figure 60. Dyneema® (286x)

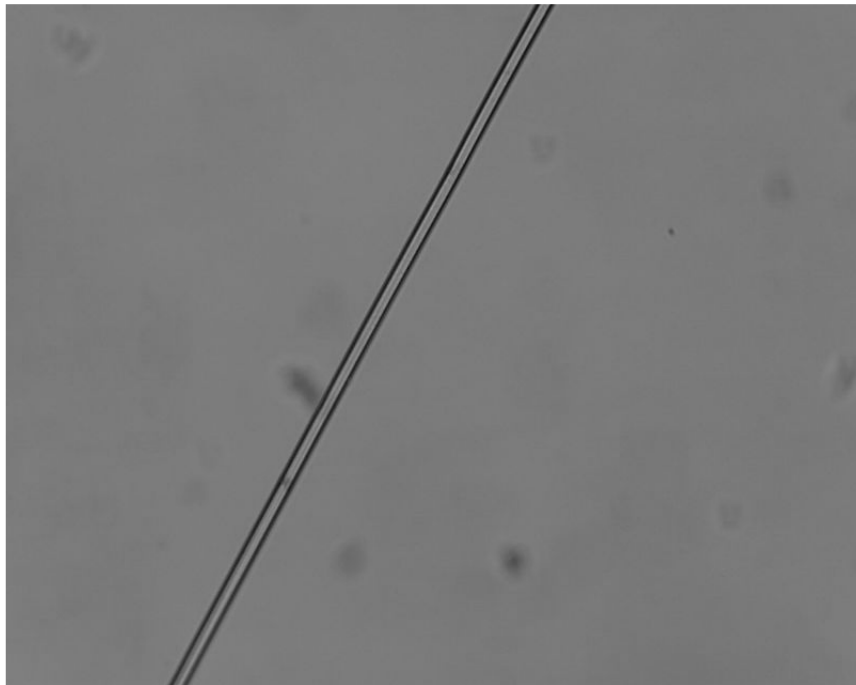


Figure 61. Twaron® (154x)

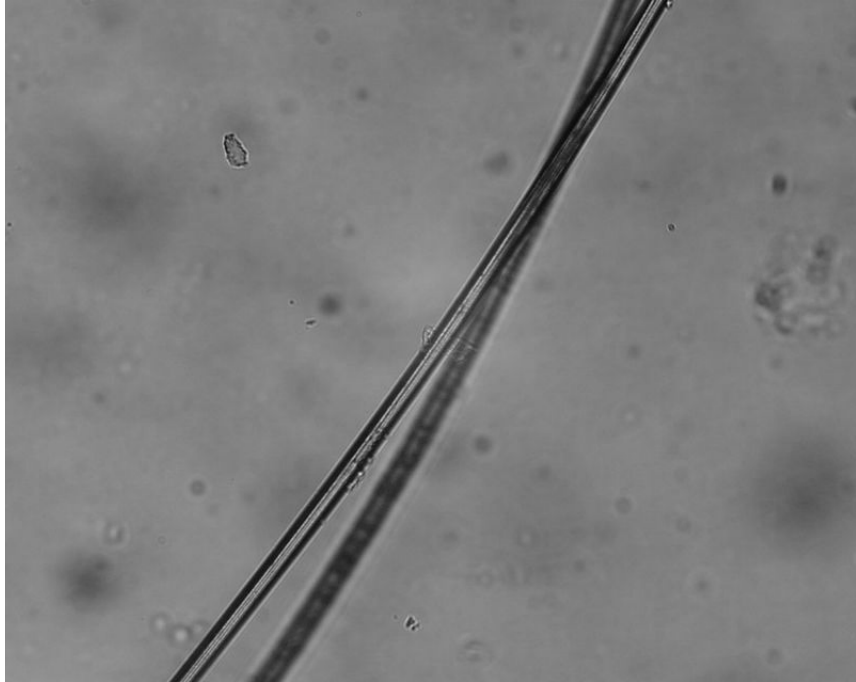


Figure 62. KM2® (139x)

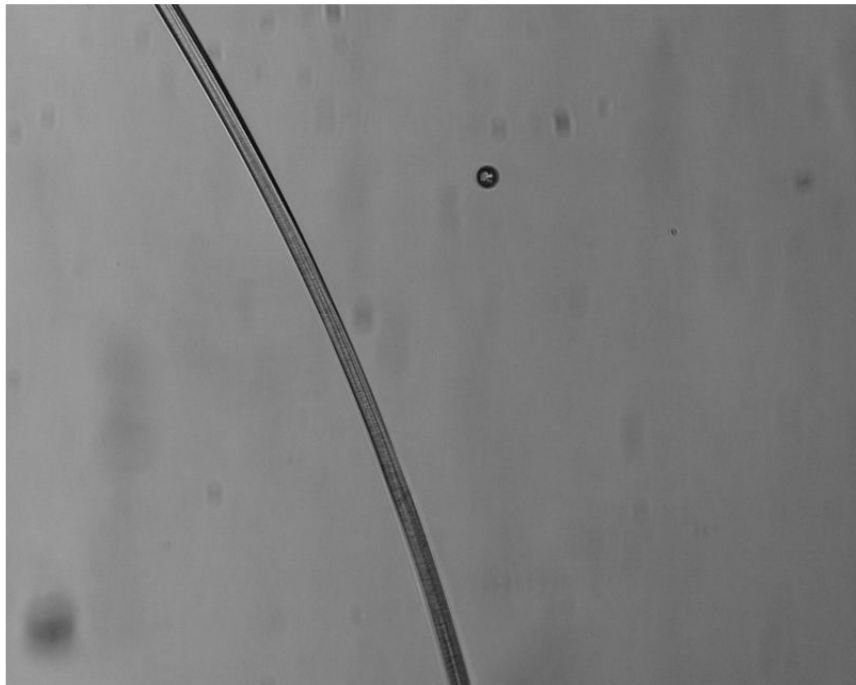



Figure 63. K129® (167x)

APPENDIX F: V₅₀ TEST RESULTS



H.P. White Laboratory, Inc.
PROTECTION BALLISTIC LIMIT TEST, V50 BL(P)

Client : PLAINSMAN ARMOR INTERNATIONAL
Job No. : 9471-01 Test Date : 8/4/04

TEST PANEL

Manufacturer : PLAINSMAN ARMOR INTERNATIONAL
Size : 13 x 13 in.
Thicknesses : NA
Avg. Thick : NA
Required BL(P) : 3300 ft/s
Description : AF 4

Sample No. : SAMPLE-13
Heat No. : NA
Weight : NA lbs.
Hardness : NA
Prest. Ammunition : 41

Date Rec'd. : 08-03-04
Via : Hand Carried
Returned : Hand Carried

PRELIMINARY
 INFORMATION PRESENTED ON THIS DATA RECORD IS SUBJECT TO CORRECTIONS AND/OR REVISIONS

SET-UP

Shot Spacing : PER CUSTOMER REQUEST
Witness Panel : 0.020" 2024-T3 ALUMINUM
Obliquity : 0 deg
Backing Material : NA
Conditioning : AMBIENT

Primary Vel. Screens : 5.0 ft., 8.0 ft.
Primary Vel. Location : 6.5 ft. From Muzzle
Residual Vel. Screens : NA
Residual Vel. Location : NA
Range to Target : 10.0 ft.
Target Size : 6.0 in.

Range No. : 5
Temp. : 75 F
RH : 29.53 in. Hg
RH : 79%
Panel No./Gun : TEST BARREL
Gunner : K. BLACK
Recorder : UNGER

AMMUNITION

Projectile : 2 grain Steel RCC
Powder : BULLSEYE
Lot No. :

APPLICABLE STANDARDS OR PROCEDURES

(1) : AIR WARRIOR
(2) :
(3) :

Shot No.	Powder/Seating	Time (usec)	Velocity (ft/s)	Vel. Loss (ft/s)	Y-Strike (ft/s)	Result	Include in V50	Footnotes
1	8.0	874	3432	158	3275	C	Y	
2	7.8	902	3326	153	3173	P	Y	
3	7.9	884	3394	156	3238	P	Y	
4	8.0	867	3460	159	3301	C	Y	
5	7.9	888	3378	155	3223	P	Y	
6	8.0	886	3386	156	3230	C	Y	
7	7.9	873	3436	158	3278	C	Y	

REMARKS :

FOOTNOTES :

V50 SUMMARY :

No. Points : 3 & 3
V50 : 3236
High Partial : 3238
Low Complete : 3230
Range of Residue : 105
Range of Mixed : 5

Forming | 9471-01 (SAMPLE 13) PLAINSMAN ARMOR INTERNATIONAL V50

Figure 64. Sample 13 (Spectra®3.6/KM2®)



TEST PANEL

Manufacturer : PLAINSMAN ARMOR INTERNATIONAL Sample No. : SAMPLE-26
 Size : 13 x 13 in. Heat No. : NA Date Recd. : 11-18-04
 Thicknesses : NA Weight : 1.74 lbs. Via : Hand Carried
 Avg. Thick. : NA Hardness : NA Returned : UPS
 Required P&P : 3300 ft/s Piles/Laminates : 37
 Description : TWARON 3504/ DYNEEMA KM2/ VECTRAN

SET-UP

Shot Spacing : PER CUSTOMER REQUEST Primary Vel. Screens : 5.0 ft., 7.0 ft. Range No. : 5
 Witness Panel : 0.020" 3024 T3 ALUMINUM Primary Vel. Location : 6.0 ft. From Muzzle Temp. : 68 F
 Obliquity : 0 deg. Residual Vel. Screens : NA Residual Vel. Location : NA EP : 29.94 in. Hg
 Backing Material : NA Range to Target : 9.0 ft. Barrel No./Dia. : TEST BARREL PH : 38%
 Conditioning : AMBIENT Target to WS : 6.0 ft. Gunner : WILSON
 Recorder : UNGER

AMMUNITION

Projectile : 2 grain Steel RCC, 2 gr. Lot No. :
 Powder : BULLSEYE

APPLICABLE STANDARDS OR PROCEDURES

- (1) : AIR WARRIOR
- (2) :
- (3) :

Shot No.	Powder/Sealing	Time (usec)	Velocity (ft/s)	Vel. Loss (ft/s)	V-Sinco (ft/s)	Result	Include in V50	Footnotes
1	8.3	580	3448	136	3312	C		
2	8.1	575	3478	138	3341	P	Y	
3	8.2	569	3515	139	3376	C		
4	8.1	583	3431	136	3295	C	Y	
5	7.9	602	3322	131	3191	C	Y	
6	7.7	574	3484	138	3347	C		
7	7.8	583	3431	136	3295	C	Y	
8	7.6	614	3257	129	3129	P		
9	7.7	593	3373	133	3239	P	Y	
10	7.8	555	3804	143	3461	C		
11	7.7	598	3344	132	3212	P	Y	

REMARKS :	FOOTNOTES :	V50 SUMMARY : No. Points : 3 & 3 V50 : 3262 High Partial : 3341 Low Complete : 3191 Range of Results : 150 Range of Mixed : 150
------------------	--------------------	--

Figure 66. Sample 26 (Dyneema®/KM2®/Vectran®)



TEST PANEL

Manufacturer : PLAINSMAN ARMOR INTERNATIONAL Sample No. : SAMPLE-27
 Size : 13 x 13 in. Heat No. : NA Date Recd. : 11-18-04
 Thicknesses : NA Weight : 1.72 lbs. Via : Hand Carried
 Avg. Thick. : NA Hardness : NA Returned : UPS
 Required D.D.P. : 3300 ft/s Piles/Laminates : 37
 Description : TWARON 3504/ DYNEEMA / TWARON

SET-UP

Shot Spacing : PER CUSTOMER REQUEST Primary Vel. Screens : 5.0 ft., 7.0 ft. Range No. : 5
 Witness Panel : 0.020 2024-T3 ALUMINUM Primary Vel. Location : 6.0 ft. From Muzzle Temp. : 68 F
 Obliquity : 0 deg. Residual Vel. Screens : NA Residual Vel. Location : NA EP : 29.94 in. Hg
 Backing Material : NA Range to Target : 9.0 ft. Range No./Dia. : TEST BARREL
 Conditioning : AMBIENT Target Wt. : 6.0 lb. Gunner : WILSON
 Recorder : UNGER

AMMUNITION

Projectile : 2 grain Steel RCC, 2 gr. Lot No. :
 Powder : BULLSEYE

APPLICABLE STANDARDS OR PROCEDURES

- (1) : AIR WARRIOR
- (2) :
- (3) :

Shot No.	Powder/Seating	Time (usec)	Velocity (ft/s)	Vel. Loss (ft/s)	V-Strike (ft/s)	Result	Include in V50	Footnotes
1	8.0	596	3366	133	3223	C	Y	
2	7.7	593	3373	133	3239	P		
3	7.8	603	3317	131	3186	P		
4	7.9	588	3401	135	3267	P	Y	
5	8.1	589	3396	134	3261	P	Y	
6	8.3	575	3478	136	3341	C	Y	
7	8.2	NR	NR	NR	NR	C		
8	8.2	580	3448	136	3312	P	Y	
9	8.3	559	3578	141	3436	C		
10	8.2	559	3578	141	3436	C		
11	8.1	582	3436	136	3301	C	Y	

REMARKS :	FOOTNOTES :	V50 SUMMARY : No. Points : 3 & 3 V50 : 3284 High Partial : 3312 Low Complete : 3223 Range of Results : 118 Range of Mixed : 89
------------------	--------------------	---

Figure 67. Sample 27(Twaron®/Dyneema®)



H.P. White Laboratory, Inc.
PROTECTION BALLISTIC LIMIT TEST, V50 BL(P)

Client : PLAINSMAN ARMOR INTERNATIONAL

Job No. : 9471-02 Test Date : 11/18/04

TEST PANEL

Manufacturer : PLAINSMAN ARMOR INTERNATIONAL Sample No. : SAMPLE-29
 Size : 13 x 13 in. Heat No. : NA Date Recd. : 11-18-04
 Thickness : NA Weight : 1.76 lbs. Via : Hand Carried
 Avg. Thick. : NA Hardness : NA Returned : UPS
 Required BL(P) : 3300 ft/s Piles/Laminates : 37
 Description : TWARON 3504/ DYNEEMA / TWARON/ VECTRAN

SET-UP

Shot Sizing : PER CUSTOMER REQUEST Primary Vel. Screen : 5.0 ft., 7.0 ft. Range No. : 5
 Witness Panel : 0.020" 2024 T3 ALUMINUM Primary Vel. Location : 6.0 ft. From Muzzle Temp. : 68 F
 Obliquity : 0 deg. Residual Vel. Screen : NA V.P. : 29.94 in. Hg
 Backing Material : NA Residual Vel. Location : NA RH : 38%
 Conditioning : AMBIENT Range to Target : 9.0 ft. Barrel Mfg. Gun : TEST BARREL
 Targeted Wt. : 6.0 in. Gunner : WILSON
 Recorder : UNGER

AMMUNITION

Projectile : 2 grain Steel RCC, 2 gr. Lot No. :
 Powder : BULLSEYE

APPLICABLE STANDARDS OR PROCEDURES

- (1) : AIR WARRIOR
- (2) :
- (3) :

Shot No.	Powder/Seating	Time (ms)	Velocity (ft/s)	Vel. Loss (ft/s)	V-Strike (ft/s)	Result	Include in V50	Footnotes
1	8.3	578	3460	137	3323	C		
2	8.0	584	3425	135	3289	C		
3	7.7	600	3333	132	3202	C	Y	
4	7.4	614	3257	129	3129	G	Y	
5	7.1	629	3180	126	3054	P		
6	7.2	597	3350	132	3218	P	Y	
7	7.3	608	3289	130	3159	P		
8	7.4	600	3333	132	3202	P	Y	
9	7.6	600	3333	132	3202	P		
10	7.7	591	3384	134	3250	P	Y	
11	7.8	584	3425	135	3289	C		
12	7.7	604	3311	131	3180	C	Y	

REMARKS :	FOOTNOTES :	V50 SUMMARY : No. Points : 3 & 3 V50 : 3197 High Partial : 3250 Low Complete : 3129 Range of Results : 121 Range of Mixed : 121
------------------	--------------------	--

Filename : 9471-02 (SAMPLE-29) PLAINSMAN ARMOR INTERNATIONAL V50

Figure 69. Sample 29(Vectran®/Dyneema®/Twaron®)



H.P. White Laboratory, Inc.
PROTECTION BALLISTIC LIMIT TEST, V50 BL(P)

Client : PLAINSMAN ARMOR INTERNATIONAL

Job No. : 9471-02

Test Date : 11/18/04

TEST PANEL

Manufacturer : PLAINSMAN ARMOR INTERNATIONAL Sample No. : SAMPLE-30
 Size : 13 x 13 in. Heat No. : NA Date Rec'd. : 11-18-04
 Thicknesses : NA Weight : 1.76 lbs. Via : Hand Carried
 Avg. Thick. : NA Hardness : NA Returned : UPS
 Required BL(P) : 3300 ft/s Plied/Laminates : 37
 Description : TWARON 3504/ DYNEEMA / TWARON/ VECTRAN AT 5.8 OZ.

SET-UP

Shot Spacing : PER CUSTOMER REQUEST Primary Vel. Screens : 5.0 ft., 7.0 ft. Range No. : 5
 Witness Panel : 0.020" 2024-T3 ALUMINUM Primary Vel. Location : 6.0 ft. From Muzzle Temp. : 68 F
 Obliquity : 0 deg. Residual Vel. Screens : NA Residual Vel. Location : NA RFL : 29.94 in. Hg
 Backing Material : NA Range to Target : 9.0 ft. Barrel No./Class : TEST BARREL
 Conditioning : AMBIENT Target Dia. : 6.0 in. Gunner : WILSON
 Recorder : UNGER

AMMUNITION

Projectile : 2 grain Steel RCC, 2 gr. Lot No. :
 Powder : BULLSEYE

APPLICABLE STANDARDS OR PROCEDURES

- (1) - AIR WARRIOR
- (2) -
- (3) -

Shot No.	Powder/Seating	Time (usec)	Velocity (ft/s)	Vel. Loss (ft/s)	V-Strike (ft/s)	Result	Include in V50	Footnotes
1	7.5	600	3333	132	3202	P	Y	
2	7.8	595	3361	133	3228	P	Y	
3	8.1	586	3413	135	3278	C	Y	
4	8.0	587	3407	135	3272	P	Y	
5	8.2	584	3425	135	3289	C	Y	
6	8.1	578	3460	137	3323	C	Y	

REMARKS :	FOOTNOTES :	V50 SUMMARY : No. Points : 3 & 3 V50 : 3265 High Partial : 3272 Low Complete : 3278 Range of Results : 121 Range of Mixed : 0
------------------	--------------------	--

Filename : 9471-02 (SAMPLE-30) PLAINSMAN ARMOR INTERNATIONAL-V50

Figure 70. Sample 30 (Vectran®/Dyneema®/Twaron®)



H.P. White Laboratory, Inc.

PROTECTION BALLISTIC LIMIT TEST, V50 BL(P)

Client : PLAINSMAN ARMOR INTERNATIONAL

Job No. : 9471-02

Test Date : 11/18/04

TEST PANEL

Manufacturer : PLAINSMAN ARMOR INTERNATIONAL Sample No. : SAMPLE-32
 Size : 13 x 13 in. Heat No. : NA Date Recd. : 11-18-04
 Thicknesses : NA Weight : 1.77 lbs. Via : Hand Carried
 Avg. Thick. : NA Hardness : NA Returned : UPS
 Required BL(P) : 3300 ft/s Piles/Laminates : 37
 Description : TWARON 3504/ SPECTRA 2.2/ VECTRAN

SET-UP

Shot Spacing : PER CUSTOMER REQUEST Primary Vel. Screens : 5.0 ft., 7.0 ft. Range No. : 5
 Witness Panel : 0.020" 2024-T3 ALUMINUM Primary Vel. Location : 6.0 ft. From Muzzle Temp. : 68 F
 Obliquity : 0 deg. Residual Vel. Screens : NA Residual Vel. Location : NA BP : 29.94 in. Hg
 Backing Material : NA Backstop Target : 9.0 ft. Barrel No/Gun : TEST BARREL Rn : 38%
 Conditioning : AMBIENT Target to Wt. : 6.0 in. Gunner : WILSON
 Recorder : LINGER

AMMUNITION

Projectile : 2 grain Steel RCC, 2-gr. Lot No. :
 Powder : BULLSEYE

APPLICABLE STANDARDS OR PROCEDURES

- (1) AIR WARRIOR
- (2)
- (3)

Shot No.	Powder Seating	Time (usec)	Velocity (ft/s)	Vel. Loss (ft/s)	V-Strike (ft/s)	Result	Include in V50	Footnotes
1	8.0	570	3509	139	3370	C		
2	7.8	586	3413	135	3278	C	Y	
3	7.5	622	3215	127	3088	P		
4	7.6	612	3258	129	3139	C	Y	
5	7.5	594	3367	133	3234	P	Y	
6	7.6	590	3390	134	3256	C	Y	
7	7.4	611	3273	129	3144	P	Y	
8	7.5	583	3431	136	3295	C		
9	7.4	598	3344	132	3212	P	Y	

REMARKS :	FOOTNOTES :	V50 SUMMARY : No. Points : 3 & 3 V50 : 3210 High Partial : 3234 Low Complete : 3139 Range of Results : 139 Range of Mixed : 95
------------------	--------------------	---

Filename : 9471-02 (SAMPLE-32) PLAINSMAN ARMOR INTERNATIONAL V50

Figure 72. Sample 32 (Twaron®/Spectra® 2.2/Vectran®)



H.P. White Laboratory, Inc.

PROTECTION BALLISTIC LIMIT TEST, V50 BL(P)

Client : PLAINSMAN ARMOR INTERNATIONAL

Job No. : 9471-02

Test Date : 11/18/04

TEST PANEL

Manufacturer : PLAINSMAN ARMOR INTERNATIONAL Sample No. : SAMPLE-33
 Size : 13 x 13 in. Heat No. : NA Date Rec'd : 11-18-04
 Thicknesses : NA Weight : 1.77 lbs. Via : Hand Carried
 Avg. Thick. : NA Hardness : NA Returned : UPS
 Required BL(P) : 3300 ft/s Flex/Laminates : 37
 Description : SPECTRA / TWARON

SET-UP

Shot Spacing : PER CUSTOMER REQUEST Primary Vel. Screens : 5.0 ft., 7.0 ft. Range No. : 5
 Witness Panel : 0.020" 2024-T3 ALUMINUM Primary Vel. Location : 6.0 ft. From Muzzle Temp. : 68 F
 Obliquity : 0 deg. Residual Vel. Screens : NA Residual Vel. Location : NA BP : 29.94 in. Hg
 Backing Material : NA Bugle to Target : 9.0 ft. Panel No./Dia. : TEST BARREL RH : 38%
 Conditioning : AMBIENT Target to Wall : 6.0 ft. Gunner : WILSON
 Recorder : UNGER

AMMUNITION

Projectile : 2 grain Steel RCC, 2 gr. Lot No. :
 Powder : BULLSEYE

APPLICABLE STANDARDS OR PROCEDURES

- (1) : AIR WARRIOR
- (2) :
- (3) :

Shot No.	Powder/Seating	Time (usec)	Velocity (ft/s)	Vel. Loss (ft/s)	V-Strike (ft/s)	Result	Include in V50	Footnotes
1	7.8	603	3317	131	3188	C	Y	
2	7.6	612	3268	129	3139	P	Y	
3	7.7	576	3472	137	3335	P	Y	
4	7.8	603	3317	131	3186	C	Y	
5	7.7	583	3431	136	3295	P	Y	
6	7.8	588	3401	135	3267	C	Y	
7	7.7	586	3413	135	3278	C	Y	
8	7.6	597	3350	132	3218	P	Y	

REMARKS :	FOOTNOTES :	V50 SUMMARY : No. Points : 3 & 3 V50 : 3248 High Partial : 3335 Low Complete : 3186 Range of Results : 149 Range of Mixed : 149
------------------	--------------------	--

Filename : 9471-02 (SAMPLE-33) PLAINSMAN ARMOR INTERNATIONAL V50

Figure 73. Sample 33 (Spectra ®3.6/Twaron®)



H.P. White Laboratory, Inc.

PROTECTION BALLISTIC LIMIT TEST, V50-BL(P)

Client : PLAINSMAN ARMOR INTERNATIONAL

Job No. : 9471-02

Test Date : 11/18/04

TEST PANEL

Manufacturer : PLAINSMAN ARMOR INTERNATIONAL
 Size : 13 x 13 in.
 Thicknesses : NA
 Avg. Thick : NA
 Required RUP : 3300 fms
 Description : SPECTRA / KM2

Sample No. : SAMPLE-34
 Heat No. : NA
 Weight : 1.79 lbs.
 Hardness : NA
 Plate Lamination : 37

Date Rec'd : 11-18-04
 Via : Hand Carried
 Returned : UPS

SET-UP

Shot Spacing : PER CUSTOMER REQUEST
 Witness Panel : 0.020" 2024 T3 ALUMINUM
 Obliquity : 0 deg.
 Backing Material : NA
 Conditioning : AMBIENT

Primary Vel. Screens : 5.0 ft., 7.0 ft.
 Primary Vel. Location : 6.0 ft. From Muzzle
 Residual Vel. Supports : NA
 Residual Vel. Location : NA
 Range to Target : 9.0 ft.
 Target to WP : 6.0 in.

Range No. : 5
 Temp. : 68 F
 BP : 29.94 in. Hg
 RH : 38%
 Barrel No./Gun : TEST BARREL
 Gunner : WILSON
 Recorder : UNGER

AMMUNITION

Projectile : 2 grain Steel RCC, 2 gr.
 Powder : BULLSEYE

Lot No. :

APPLICABLE STANDARDS OR PROCEDURES

- (1) - AIR WARRIOR
- (2) -
- (3) -

Shot No.	Powder/Seating	Time (usec)	Velocity (ft/s)	Vel. Loss (ft/s)	V-Strike (ft/s)	Result	Include in V50	Footnotes
1	8.0	584	3425	135	3289	P	Y	
2	8.3	571	3503	139	3364	P	Y	
3	8.5	557	3591	142	3449	P	Y	
4	8.7	567	3527	139	3388	C	Y	
5	8.6	585	3419	135	3284	C	Y	
6	8.5	571	3503	139	3364	C	Y	

REMARKS :

FOOTNOTES :

V50 SUMMARY :

No. Points : 3 & 3
 V50 : 3356
 High Partial : 3449
 Low Complete : 3284
 Range of Results : 165
 Range of Mixed : 165

Filename : 9471-02 (SAMPLE-34) PLAINSMAN ARMOR INTERNATIONAL V50

Figure 74. Sample 34 (Spectra ®3.6/KM2®)



H.P. White Laboratory, Inc.
PROTECTION BALLISTIC LIMIT TEST, V50 BL(P)

Client: PLAINSMAN ARMOR INTERNATIONAL
 Job No.: 0471-03 Test Date: 12/10/04

TEST PANEL

Manufacturer: PLAINSMAN ARMOR INTERNATIONAL
 Size: 13 x 13 in.
 Thickness: NA
 Avg. Thick: NA
 Required BLPI: 3300 ft/s
 Description: K129 + SPECTRA 435 + TWARON 3504

Sample No.: SAMPLE-37
 Heat No.: NA
 Weight: 1.74 lbs.
 Hardness: NA
 Piles/Laminates: 43

Date Recd.: 12-09-04
 Via: U/PS
 Returned: U/PS

SET-UP

Shot Spacing: PER CUSTOMER REQUEST
 Witness Panel: 0.020", 2024-T3 ALUMINUM
 Obliquity: 0 deg.
 Backing Material: NA
 Conditioning: AMBIENT

Primary Vel. Screens: 5.0 ft., 7.0 ft.
 Primary Vel. Location: 8.0 ft. From Muzzle
 Residual Vel. Screens: NA
 Residual Vel. Location: NA
 Range to Target: 9.0 ft.
 Target to WL: 8.0 in.

Range No.: 5
 Temp.: 66 F
 BP: 29.23 in. Hg
 RH: 54%
 Barrel No./Gun: TEST BARREL
 Gunner: UNGER
 Recorder: UNGER

AMMUNITION

Projectile: 2 grain Steel RCC, 2 gr.
 Powder: BULLSEYE

Lot No.:

APPLICABLE STANDARDS OR PROCEDURES

- (1): AIR WARRIOR
- (2):
- (3):

Shot No.	Powder Seating	Time (usec)	Velocity (ft/s)	Vel. Loss (ft/s)	V-Strike (ft/s)	Result	Include in V50	Footnotes
1	8.2	581	3442	136	3306	P	Y	
2	8.4	579	3454	137	3318	P	Y	
3	8.5	577	3466	137	3329	C	Y	
4	8.5	572	3497	138	3358	C	Y	
5	8.4	585	3413	135	3278	C	Y	
6	8.2	599	3339	132	3207	P	Y	

REMARKS:

FOOTNOTES:

V50 SUMMARY:

No. Points: 3 & 3
 V50: 3288
 High Partial: 3318
 Low Complete: 3278
 Range of Results: 151
 Range of Mixed: 40

Figure 75. Sample 38 (8 oz. K129®/Dyneema®)



H.P. White Laboratory, Inc.

PROTECTION BALLISTIC LIMIT TEST, V50 BL(P)

Client: PLAINSMAN ARMOR INTERNATIONAL

Job No. 9471-03

Test Date: 12/10/04

TEST PANEL

Manufacturer: PLAINSMAN ARMOR INTERNATIONAL
 Size: 13 x 13 in.
 Thickness: NA
 Avg. Thick: NA
 Required BLPI: 3300 ft/s
 Description: K129 + SPECTRA 650 + TWARON 3504

Sample No.: SAMPLE-38
 Heat No.: NA
 Weight: 1.77 lbs.
 Hardness: NA
 Ply/Laminated: 42

Date Rec'd: 12-09-04
 Via: UPS
 Returned: UPS

SET-UP

Shot Spacing: PER CUSTOMER REQUEST
 Witness Panel: 0.020", 2024-T3 ALUMINUM
 Obliquity: 0 deg.
 Backing Material: NA
 Conditioning: AMBIENT

Primary Vel. Screens: 5.0 ft., 7.0 ft.
 Primary Vel. Location: 6.0 ft. From Muzzle
 Residual Vel. Screens: NA
 Residual Vel. Location: NA
 Range to Target: 0.0 ft.
 Target to Wall: 6.0 in.

Range No.: 5
 Temp: 66 F
 BP: 29.23 in. Hg
 RH: 54%
 Barrel No./Gun: TEST BARREL
 Gunner: UNGER
 Recorder: UNGER

AMMUNITION

Projectile: 2 grain Steel RCC, 2 gr.
 Powder: BULLSEYE

Lot No. 1

APPLICABLE STANDARDS OR PROCEDURES

- (1) AIR WARRIOR
- (2) -
- (3) -

Shot No.	Powder/Boatling	Time (ms)	Velocity (ft/s)	Vel. Loss (ft/s)	V-Score (ft/s)	Result	Include in V50	Footnote
1	8.1	599	3339	132	3207	P	Y	
2	8.3	593	3373	133	3239	C	Y	
3	8.2	595	3361	133	3228	P	Y	
4	8.3	595	3361	133	3228	P	Y	
5	8.4	583	3431	136	3295	G	Y	
6	8.3	592	3378	134	3245	P	Y	
7	8.4	575	3478	138	3341	C	Y	

REMARKS:

FOOTNOTES:

V50 SUMMARY:

No. Points: 3 & 3
 V50: 3263
 High Percent: 3245
 Low Percent: 3239
 Range of Results: 115
 Range of Mean: 8

Figure 76. Sample 37 (8.5 oz. K129®/Spectra® 3.6)



H.P. White Laboratory, Inc.

PROTECTION BALLISTIC LIMIT TEST, V50 BL(P)

Client : PLAINSMAN ARMOR INTERNATIONAL

Job No. : 9471-03

Test Date : 12/10/04

TEST PANEL

Manufacturer : PLAINSMAN ARMOR INTERNATIONAL
 Size : 13 x 13 in.
 Thickness : NA
 Avg. Thick : NA
 Required BL(P) : 3300 f/s
 Description : K129 + DYNEMA + TWARON

Sample No. : SAMPLE-39
 Heat No. : NA
 Weight : 1.77 lbs.
 Hardness : NA
 Piles/Laminates : 43

Date Rec'd. : 12-09-04
 Via : UPS
 Returned : UPS

SET-UP

Shot Spacing : PER CUSTOMER REQUEST
 Witness Panel : 0.020", 2024-T3 ALUMINUM
 Obliquity : 0 deg.
 Backing Material : NA
 Conditioning : AMBIENT

Primary Vel. Screens : 5.0 ft., 7.0 ft.
 Primary Vel. Location : 6.0 ft. From Muzzle
 Residual Vel. Screens : NA
 Residual Vel. Location : NA
 Range to Target : 9.0 ft.
 Target to Wt. : 6.0 in.

Range No. : 5
 Temp. : 68 F
 RP : 29.23 in. Hg
 RH : 54%
 Barrel No./Gun : TEST BARREL
 Gunner : UNGER
 Recorder : UNGER

AMMUNITION

Projectile : 2 grain Steel ROO, 2 gr.
 Powder : BULLSEYE

Lot No. :

APPLICABLE STANDARDS OR PROCEDURES

- (1) : AIR WARRIOR
- (2) :
- (3) :

Shot No.	Powder Seating	Time (usec)	Velocity (f/s)	Vel. Loss (f/s)	V-Strike (f/s)	Result	Include in V50	Footnotes
1	8.4	567	3527	139	3388	C	Y	
2	8.9	586	3413	135	3278	P	Y	
3	8.4	577	3486	137	3329	C	Y	
4	8.3	587	3407	135	3272	C	Y	
5	8.1	593	3373	133	3209	P	Y	
6	8.2	590	3390	134	3256	P	Y	

REMARKS :

FOOTNOTES :

V50 SUMMARY :

No. Points : 3 & 3
 V50 : 3294
 High Partial : 3278
 Low Complete : 3272
 Range of Results : 149
 Range of Misses : 6

Figure 77. Sample 39 (5.8 oz K129®/Dyneema®)



H.P. White Laboratory, Inc.
PROTECTION BALLISTIC LIMIT TEST, V50 BL(P)

Client: PLAINSMAN ARMOR INTERNATIONAL

Job No.: 9471-03

Test Date: 12/10/04

TEST PANEL

Manufacturer: PLAINSMAN ARMOR INTERNATIONAL
 Size: 13 x 13 in.
 Thickness: NA
 Avg. Thick: NA
 Required BL(P): 3300 ft/s
 Description: 807 + K129 DYNEMA + 38 TWARON 3504

Sample No.: SAMPLE-40
 Heat No.: NA
 Weight: 1.77 lbs.
 Hardness: NA
 Piles/Laminates: 42



Date Recd.: 12-09-04
 Via: UPS
 Returned: UPS

SET-UP

Shot Spacing: PER CUSTOMER REQUEST
 Witness Panel: 0.020", 2024-T3 ALUMINUM
 Obliquity: 0 deg.
 Backing Material: NA
 Conditioning: AMBIENT

Primary Vel. Screens: 5.0 ft., 7.0 ft.
 Primary Vel. Location: 8.0 ft. From Muzzle
 Residual Vel. Screens: NA
 Residual Vel. Location: NA
 Range to Target: 9.0 ft.
 Target to Vel.: 8.0 in.

Range No.: 5
 Temp.: 66 F
 SP: 29.23 in. Hig
 RH: 54%
 Barrel No./Gun: TEST BARREL
 Gunner: UNGER
 Recorder: UNGER

AMMUNITION

Projectile: 2 grain Steel FCC, 2 gr.
 Powder: BULLSEYE

Lot No.:

APPLICABLE STANDARDS OR PROCEDURES

- (1): AIR WARRIOR
- (2):
- (3):

Shot No.	Prvd/Grating	Time (ms)	Velocity (ft/s)	Vel. Loss (ft/s)	V-Strike (ft/s)	Result	Include in V50	Footnotes
1	8.3	582	3436	136	3301	P	Y	
2	8.4	572	3497	138	3358	C	Y	
3	8.3	571	3503	139	3364	C	Y	
4	8.2	595	3361	133	3228	C	Y	
5	8.1	593	3373	133	3239	P	Y	
6	8.2	595	3361	133	3228	P	Y	

REMARKS:

FOOTNOTES:

V50 SUMMARY:
 No. Pts: 3 & 3
 V50: 3286
 High Partial: 3301
 Low Complete: 3228
 Range of Results: 136
 Range of Missed: 73

File Name: 9471-03 (SAMPLE 40) PLAINSMAN ARMOR INTERNATIONAL V50

Figure 78. Sample 40 (8 oz. K129®/Dyneema®)

APPENDIX G: DSC PLOTS

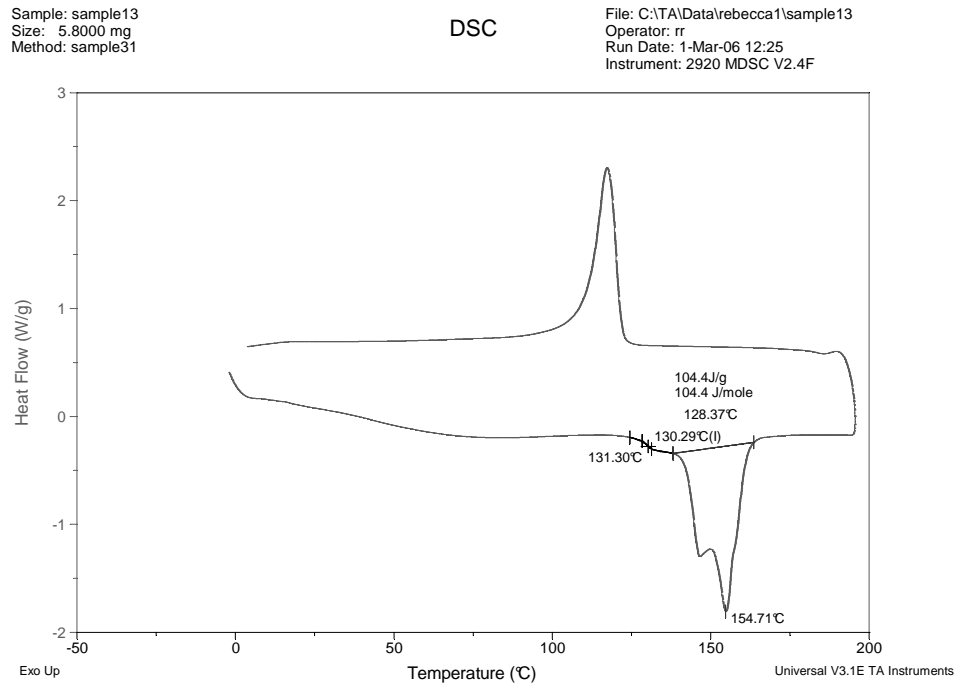


Figure 79. Sample 13: Spectra® 3.6 Impact

Sample: sample25
Size: 5.7000 mg
Method: sample31

DSC

File: C:\TA\Data\rebecca1\sample25
Operator: rr
Run Date: 1-Mar-06 11:27
Instrument: 2920 MDSC V2.4F

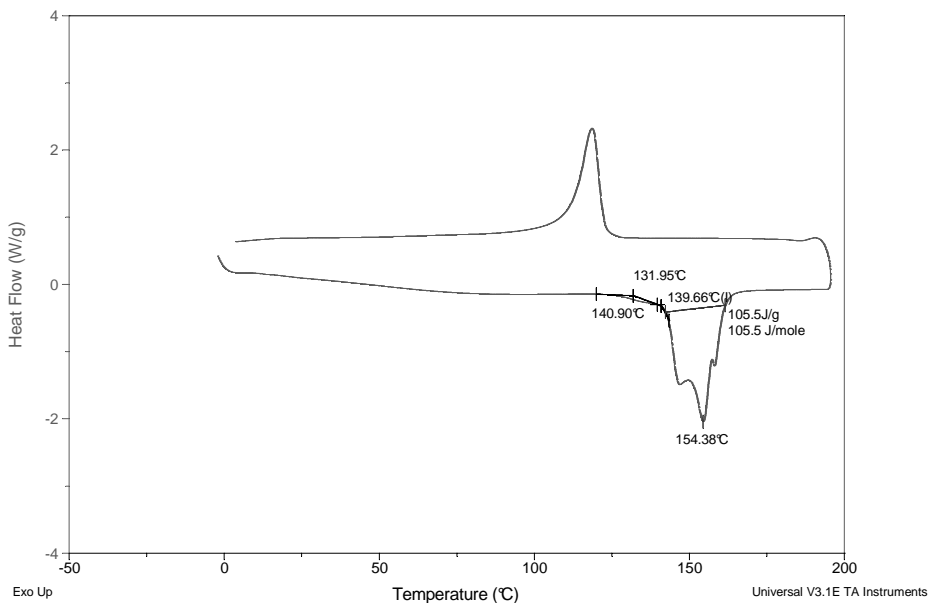


Figure 80. Sample 25: Dyneema® Impact

Sample: sample26
Size: 6.2000 mg
Method: sample31

DSC

File: C:\TA\Data\rebecca1\sample26
Operator: rr
Run Date: 1-Mar-06 10:20
Instrument: 2920 MDSC V2.4F

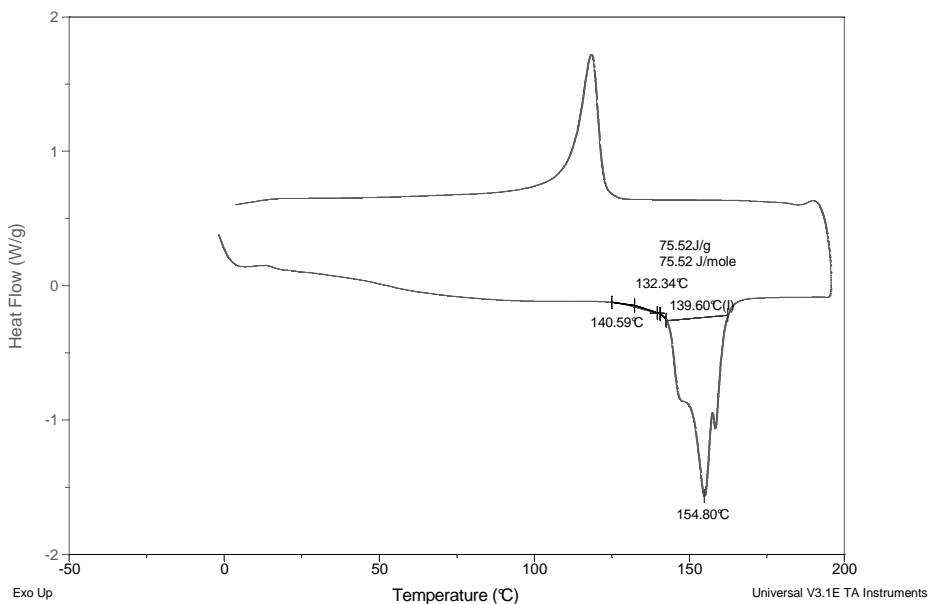


Figure 81. Sample 26: Dyneema® Impact

Sample: sample27
Size: 6.7000 mg
Method: sample31

DSC

File: C:\TA\Data\rebecca1\sample27
Operator: rr
Run Date: 1-Mar-06 09:29
Instrument: 2920 MDSC V2.4F

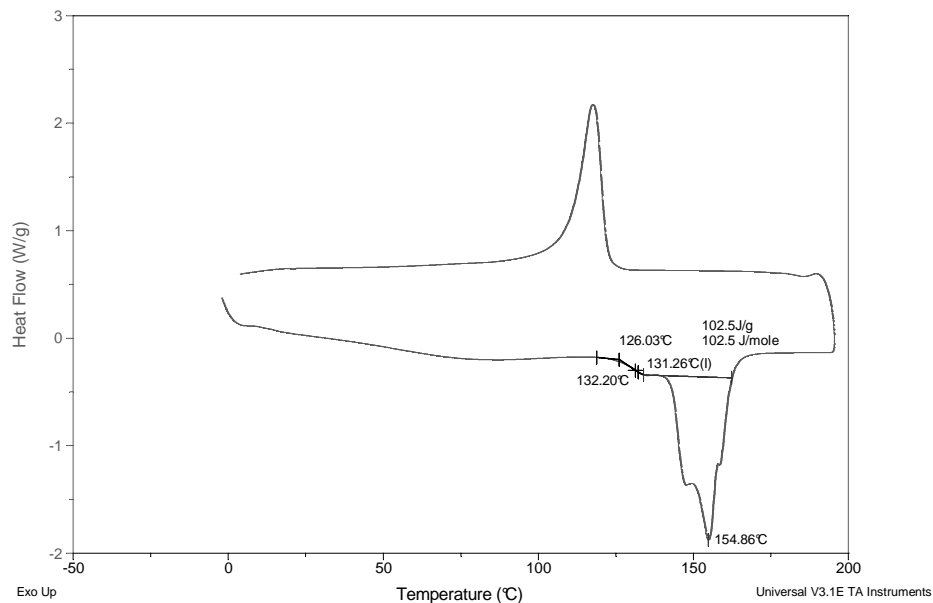


Figure 82. Sample 27: Dyneema® Impact

Sample: sample28
Size: 6.8000 mg
Method: sample31

DSC

File: C:\TA\Data\rebecca1\sample28
Operator: rr
Run Date: 28-Feb-06 16:15
Instrument: 2920 MDSC V2.4F

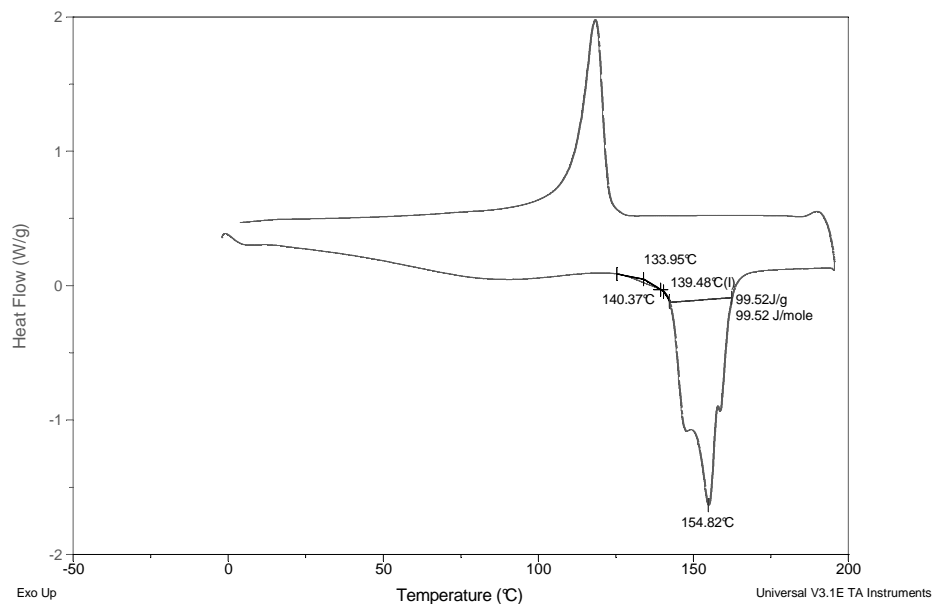


Figure 83. Sample 28: Dyneema® Impact

Sample: sample29
Size: 6.2000 mg
Method: sample31

DSC

File: C:\TA\Data\rebecca1\sample29
Operator: rr
Run Date: 28-Feb-06 14:31
Instrument: 2920 MDSC V2.4F

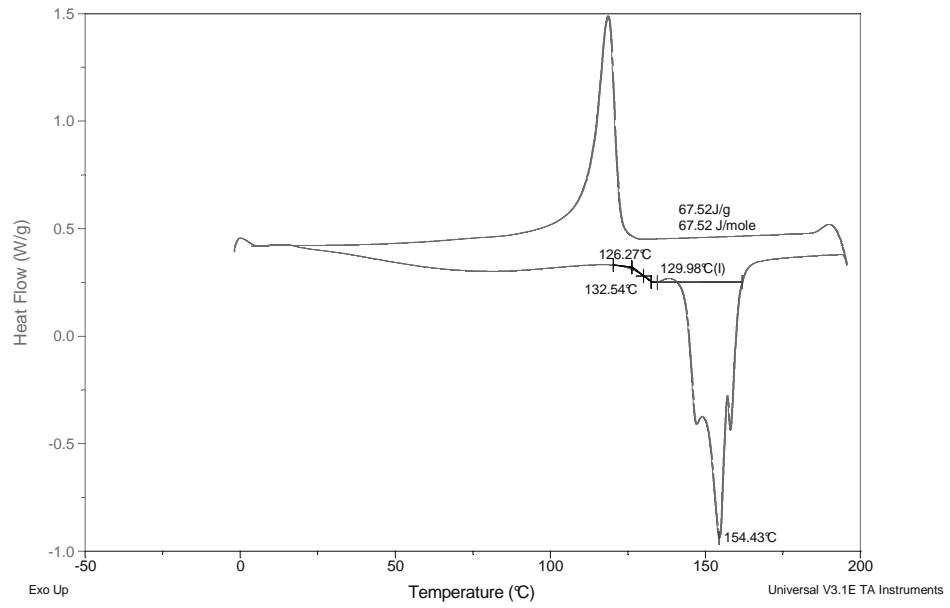


Figure 84. Sample 29: Dyneema® Impact

Sample: sample30
Size: 10.0000 mg
Method: sample30

DSC

File: C:\TA\Data\rebecca1\sample30.001
Operator: wwang
Run Date: 17-Jan-06 11:38
Instrument: 2920 MDSC V2.4F

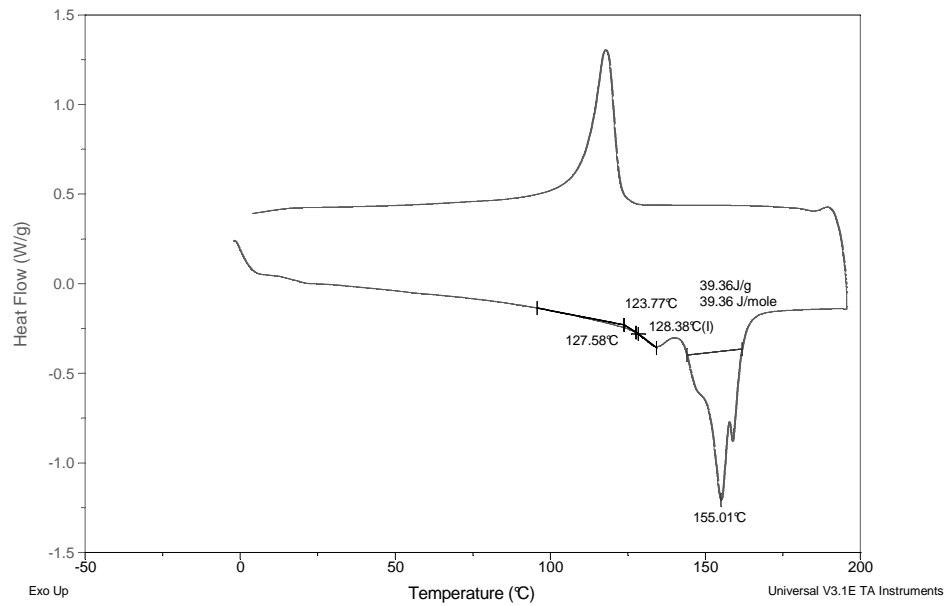


Figure 85. Sample 30: Dyneema® Impact

Sample: sample31
Size: 5.3000 mg
Method: sample31

DSC

File: C:\TA\Data\rebecca1\sample31
Operator: skh
Run Date: 28-Feb-06 12:36
Instrument: 2920 MDSC V2.4F

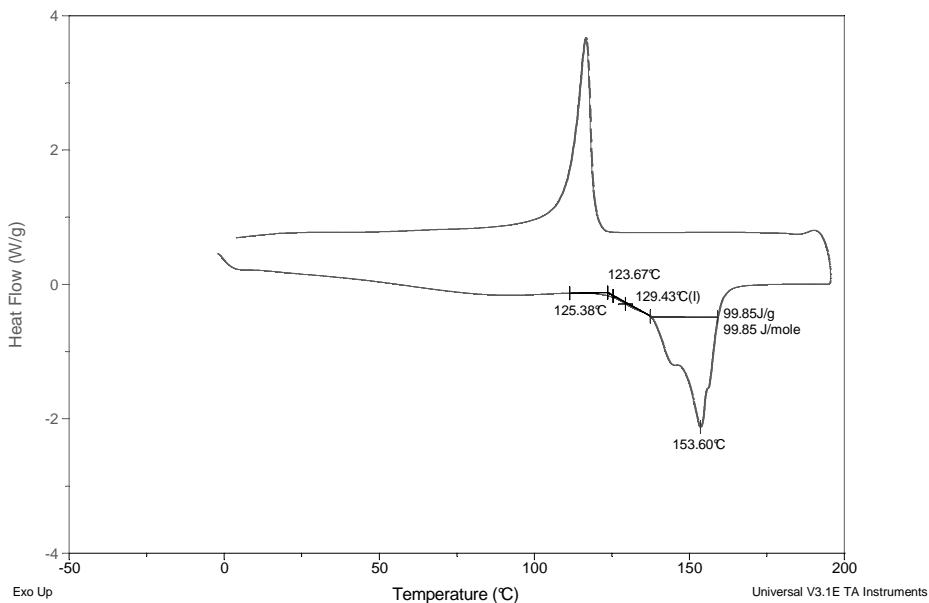


Figure 86. Sample 31: Spectra® 2.2 Impact

Sample: sample31n
Size: 7.2000 mg
Method: sample30

DSC

File: C:\TA\Data\rebecca1\sample31n
Operator: wwang
Run Date: 17-Jan-06 12:29
Instrument: 2920 MDSC V2.4F

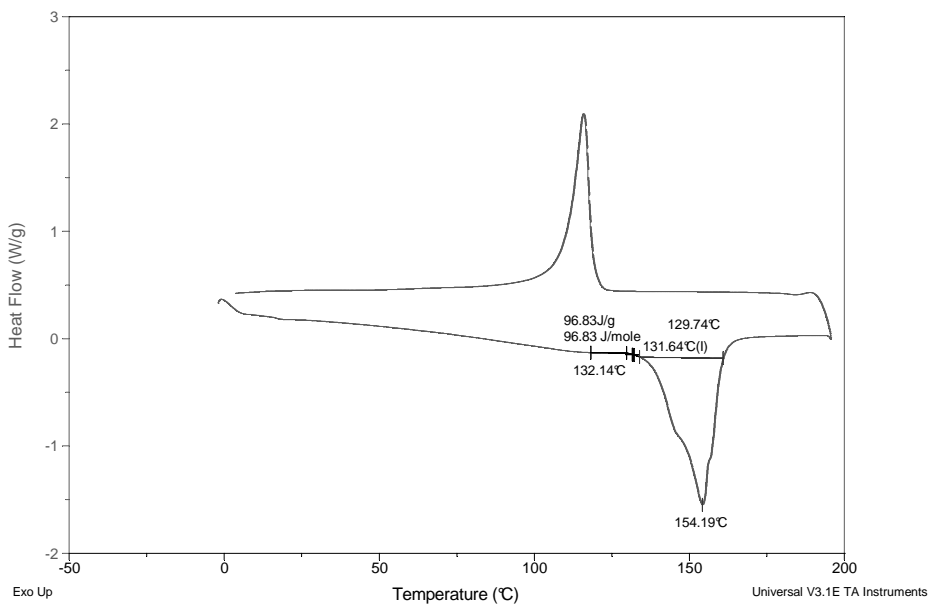


Figure 87. Sample 31: Spectra® 2.2 Non-Impact

Sample: sample32
Size: 9.0000 mg
Method: sample37

DSC

File: C:\TA\Data\rebecca1\sample32
Operator: wwang
Run Date: 9-Dec-05 11:03
Instrument: 2920 MDSC V2.4F

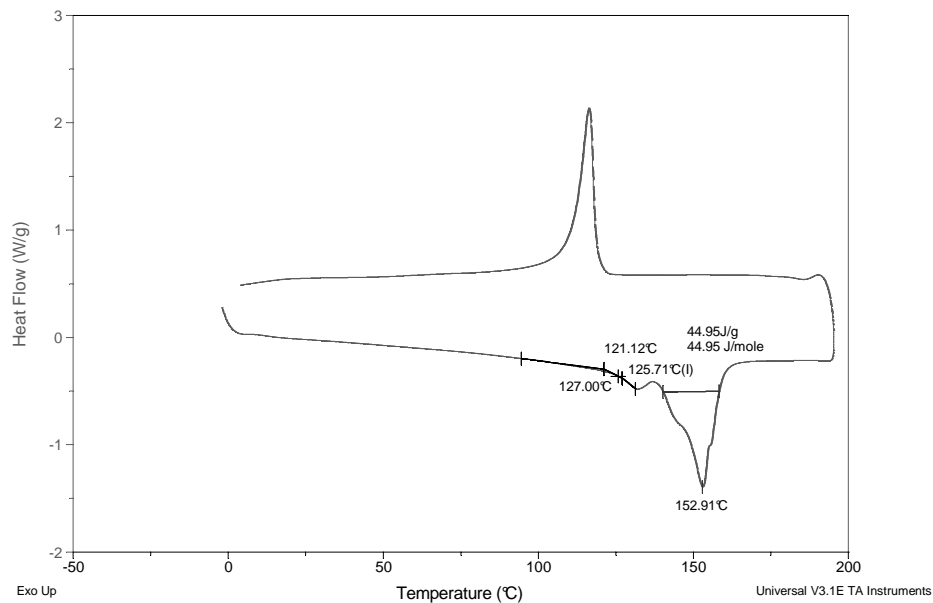


Figure 88. Sample 32: Spectra® 2.2 Impact

Sample: sample32n
Size: 8.3000 mg
Method: sample37

DSC

File: C:\TA\Data\rebecca1\sample32n
Operator: wwang
Run Date: 9-Dec-05 11:52
Instrument: 2920 MDSC V2.4F

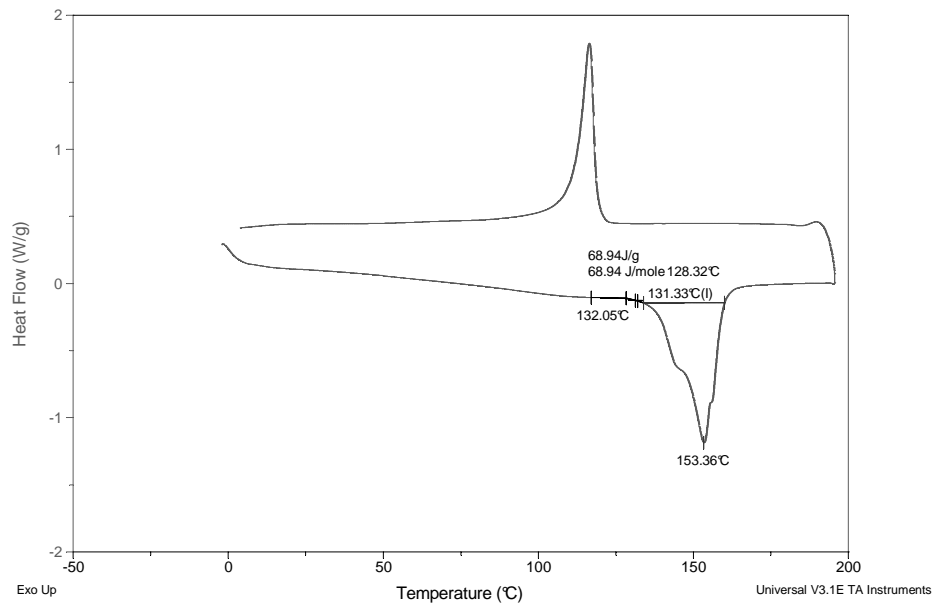


Figure 89. Sample 32: Spectra® 2.2 Non-Impact

Sample: sample33
Size: 9.1000 mg
Method: sample33

DSC

File: C:\TA\Data\rebecca1\sample33
Operator: wwang
Run Date: 6-Dec-05 11:26
Instrument: 2920 MDSC V2.4F

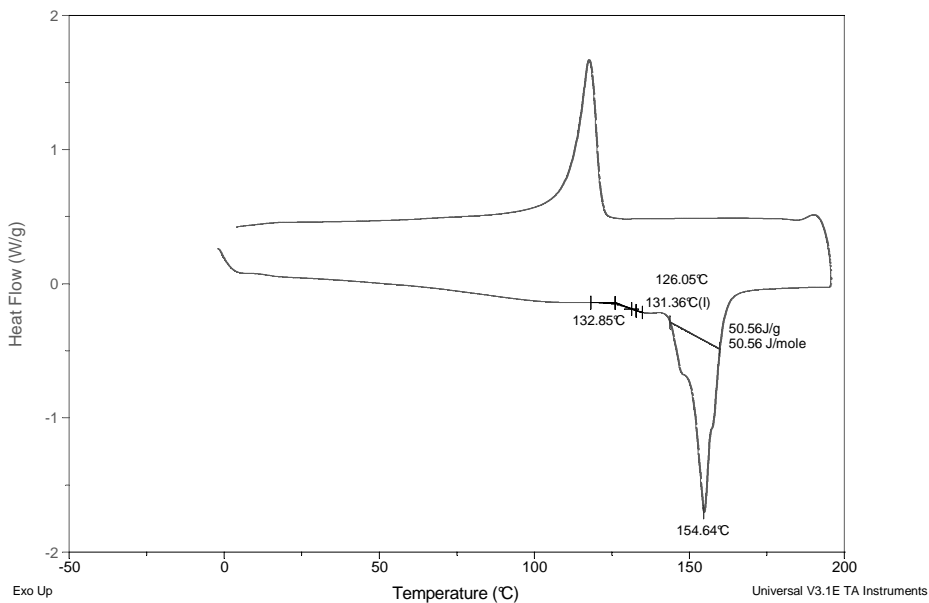


Figure 90. Sample 33: Spectra® 3.6 Impact

Sample: sample34
Size: 8.9000 mg
Method: sample34

DSC

File: C:\TA\Data\rebecca1\sample30
Operator: wwang
Run Date: 6-Dec-05 09:35
Instrument: 2920 MDSC V2.4F

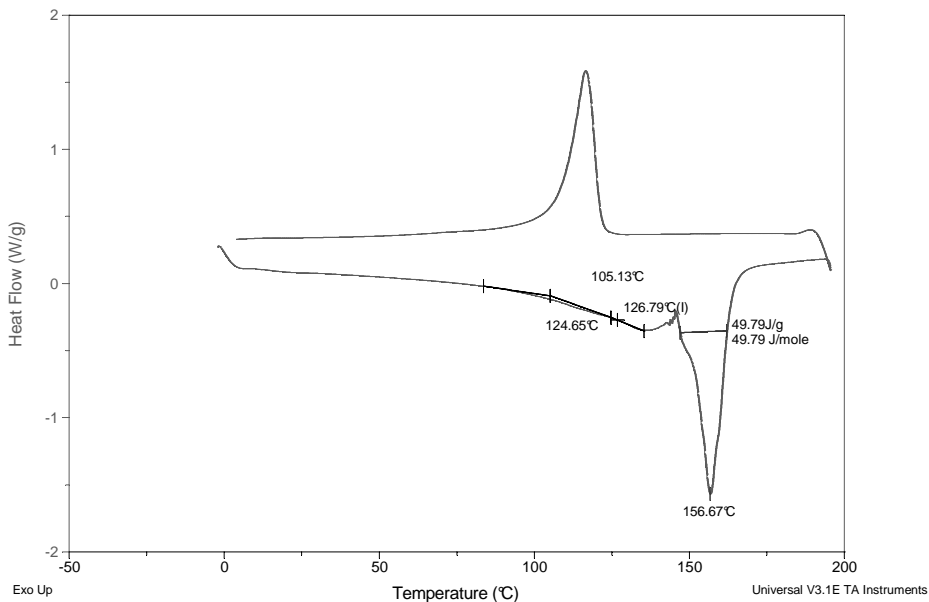


Figure 91. Sample 34: Spectra® 3.6 Impact

Sample: sample34n
Size: 8.5000 mg
Method: sample34

DSC

File: C:\TA\Data\rebecca1\sample34n
Operator: wwang
Run Date: 6-Dec-05 10:26
Instrument: 2920 MDSC V2.4F

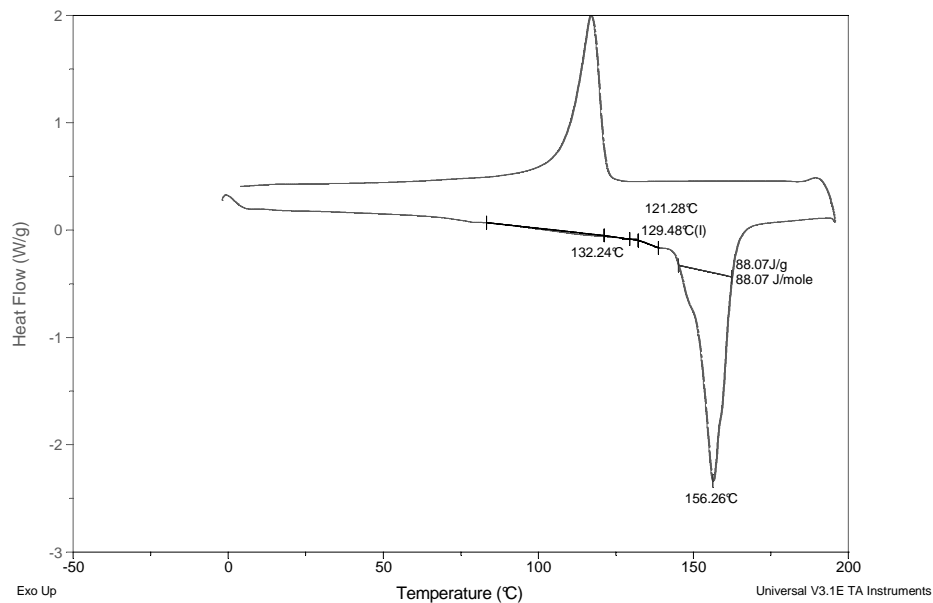


Figure 92. Sample 34: Spectra® 3.6 Non-Impact

Sample: sample35
Size: 7.9000 mg
Method: sample35

DSC

File: C:\TA\Data\rebecca1\sample35
Operator: wwang
Run Date: 2-Dec-05 14:26
Instrument: 2920 MDSC V2.4F

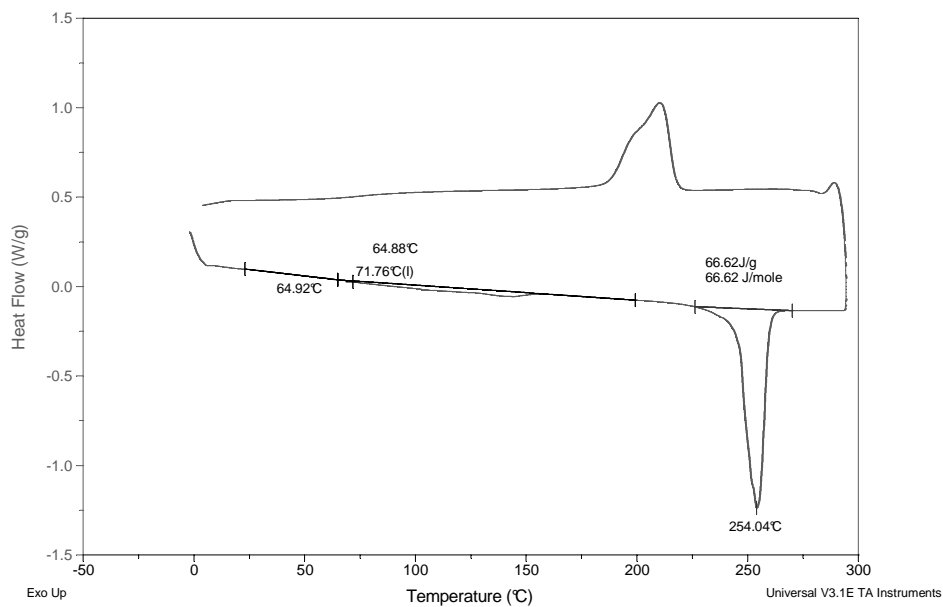


Figure 93. Sample 35: PET Impact

Sample: sample35n
Size: 7.9000 mg
Method: sample35

DSC

File: C:\TA\Data\rebecca1\sample35n
Operator: wwang
Run Date: 2-Dec-05 15:34
Instrument: 2920 MDSC V2.4F

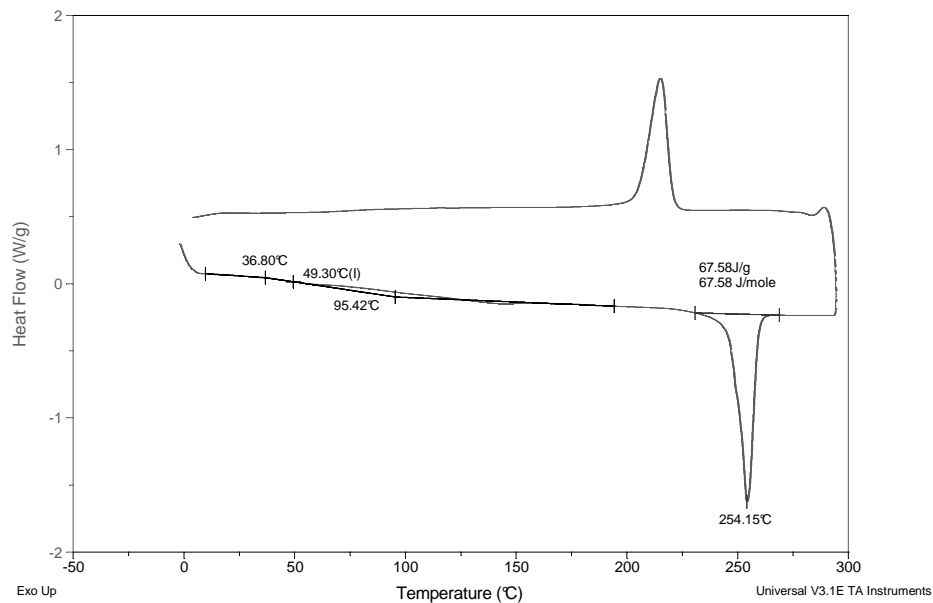


Figure 94. Sample 35: PET Non-Impact

Sample: sample372
Size: 7.1000 mg
Method: sample31

DSC

File: C:\TA\Data\rebecca1\sample372
Operator: skh
Run Date: 28-Feb-06 13:45
Instrument: 2920 MDSC V2.4F

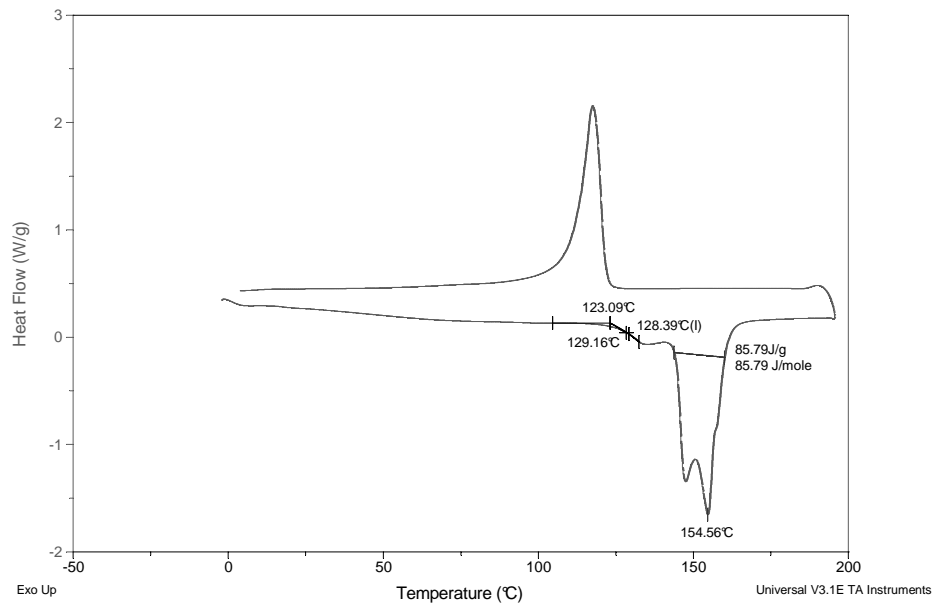


Figure 95. Sample 37: Spectra® 3.6 Impact

Sample: sample38
Size: 9.0000 mg
Method: sample38

DSC

File: C:\TA\Data\rebecca1\sample38
Operator: wwang
Run Date: 2-Dec-05 12:36
Instrument: 2920 MDSC V2.4F

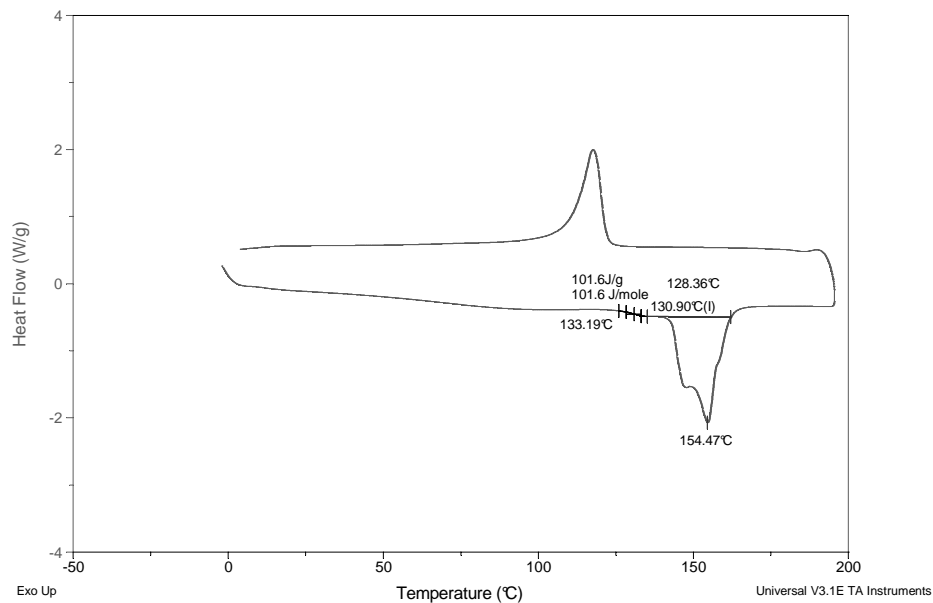


Figure 96. Sample 38: Spectra® 6.3 Impact

Sample: sample38n
Size: 9.4000 mg
Method: sample38

DSC

File: C:\TA\Data\rebecca1\sample38n
Operator: wwang
Run Date: 2-Dec-05 13:24
Instrument: 2920 MDSC V2.4F

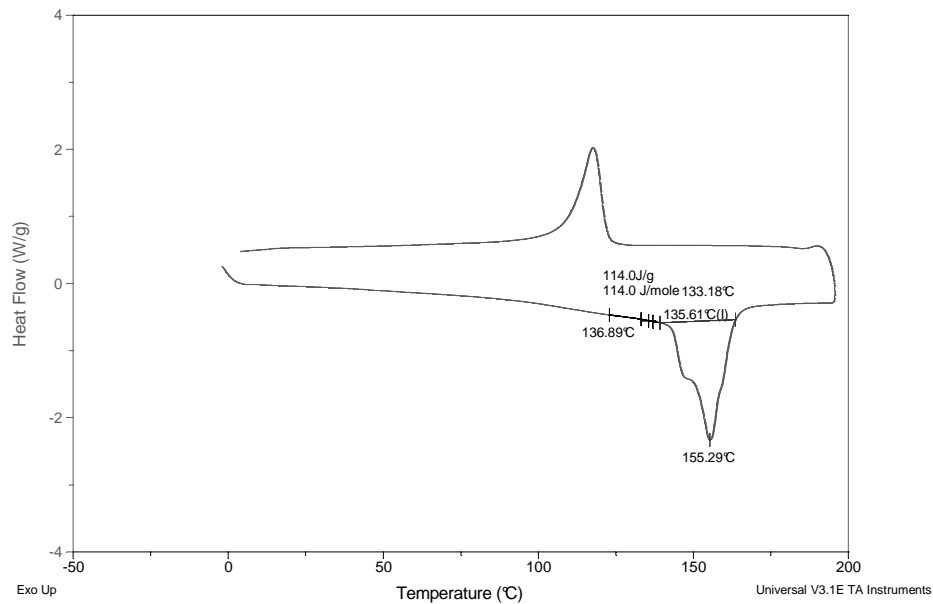


Figure 97. Sample 38: Spectra® 6.3 Non-Impact

Sample: sample39
Size: 10.0000 mg

DSC

File: C:\TA\Data\rebecca1\sample39.000
Operator: wwang
Run Date: 2-Dec-05 10:54
Instrument: 2920 MDSC V2.4F

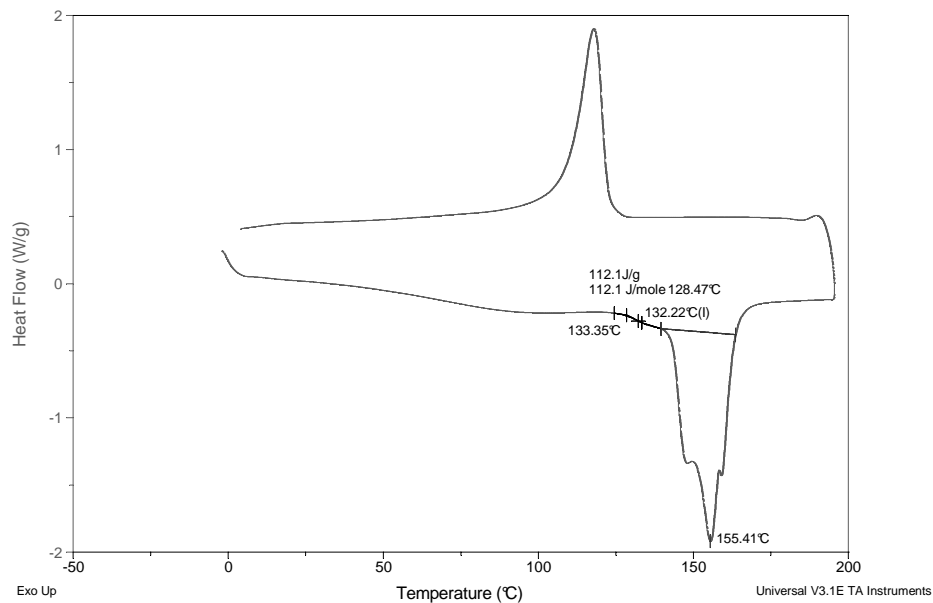


Figure 98. Sample 39: Dyneema® Impact

Sample: sample 40
Size: 9.2000 mg

DSC

File: C:\TA\Data\rebecca1\sample40
Operator: wwang
Run Date: 30-Nov-05 15:56
Instrument: 2920 MDSC V2.4F

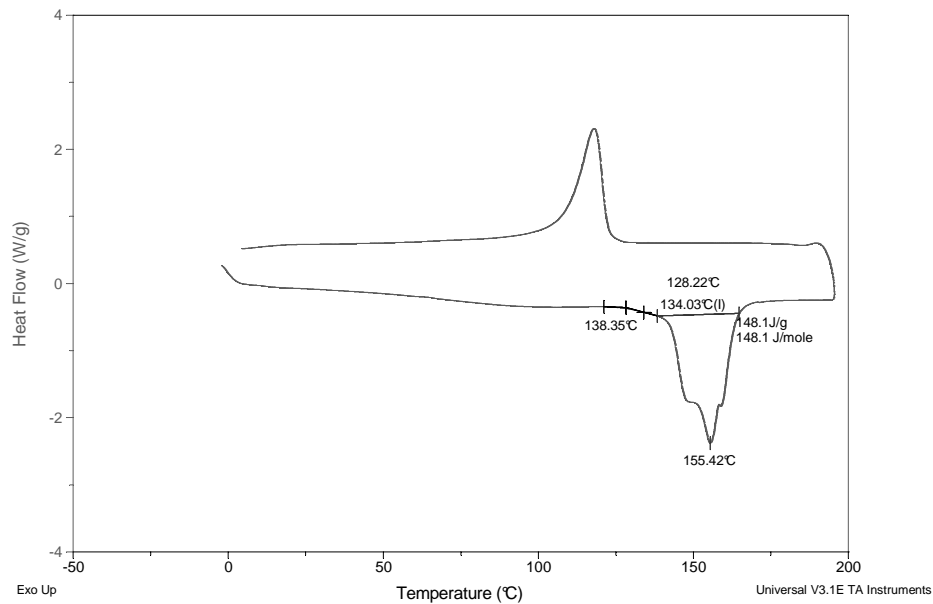


Figure 99. Sample 40: Dyneema® Impact

Sample: sample40n
Size: 9.0000 mg

DSC

File: C:\TA\Data\rebecca1\sample40n
Operator: wwang
Run Date: 2-Dec-05 09:57
Instrument: 2920 MDSC V2.4F

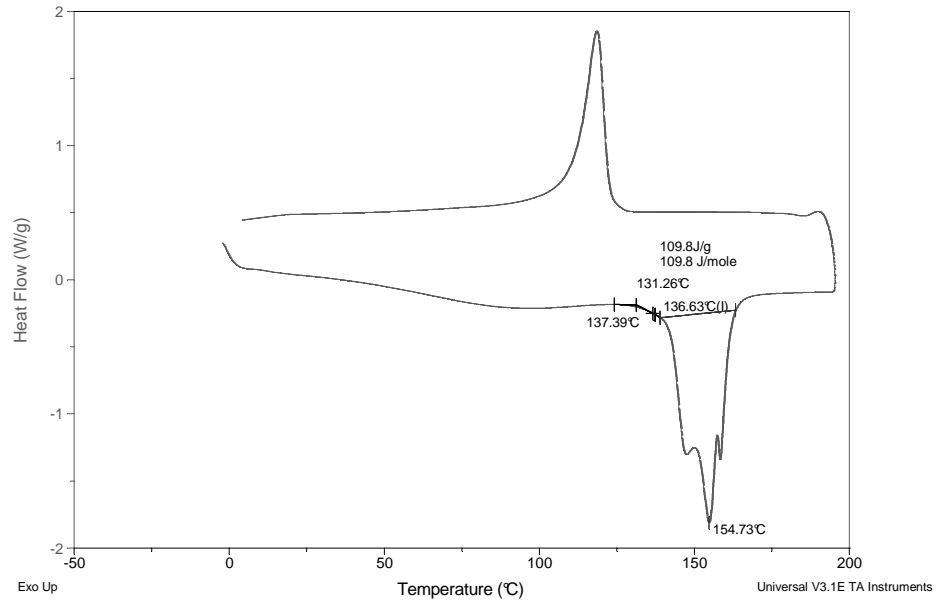


Figure 100. Sample 40: Dyneema® Non-Impact